Analysis of slender reinforced concrete wall panels (tilt-up) utilizing lightweight concrete

by

Connor Lewer

B.S., Kansas State University, 2019

A THESIS

submitted in partial fulfillment of the requirements for the degree

MASTER OF SCIENCE

Department of Architectural Engineering
Carl R. Ice College of Engineering

KANSAS STATE UNIVERSITY
Manhattan, Kansas

2019

Approved by:

Major Professor
Kimberly Kramer

Copyright

Abstract

With tilt-up panels gaining popularity in the construction industry due to their affordability and quick construction times, more analysis of lightweight concrete in slender tilt-up wall panels is in order. Lightweight concrete offers benefits over normal weight concrete as it reduces the overall weight of the structure, thus reducing seismic loading. This reduction in weight also allows for the lifting of larger panels, which reduces the quantity of panels and reduces construction time. For panels of the same size, lightweight panels also allow for longer reach from the crane due to the reduced weight. Lightweight concrete, however, has different material properties than normal weight concrete, which impact design. The three primary differences between lightweight and normal weight concrete in the design of slender tilt-up panels are: the concrete unit weight, the modulus of rupture factor, and the lightweight modification factor. This thesis investigated the effect that each of these properties have on the performance of tilt-up panels through a parametric study using current ACI 318 code. Deflections calculated were compared to determine the impact these factors have on the panel deflections.

Table of Contents

List of Figures

List of Tables

List of Terms

A_g – Gross area of concrete section

A_s – Area of tension reinforcement

A_{se} – Effective area of tension reinforcement

a – Depth of equivalent rectangular stress block

b – Width of concrete section

C_t – Creep coefficient

c – Distance from the extreme compression fiber to the neutral axis

D – Dead load

d – Distance from the extreme compression fiber to the centroid of tension reinforcement

E – Loads due to seismic force

E_c – Concrete modulus of elasticity

E_s – Steel modulus of elasticity

e_{cc} – Eccentricity of applied axial load

e_a – Additional eccentricity due to creep

f'_c – Specified concrete compressive strength

f_r – Modulus of rupture

f_y – Steel reinforcement yield stress

h – Panel thickness

I_{cr} – Cracked section moment of inertia

I_e – Effective moment of inertia

I_g – Gross moment of inertia

K – Modulus of rupture factor

K_b – Bending stiffness

L – Live load

L_r – Roof live load

l – Span of member between supports

l_c – Cantilever height

l_{total} – Total panel height

l_w or l_b or t – Width of concrete section

M_a – Maximum moment at panel midheight due to service lateral loads and eccentric vertical loads (including P-Δ effects)

M_{cr} – Moment causing flexural cracking of the concrete section

M_n – Nominal moment strength at panel midheight due to service lateral loads and eccentric vertical loads

M_{sa} – Maximum moment at panel midheight due to service lateral loads and eccentric vertical loads (including P-Δ effects)

M_u – Maximum factored combined bending moment

M_{ua} – Maximum factored moment at panel midheight due to lateral loads and eccentric vertical loads (including P-Δ effects)

n – Modular ratio

P – Applied axial load

P-Δ – Secondary moment caused by axial load acting on a deflected shape with displacement

P_u – Factored axial load

psf – Pounds per square foot

pcf – Pounds per cubic foot

W – Wind load

W_a – Service level wind load

w_c – Concrete unit weight

β – Ratio of sustained design load to total design load

Δ_{cr} – Deflection that occurs at panel cracking

Δ_n – Maximum potential deflection at panel midheight

ρ – Reinforcement ratio

λ – Lightweight concrete modification factor

$\emptyset$ – Strength reduction factor

Acknowledgements

I would like to express my gratefulness for my major professor, Kimberly Kramer, whose contributions, advice, and invaluable experience were instrumental in the composition of this thesis. I'd also like to extend my gratitude to the members of my graduate committee, Dr. Hayder Rasheed, Dr. Bill Zhang, and Professor Katie Loughmiller for their flexibility, support, and guidance. Additionally, I'd like to give thanks to all my past professors at Kansas State University who have educated and inspired me throughout my years of study.

My academic success would also not have been possible without the love and support of my parents, Gregory and Julie Lewer. The sacrifices they have made for me and the experiences they have given me throughout my educational career have contributed to my growth as a developing engineer.

I am also filled with gratitude for the love and encouragement from my fiancé, Kali Babich. From our freshman year through my second senior year, she has guided me in my decisions and advocated for my success.

A final expression of my gratitude is owed to my Catholic faith, which has been my primary support system throughout my college career.

Dedication

I dedicate this thesis to my late grandfather, Dorvon Chuck Lewer, for teaching me priceless life lessons and being a primary source of my inspiration.

Chapter 1 - Introduction

Concrete tilt-up wall panels are increasingly being used in structural design. The Tilt-Up Concrete Association (TCA, 2018) states that over 10,000 buildings with over 650 million square feet are constructed annually using site-cast tilt-up construction. Until recently, normal weight concrete was typically used for the design of slender tilt-up wall panels. Lightweight concrete, however, is gaining popularity among tilt-up designers due to its properties such as reduced self-weight/dead load.

The Tilt-up Concrete Association (TCA) has a hotline which allows architects, engineers, and contractors to ask questions and TCA's hotline experts reply to the questions/inquires. Contractors have posed questions about replacing normal weight concrete with lightweight concrete to reduce the overall weight of an individual panel for construction purposes (N. Schnell, personal communication, October 1, 2018). While this would allow for reduced loads on the crane during the lifting process, the engineer of record will need to consider the impact of using lightweight concrete on the structural integrity of the slender wall panel. Lightweight concrete has a reduced modulus of elasticity, E_c, and modulus of rupture, f_r, when compared to normal weight concrete. This reduces flexural stiffness, increasing the deflection of the wall and in turn decreases the capacity of the slender wall due to P-delta effects. Lightweight concrete, however, has a lower density (ranging from 90 pounds per cubic foot to 120 pounds per cubic foot (pcf)) than normal weight concrete (approximately 145 pcf), which may offset some of the reduced mechanical properties. The American Concrete Institute (ACI) 318-19 *Building Code Requirements for Structural Concrete* (ACI 318-19) in Section 19.2.4.1 defines lightweight concrete based on equilibrium density ranges from less than 100 pcf to 135 pcf and normal weight concrete with an equilibrium density greater than 135 pcf.

Modern concrete tilt-up construction was first conceptualized in the early 1900's, but only within the past forty years has it gained traction as a viable method of wall construction (Ward, 2011). With advancements in concrete, reinforcement, and crane technology, tilt-up has evolved to become widely used. Tilt-up wall panels are site cast by placing the fresh concrete horizontally on a flat casting surface, typically the slab-on-grade for the building. Once the concrete has reached 75 percent of the 28-day specified compressive strength, typically 3,000 pounds per square inch (psi), the panels are lifted into place with a crane into their final vertical position. An experienced tilt-up contractor can lift and place 30 tilt-up panels in a single day (Ward, 2011). Tilt-up construction also requires less formwork when compared to cast-in-place construction, saving time, money, and labor.

While slender tilt-up panels and lightweight concrete have both been separately studied, more work must be done to better understand the behavior of lightweight concrete used within slender tilt-up panels. This report analyzes previous studies and existing literature, conducts a parametric study of lightweight slender tilt-up panels, offers other considerations regarding the use of lightweight tilt-up wall panels, and makes recommendations for future research into the subject.

A review on existing literature begins with an analysis of the material properties of lightweight concrete in comparison with normal weight concrete. Next, experimental data from previous full-scale testing on slender wall panels constructed with normal weight concrete is discussed. Finally, analysis methods for the design of tilt-up wall panels are included as the foundation for the research done in this report.

The parametric study included in this report begins by describing the building and site conditions taken into consideration. The panel parameters used for the study are described.

Once the constraints of the study are established, the methods and results are discussed. The results of the study are used to describe the impact that using lightweight concrete has in the design of slender tilt-up wall panels. The deflection equations used for analysis are also discussed.

Other considerations involved in the selection of lightweight concrete are also discussed. The cost, fireproof rating, and sustainability are described to show non-strength considerations involved with lightweight concrete.

As a conclusion, a summary of the report discusses the findings of the parametric study and the current equations used to calculate the deflection in slender tilt-up wall panels. Recommendations for design is included to assist in engineering design in accordance with current code. Additionally, recommendations for future research discuss potential tests for lightweight concrete in slender tilt-up walls and further analysis of the deflection equations report.

Chapter 2 - Literature Review

This chapter discusses the research done in relation to this thesis and is divided into three sections: lightweight concrete and reinforcing steel material properties, an analysis of previous test results, and design criteria for slender tilt-up panels.

2.1 Lightweight Concrete and Reinforcing Steel Material Properties

This section discusses the material properties of lightweight concrete and reinforcing steel. Material properties such as the modulus of rupture, modulus of elasticity, and material strength influence the design capacity of slender wall panels and must be understood for a proper analysis.

Lightweight aggregates have a low-particle relative density because of the cellular pore system. Raw materials are heated to incipient fusion which causes cellular structure to form due to gases evolve with the pyroclastic mass, causing expansion that is retained upon cooling (ACI 213R, 2014). Each of the properties of lightweight aggregate may have some bearing on properties of the fresh and hardened concrete. The properties of lightweight concrete are greatly influenced by the cementitious matrix. Particle shape may be cubical and regular or rounded, irregular, and surface texture may be relatively smooth with small exposed pores to irregular with large pores - these properties varying depending on the source. Proportioning of mixtures are influenced by surface textures and particle shape. Workability, pump-ability, fine-to-coarse aggregate ratio, binder content, and water requirement are all influenced. Workability, pump-ability and water requirements effect the construction aspects of concrete tilt-up wall panels. The binder content, fine-to-coarse aggregate ratio, and water requirement effect the strength of the panels.

As previously indicated, the specific gravity of lightweight concrete is less than that of normal weight concrete. This is due to the cellular structure of the lightweight aggregates and varies greatly due to the processing methods. The strength of lightweight aggregate particles also varies with type and source and is measurable only in a qualitative way. Some particles may be strong and hard while other are weak and friable. Currently, no reliable correlation between aggregate intrinsic strength and concrete strength for compressive strengths up to approximately 5000 psi exists (ACI213R, 2014).

Compressive strength levels commonly required by the construction industry for design strengths of cast-in-place, precast, or prestressed concrete are economically obtained with lightweight concrete (Shideler 1957; Hanson 1964; Holm 1980a; Trumble & Santizo 1992). Design strengths of 3000 to 5000 psi are common. Videla and Lopez (2000, 2002) have found a relationship between compressive strength and the amount and strength of lightweight aggregates for concrete made with natural lightweight aggregates. The strength ceiling is influenced predominantly by the coarse aggregate. The strength ceiling can be increased appreciably by reducing the maximum size of the coarse aggregate for most LWAs. This effect is more apparent for the weaker and more friable aggregates. In one case, strength attained in the laboratory, for concrete containing 3/4 in. maximum size of a specific lightweight aggregate, was 5000 psi (35 MPa). The strength, however, was increased to 6100 and 7600 psi (42 and 52 MPa) when the maximum size of the aggregate was reduced to 1/2 and 3/8 in. (13 and 10 mm), respectively, without changing the cement content. Consequently, concrete unit weight increased by 3 and 5 lb/ft^3 (48 and 80 kg/m^3) when the maximum size of the aggregate was reduced to 1/2 and 3/8 in. (13 and 10 mm), respectively. All aggregates have strength ceilings, and with lightweight aggregates, the strength ceiling generally can be increased by reducing the maximum size of the coarse aggregate. Since concrete tilt-up panels are typically are specified/designed for a compressive strength of concrete of 3000 psi to 5000 psi with ¾-inch or 1-inch maximum aggregate size (Baty, 2006), the strength ceiling has little bearing on the design of lightweight concrete tilt-up panels.

Meyer, Buchberg, & Kahn (2003) reported that the tensile strength for a given lightweight aggregate may not increase in a manner comparable to the increase in compressive strength. Increases in tensile strength occur at a lower rate relative to increases in compressive strength. This becomes more pronounced as compressive strength exceeds 5000 psi which is outside the scope of this thesis.

The modulus of rupture, f_r, (ASTM C78/C78M) is also a measure of the tensile strength of concrete. For prism specimens, a nonuniform moisture distribution will reduce the modulus of rupture, but the moisture distribution within the structural member is not known and is unlikely to be completely saturated or dry. Studies have indicated that modulus of rupture tests of concrete undergoing drying are extremely sensitive to the transient moisture content and, under these conditions, may not furnish reliable results that are satisfactorily reproducible (Hanson 1961). The values of the modulus of rupture determined from tests on high-strength lightweight concrete yield inconsistent correlation with code requirements. While Huffington (2000) reported that the tensile splitting and modulus of rupture test results generally met AASHTO requirements for high-strength lightweight concrete, Nassar (2002) found that the modulus of rupture of high-strength lightweight concrete was approximately 60 to 85 percent of code requirements of $\lambda \times 7.5\sqrt{fc'}$, where λ for sand lightweight concrete is recommended to be 0.85. Meyer (2002), however, found that no additional reduction was required for high-strength lightweight concrete mixtures. Knowing the actual modulus of rupture is important to determine the cracking moment of the tilt-up panel and its implication of the P-delta effects for design.

Proportioning concrete mixtures and making field adjustments of lightweight concrete require a comprehensive understanding of porosity, absorption, and the degree of saturation of lightweight-aggregate particles. The degree of saturation, which is the fractional part of the pores filled with water, can be evaluated from pycnometer measurements. These measurements determine the relative density at various levels of absorption, thus permitting proportioning by the absolute volume procedure. Pores are the air space inside an individual aggregate particle and voids are the interstitial space between aggregate particles. Total porosity that is found within and between the particles is determined from measured values of particle relative density and bulk density.

Due to their cellular structure, the moisture content and absorption of lightweight aggregates are capable of absorbing more water than normal weight aggregates. Based on a standard ASTM C127 absorption test, LWAs absorb from 5 to 25 percent or more by mass of dry aggregate after soaking for 24 hours, depending on the aggregate pore system. In contrast, most normal weight aggregates will absorb less than 2 percent moisture. The moisture content in a normal weight aggregate stockpile, however, may be as high as 5 percent or more. The important difference is that the moisture content with lightweight aggregates is absorbed into the interior of the particles, as well as on the surface, while in normal weight aggregates it is largely surface moisture. This difference becomes important for mixture proportioning, batching, and control of concrete. Depending on the aggregate pore characteristics, the rate of absorption in lightweight aggregates is another factor that has a bearing on mixture proportioning, handling, and properties of concrete. The water, which is internally absorbed in the lightweight aggregate, is not immediately available to the cement and should not be counted as mixing water or considered in the water/cementitious material ratio calculations. Therefore, a tilt-up panel made of lightweight concrete may weigh more than expected at the time of lifting since it may have more water in the aggregate than considered.

The water-cementitious material ratio (w/cm) describes the mass of water divided by the mass of cementitious material in a concrete mix. Concrete 28-day compressive strength is directly influenced by the w/cm ratio (Kosmatka & Wilson, 2017). Higher w/cm ratios yield lower 28-day compressive strengths. The same w/cm ratios are used in mix design of lightweight concrete and normal weight concrete (Embry, 2016). While the ratio is not altered for lightweight concrete, more water must be used in lightweight mixes to achieve the same strength due to the lower density of LWAs. The water content in a lightweight mix will vary depending on the density of the aggregates used, exposure conditions, and the desired 28-day compressive strength, but lightweight concrete mixes will generally require more water than normal weight mixes. The increase in weight due to water is offset by the reduction in density of LWAs, resulting in a lower overall mix density.

The modulus of elasticity of concrete, E_c, is a function of the moduli of its constituents. Concrete may be considered a three-phase material (aggregates, cement paste, and interfacial transition zone); however, lightweight aggregate concrete may be considered a two-phase material consisting of coarse-aggregate inclusions within a continuous mortar fraction that includes cement paste, entrained air, and fine aggregate. For this reason, it is relevant to consider the lightweight aggregate modulus of elasticity and its influence in the modulus of elasticity on concrete. One approximation to assess lightweight aggregate modulus of elasticity is to use dynamic measurements on aggregates alone, which have shown a relationship corresponding to the function $E = 0.008p^2$ (Bremner and Holm 1986), where E is the dynamic modulus of elasticity of the particle, in psi, and p is the dry mean particle density in lb/ft^3. Dynamic moduli for typical expanded aggregates have a range of 1.45 to 2.3×10^6 psi, whereas the range for strong normal weight aggregates is approximately 4.35 to 14.5×10^6 psi (Muller-Rochholz 1979).

The modulus of elasticity of concrete depends on the relative amounts of paste and aggregate and the modulus of each constituent (LaRue 1946; Pauw 1960). Normal weight concrete has a higher E_c than lightweight concrete because the moduli of sand, stone, and gravel are greater than the moduli of lightweight aggregate. Figure 2-1 gives the range of modulus of elasticity values for lightweight concrete. Generally, the modulus of elasticity for lightweight concrete is considered to vary between 50 and 75 percent of the modulus of sand and gravel concrete of the same strength. Variations in lightweight aggregate grading usually have little effect on modulus of elasticity if the relative volumes of cement paste and aggregate remain constant.

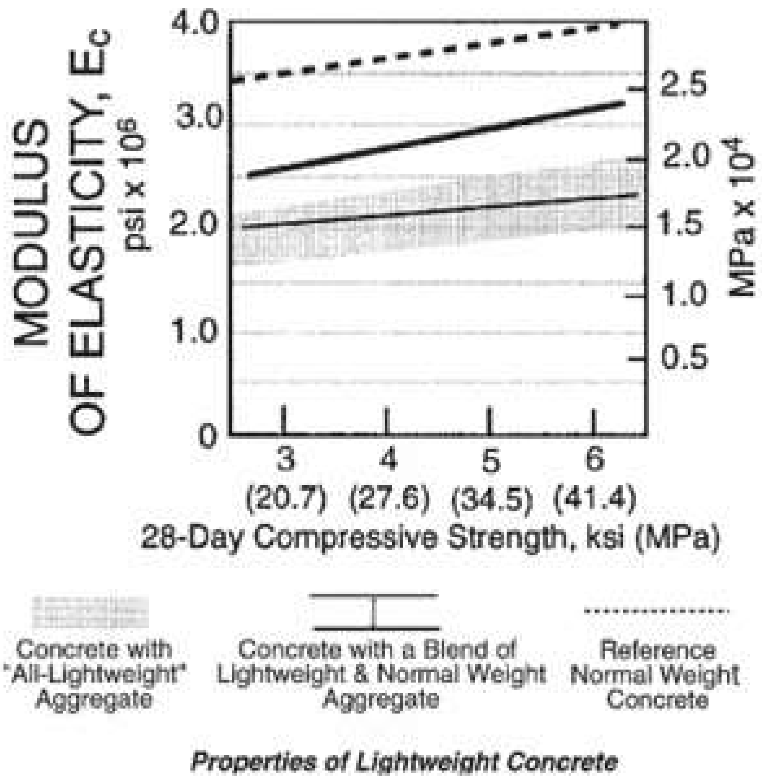

Figure 2-1: Concrete Modulus of Elasticity, adapted from (ACI Committee 213, 2014)

While most researches agree the modulus of elasticity of concrete depends on its density and compressive strength as expressed by the equation for E_c given in ACI 318, some research has shown that such formulas may not adequately represent the relationship between density and compressive strength and the modulus of elasticity. Russell (2009) analyzed the material properties of lightweight concrete for structural design. The modulus of elasticity, E_c, is currently calculated in the American Association of State Highway and Transportation Officials (AASHTO) Load Factor Resistance Design (LRFD) Bridge Design Specification as:

$$\boldsymbol{E_c = 33,000K_1 w_c^{1.5}\sqrt{f'_c}} \qquad (2\text{-}1)$$

Where: K_1, the correction factor for source of aggregate, is taken as 1.0 unless determined by a physical test, w_c is the unit weight of concrete (pcf), and f'_c is the minimum specified compressive strength of concrete (psi). Based on a project conducted by the National

Cooperative Highway Research Program (NCHRP), 4,388 data points where collected and analyzed to recommend a change in the original modulus of elasticity equation. Russell proposed a new equation, Equation 2-2, which is assumed to provide a more accurate representation of the true modulus of elasticity based on the research data.

$$\boldsymbol{E_c = 310{,}000 K_1 w_c^{2.5} f_c'^{0.33}} \qquad (2\text{-}2)$$

Cook (2007) has developed a new formula for modulus of elasticity that provides a better estimate of lightweight concrete and high-strength concrete than the following equation.

$$\boldsymbol{E_c = w_c^{2.687} (f'_c)^{0.24}} \qquad (2\text{-}3)$$

The formula has proven that it may be used for values of w_c between 100 and 155 lb/ft^3 and strength levels of 1000 to 23,000 psi. Concretes in service may deviate from this formula; thus, when an accurate evaluation of E_c is required for a particular concrete, a laboratory test in accordance with the methods of ASTM C469/C469M should be used to determine the modulus of elasticity of the concrete. The accurate value of the modulus of elasticity is significant in the flexural stiffness determination.

In addition, data from several sources, Messenger et al. (2005), Heffington (2000), Hoff (1992), Malhotra (1990), Meyer (2002), Ozyildirim & Gomez (2005), Ramirez, Olek, & Malone (2000), Shideler (1957), and Tasillo, Neeley, & Bombich (2004), was analyzed by Russell (2009) to determine an equation for the modulus of rupture. The modulus of rupture, f_r, was recommended to be taken as $0.21\sqrt{f_c'}$ for moist cured lightweight concrete with a compressive strength of 3.0 ksi to 9.0 ksi. For dry-cured lightweight concrete, no satisfactory correlation was made as the modulus of rupture varies greatly with the conditions of the environment. Dry-cured lightweight concrete develops tensile stresses at the surface, which alters the modulus of rupture.

Dry-cured is the scenario for lightweight concrete used as site cast tilt-up panels where moist cured is used in precast plants.

Additional consideration is bond strength. ACI 318 includes a factor for development length of 1.3 to reflect the lower tensile strength of lightweight aggregate concrete and allows that factor to be taken as $6.7\sqrt{f'_c}/f_{ct} \geq 1.0$ if the average splitting strength f_{ct} of the lightweight aggregate concrete is specified. In general, design provisions require longer development lengths for lightweight-aggregate concrete. Due to the lower strength of the aggregate, lightweight concrete should be expected to have lower tensile strength, fracture energy, and local bearing capacity than normal weight concrete with the same compressive strength which result in lower bond strength of bars cast in lightweight concrete (Shideler 1957). In other words, longer development lengths are required when lightweight concrete is used.

Shrinkage, either autogenous or drying, is an important property that can affect the extent of cracking, effective tensile strength, and warping. ACI 213R-14 indicates that large size concrete members might undergo substantially less shrinkage than that exhibited by small laboratory specimens stored at 50 percent relative humidity. Low-strength lightweight concrete generally has greater drying shrinkage than the normal weight concrete.

Ultimate strain is important for the design of concrete tilt-up walls governed by flexural tension. Figure 2-2 gives a range of values for ultimate compressive strain for concrete containing both coarse and fine lightweight aggregate and for normal weight concrete. These data were obtained from unreinforced specimens eccentrically loaded to simulate the behavior of the compression side of a reinforced beam in flexure (Hognestad, Hanson, & McHenry, 1955). The diagram indicates that the ultimate compressive strain of most lightweight concrete may be slightly greater than the value of 0.003 assumed for design purposes.

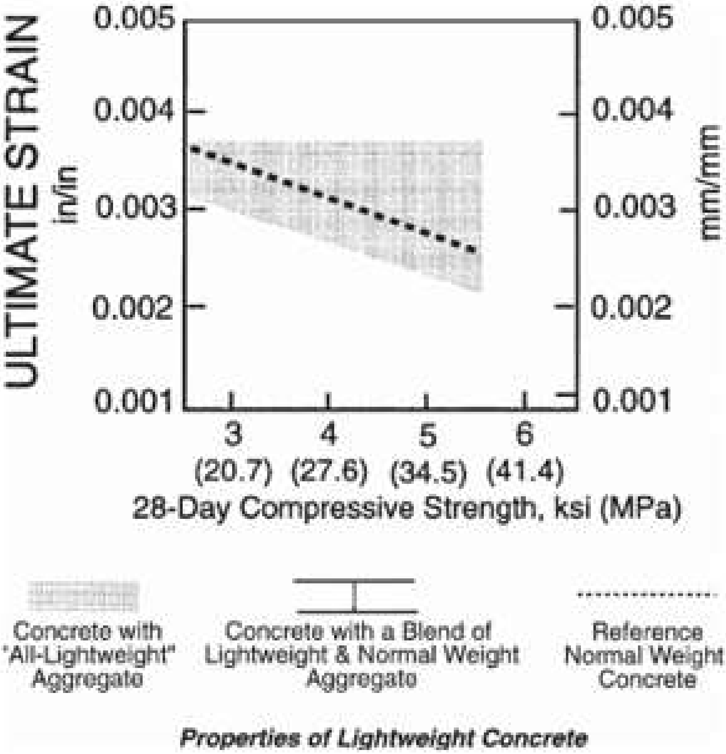

Figure 2-2: Ultimate Strain, adapted from (ACI Committee 213, 2014)

2.2 Previous Test Results

The *Report of the Task Committee on Slender Walls* (Simpson et al., 1982) was written to analyze the performance of slender concrete and masonry walls under lateral and axial loads. This thesis focuses on the concrete tilt-up portion of the *Report of the Task Committee on Slender Walls*. Twelve reinforced concrete panels of various slenderness ratios were tested.

The concrete used for the testing of the tilt-up panels used a 0.67 water/cement ratio. The mix consisted of 470 lbs of Portland cement, 1,420 lbs (~14 cu. ft.) of washed concrete sand, 1,815 lbs (~18 cu. ft.) of 1-in. gravel, and 317 lbs (38 gal.) of water. The 7-day compressive strength as provided by Conrock, the concrete supplier, of the concrete was given as 2,282 psi and the 28-day compressive strength was given as 3,181 psi. In addition, Twining Laboratories tested the concrete mix using 16 cylinders and 6 concrete beams. The results at 7-days, 28-days, and 167-days (job cured) are shown in Table 2-1.

Table 2-1: Twining Laboratories Concrete Test Results

	7-Day (psi)	28-Day (psi)	167-Day (psi)
Compressive Strength	2,300	3,225	4,009
Modulus of Elasticity	-	3,360,000	3,540,000
Splitting Tensile Strength	270	355	-
Modulus of Rupture	-	695	520

The reinforcing steel used for the vertical reinforcement was Grade 60 and was provided by Bethlehem Steel with a reported yield strength of 72,250 psi and an ultimate tensile strength of 102,750 psi. Samples of the steel were sent to Twining Laboratories which gave test results of a yield strength of 67,500 psi and an ultimate yield strength of 102,000 psi. The average yield strength was given was 70,000 psi. The elongation of an 8 in. sample was 17%. The bars had a measured modulus of elasticity of 28.6 x 10^6 psi. The vertical reinforcement was used in full length without any splices. The vertical reinforcement resists the axial and flexural loads placed on the slender wall.

The horizontal reinforcing steel chosen was Grade 40 steel, with a mill reported yield strength of 52,730 psi and an ultimate tensile strength of 75,910 psi. Samples sent to Twining Laboratories were tested and showed a yield strength of 52,000 psi and an ultimate tensile strength of 79,100 psi. The elongation in an 8” bar was measured at 18%, and the modulus of elasticity reported was 28.0 x 10^6 psi.

The tests performed for the *Report of the Task Committee on Slender Walls* used full-scale wall panels with the intent to have an accurate representation of the wall slenderness, the P∆ effect, and the moment eccentricity. The panels constructed were 4’-0” wide, 24’-8” high, and had a bearing elevation (unbraced length) of 24’-0”. Four different thicknesses were constructed to evaluate slenderness ratios ranging from 30 to 60. The four thicknesses chosen were 4-3/4", 5-3/4", 7-1/4", and 9-1/2", representing slenderness (h/t) ratios of 60, 50, 40, and 30 respectively. Three tilt-up wall panels of each thickness were constructed and tested.

To provide a true pin support connection, the wall panels were constructed with a base of half of a 4 in. pipe welded to a ½ in. base plate, refer to Figure 2-5. These supports were attached to the panels through three 1'-8" #4 dowels. The pin connection allowed the panels to have zero moment at the base. The support used at the top of the panels was designed to prevent lateral translation, but allow rotation and vertical translation. 6" x 6" x 3/8" angles were used for the bearing on the panels and were attached using four ¾" bolts.

The wall panels were cast with the exterior face down with ledger bolts protruding from the exposed face. The 4-3/4" thick and 5-3/4" thick panels used four continuous #4 bars for vertical reinforcement and #3 bars spaced at 2'-0" on center for horizontal reinforcement. The 7-1/4" thick and 9-1/2" thick panels used four continuous ½" #4 bars for vertical reinforcement and #4 bars spaced at 2'-0" on center for horizontal reinforcement. Once the panels had been cast, they were lifted and stored on the long edge for a drying period of 160 days before being lifted into their final resting position on the pin-supported surface.

After the panels had been tested, the panels were broken apart in the middle-third of the panel height and the distance between the reinforcing steel and the loading face was measured. The data measured is shown in Table 2-2. The discrepancies between the distance measured and the design distance may increase or decrease the capacity of the wall panels. These discrepancies are adjusted for through the Φ factor (ACI 318-19 Equation 11.8.3.1d) during design.

Table 2-2: Placement of Steel Reinforcement

Panel No.	Nominal Thickness	Measured Thickness (in.)	Distance (d) from Outer Wall Face to Center Line of Steel (in.)					Variation in d	
			Bar #1	Bar #2	Bar #3	Bar #4	Ave. d	%	in.
19	9.5	9.60	4.67	5.24	4.48	4.24	4.66	3%	0.14
20	9.5	9.40	4.76	4.59	4.70	4.76	4.70	0%	0.00
21	9.5	9.50	4.40	4.60	4.70	4.80	4.63	3%	0.13
22	7.25	7.40	3.88	4.00	4.13	4.38	4.10	11%	0.40
23	7.25	7.34	2.85	3.35	3.48	3.48	3.29	10%	0.38
24	7.25	7.38	4.80	4.70	4.30	4.30	4.53	23%	0.84
25	5.75	6.13	3.70	3.80	3.70	3.60	3.70	21%	0.64
26	5.75	5.88	3.40	3.70	3.80	3.60	3.63	23%	0.69
27	5.75	6.00	3.38	3.50	3.25	3.25	3.35	12%	0.35
28	4.75	4.82	2.21	2.45	2.86	2.74	2.57	6%	0.16
29	4.75	4.78	2.46	2.58	2.90	3.16	2.78	16%	0.39
30	4.75	4.89	2.24	2.37	2.66	2.92	2.55	4%	0.10

The intent for the tests performed on the wall panels was to determine the effect of lateral deflection on the stability of walls subjected to vertical and lateral loading. The walls were tested in the upright position to allow for the self-weight of the walls to be included in the vertical gravity loads.

A welded steel trussed frame was used to apply the loading and provide the support for the top of the wall. To apply lateral loads to the wall panels, an air bladder was used. A wooden structure of plywood was secured to the face of the frame to provide support for the air bladder. The wall panels were held in place against the bladder using a 1” threaded rod at each corner of the wall panel attached to the steel frame. These threaded rods were welded to a 6” x 3” x ¼” rectangular steel tube across the base of the outer wall face to resist the lateral force applied by the bladder. A lever system was used for vertical loading. For safety measures, loose cables were attached to the top of the walls and to outriggers to minimize risk in the event of rupture. Also included in the steel frame was a ladder and work platform to safely make attachments at the top of the wall.

The steel frame rested on wheels for mobility. Figure 2-3 indicates the side elevation of the test setup, and Figure 2-4 shows a picture taken of the test setup in use.

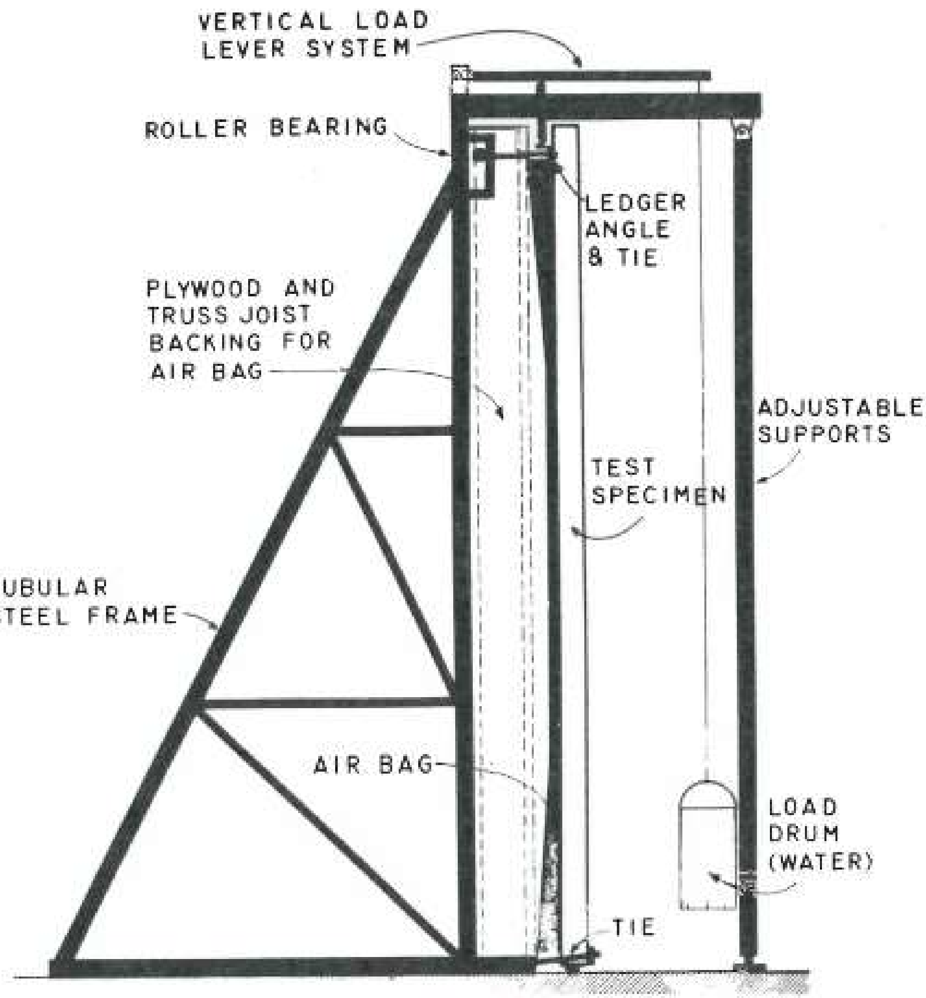

Figure 2-3: Loading Frame for the *Report of the Task Committee on Slender Walls*, adapted from (Simpson et al., 1982)

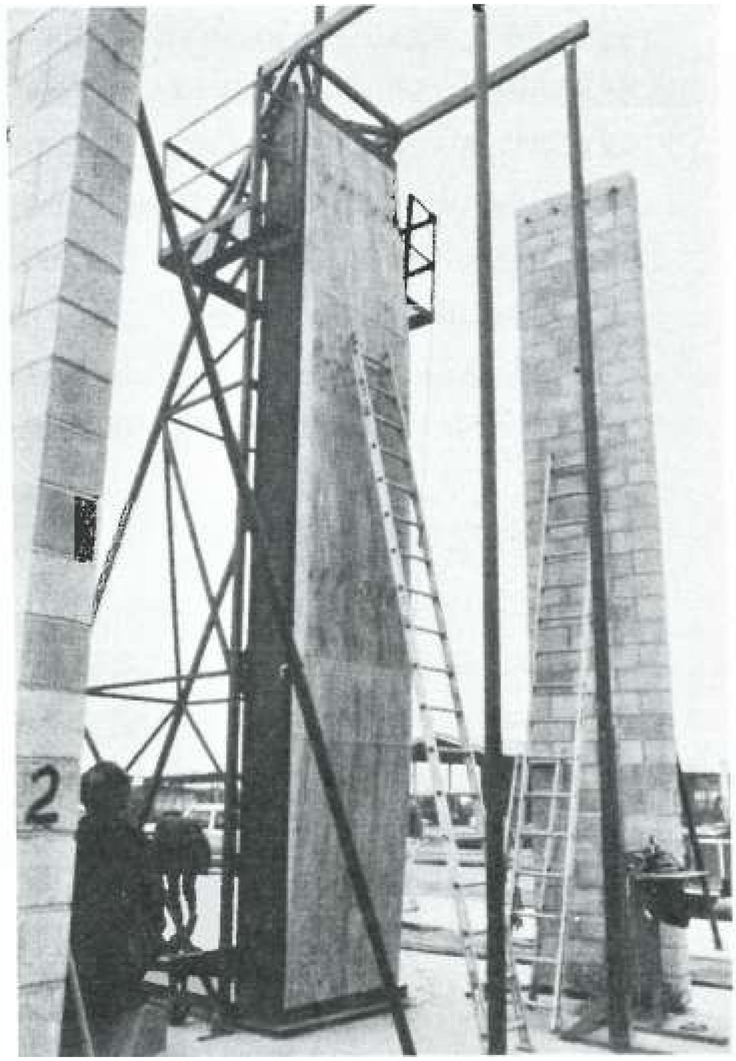

Figure 2-4: Loading Frame Showing Scab Plywood Forming to Conform to the Loaded Panel for the *Report of the Task Committee on Slender Walls*, adapted from (Simpson et al., 1982)

For applying vertical loads at the top support, a 6” x 4” x 3/8” steel ledger angle which was embedded in the wall panel was welded to the threaded rods. To allow for vertical and angular moment, the threaded rods for the top support were attached to the steel frame via a roller bearing, as shown in Figure 2-5.

The safety cables used for protection in the event of rupture consisted of two loops of light steel cable passing through a connection at each edge of the ledger angle. These safety cables prevented the walls from falling during rupture of the wall panels.

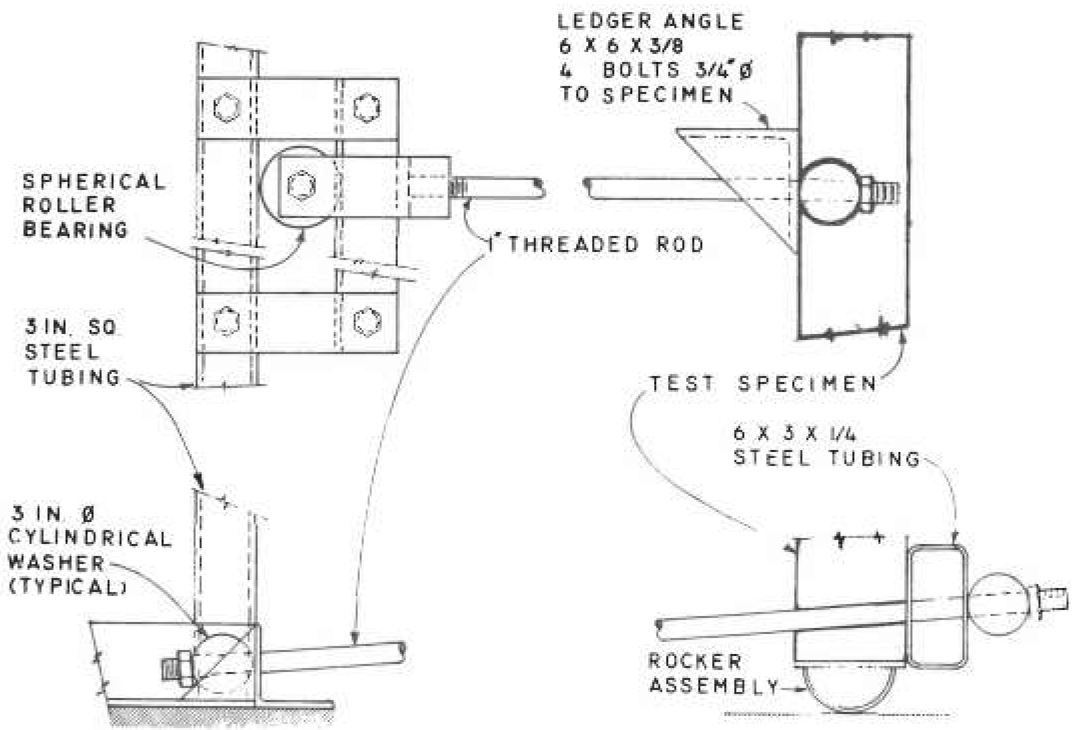

Figure 2-5: Ties to Test Frame for the *Report of the Task Committee on Slender Walls*, adapted from (Simpson et al., 1982)

The vertical loads were applied through a lever system, which pivoted at the top of the main frame. Two lever arms were used to apply loads. Steel drums were attached to the lever arms and filled with water to achieve a desired vertical load. The uniformly distributed lateral load was applied to the wall panel through the air bladder. The air bladder was composed of a 20-millimeter vinyl material with welded seams and an exterior layer of 22 ounce vinyl-coated nylon with sewed seams. The bag measured 18” x 48” x 24’. The bag had two openings, one for inflation, and one for pressure readings which was located on the opposite end of the bag. Grommeted flaps were used to attach bag to the outriggers from the steel frame.

The wall panels were held in place before testing with telescoping pipe bracing anchored into the floor. Once the wall was in place and attached to the frame, the bracing was removed for testing. After testing, the bracing was installed again, the steel frame was detached, and the wall remained in its upright position until multiple walls could be removed at once.

Air pressure was applied by inflating the bag with a ½ HP compressor. A pressure regulator was provided, but a needle valve was primarily used for control of inflation. The pressure within the bag was measured by a double water tube manometer. After a few trial tests had been performed, the double water tube manometer was replaced with a single tube manometer. The equipment used for pressure measurements is shown in Figure 2-6. A vacuum cleaner was used to assist with deflation.

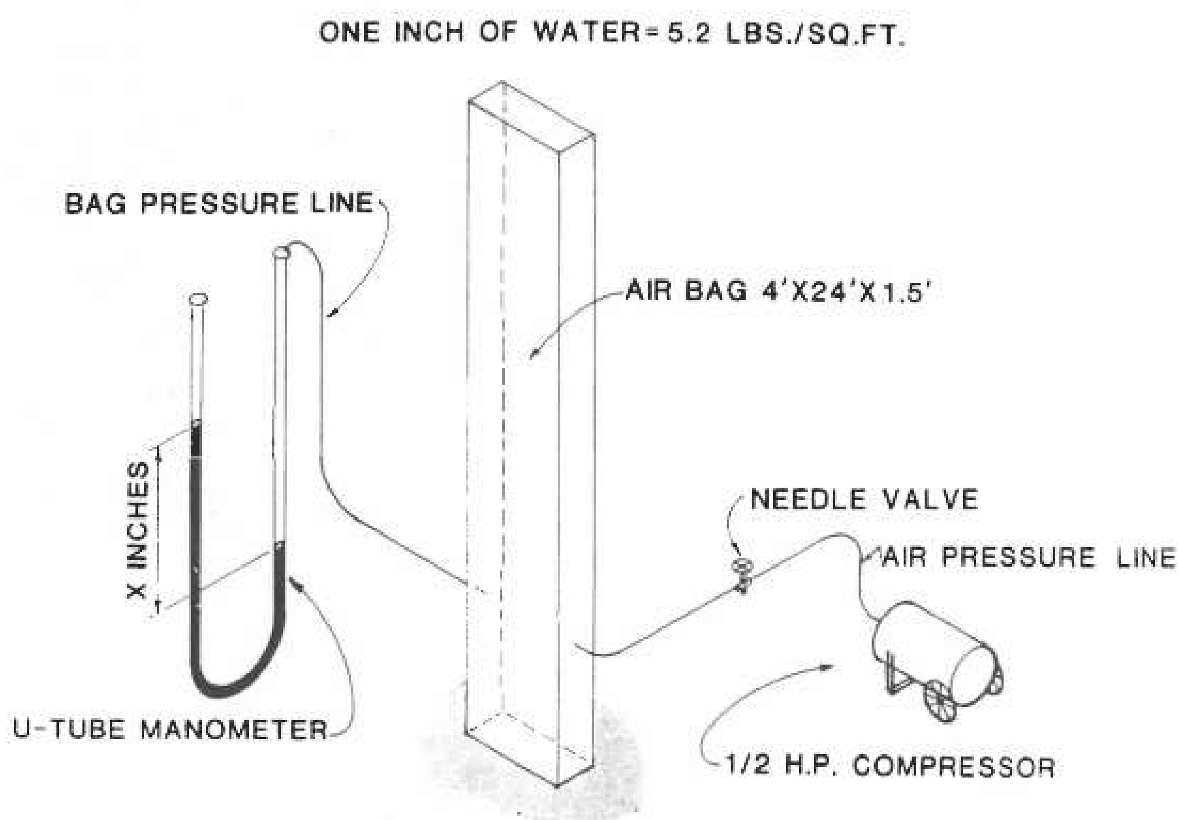

Figure 2-6: Schematic of Lateral Load System for the *Report of the Task Committee on Slender Walls*, adapted from (Simpson et al., 1982)

Deflection measurements were taken at each support of the walls and at tenth points to determine the deflected shape using three test methods. The first method used yardsticks attached to the walls and deflections were observed through a transit sight parallel to the wall panel (Figure 2-7). These readings were accurate to the nearest 1/16". The second method used dial gages which were calibrated in thousandths of an inch and had a max reading of 3". The dial gages were supported by a steel pylon independent of the test frame. Nylon coated steel wire tension line connected the gages to the wall to prevent damage to the equipment. The data from these gages was not used because the deflection in the panels exceeded the 3" travel and because reading the gages from a distance using a telescope was inefficient. The third and final method used to measure deflection consisted of a steel wire tension line from the wall which was wrapped around a capstan pulley that was mounted on the shaft of a ten-turn precision potentiometer. This allowed measurements of a range of about 50" with accuracy of 0.02". A test of this system over 2' proved that this system was accurate and repeatable. During testing, electrical leads from 11 electric displacement transducers were taken from the reference pylon. These electrical leads led to a switch box and digital voltmeter with .001 volt precision (Figure 2-8). This system was used as the primary source of measurement, but transit readings using the first method were taken for accuracy verification. The displacement measurements were recorded with the time and temperature at set intervals during loading and unloading of the wall panels.

Figure 2-7: Securing Yardstick to Side of Panel for the *Report of the Task Committee on Slender Walls*, adapted from (Simpson et al., 1982)

While displacement control was attempted to be used to control the loading, load control was primarily used. Load increments decreased as the maximum load was approached. Loads were applied monotonically until the panels were nearing failure, with displacement measurements being read as quickly as possible. The average loading period for each wall panel was two hours, while the entire testing process, including setup, usually average one day per panel.

While thirty wall panels were tested, this review focuses on the results from the twelve concrete tilt-up panels. Mid-height readings were taken for deflection measurements. Table 2-3 lists the test results for deflection for different applied loads. Figures 2-9 through 2-12 show the maximum lateral loads in load deflection test curves. These curves do not account for a

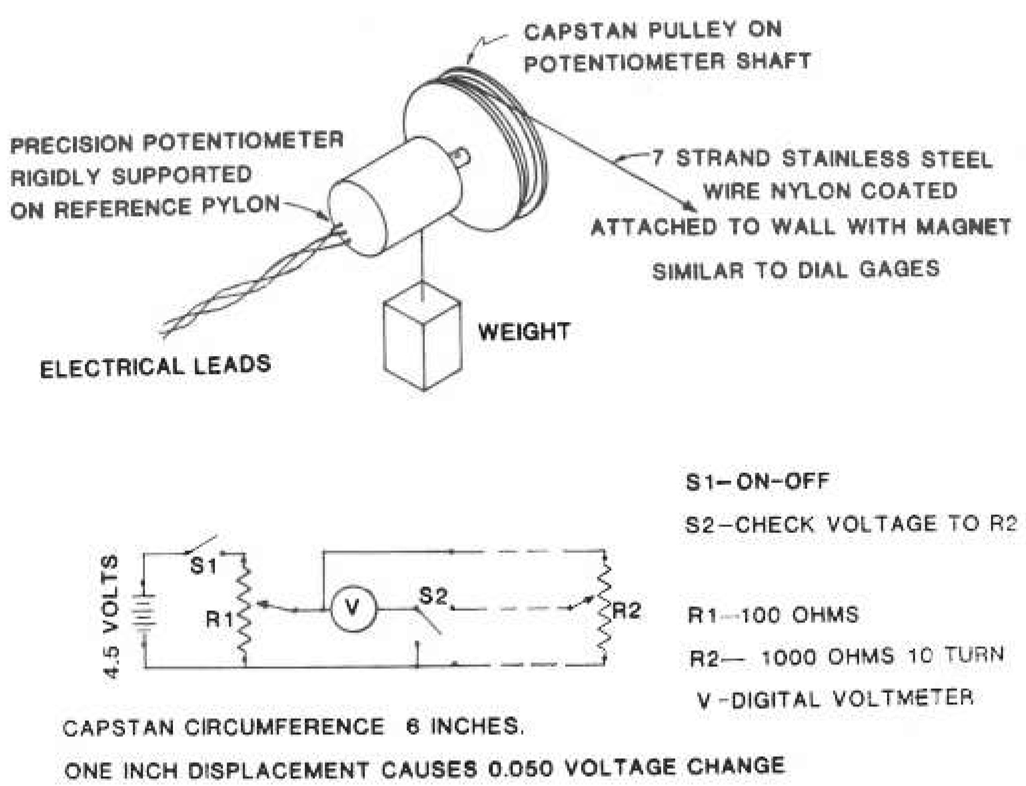

Figure 2-8: Electrical Displacement Transducer for the *Report of the Task Committee on Slender Walls*, adapted from (Simpson et al., 1982)

correction due to the loss of contact between the air bag and the test panel when the deflections exceeded 7” to 8”. Figure 2-13 shows a curve including these corrections. A sharp break at the cracking moment and a change in slope at yield moment is observed in these curves. Cracks in the tilt-up wall panels were spaced apart by approximately two times the panel thickness at maximum deflection.

Table 2-3: Slender Walls Test Results for the *Report of the Task Committee on Slender Walls*

Wall No.	t (in.)	f'c (psi)	h/t	Vertical Load (plf)	Lateral Load at f_y (psf)	Deflection at Yield (in.)	Lateral Deflection (in.)
19	9.5	4000	30.3	320	87	7.3	9.9
20	9.5	4000	30.3	320	83	5.3	7
21	9.5	4000	30.3	320	83	7.5	12.3
22	7.25	4000	39.7	320	57	5.4	12.2
23	7.25	4000	39.7	320	52	7.4	11.8
24	7.25	4000	39.7	860	57	7.6	11.8
25	5.75	4000	52.4	860	51	8.1	13.2
26	5.75	4000	52.4	860	42	7.2	11.1
27	5.75	4000	52.4	320	42	7.6	12.4
28	4.75	4000	60.6	320	32	11.6	13
29	4.75	4000	60.6	320	34	12.6	19.2
30	4.75	4000	60.6	320	34	13.1	15.2

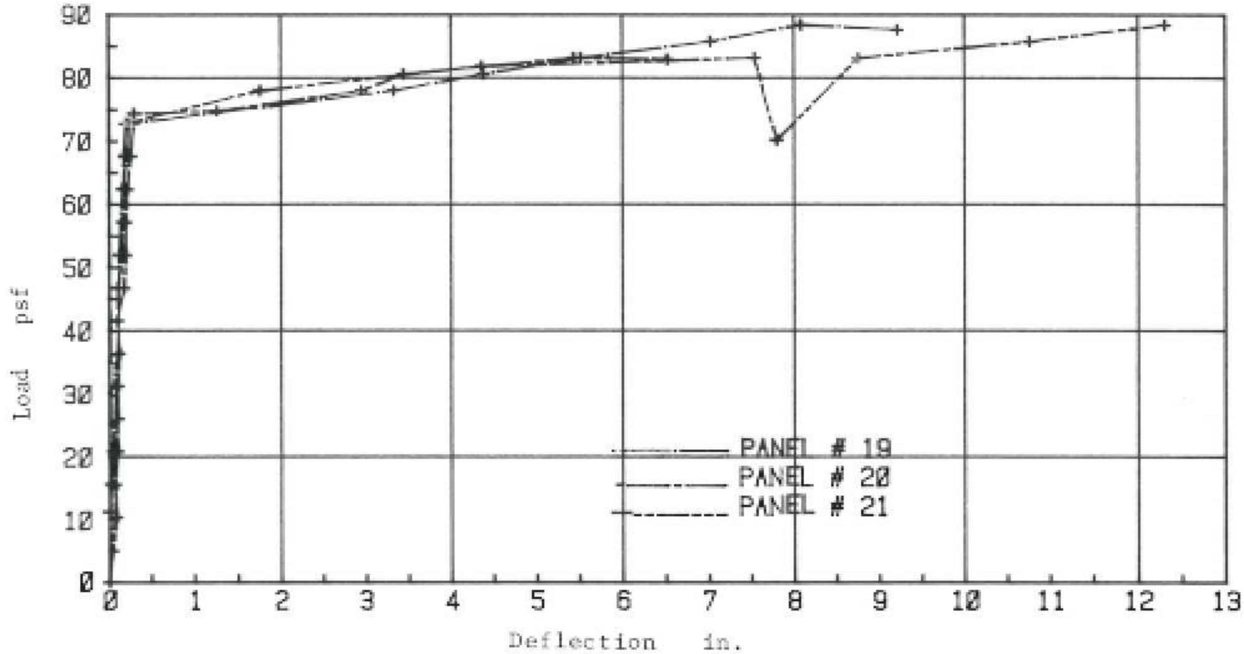

Figure 2-9: Load-Deflection Curves, 9.50" Concrete Tilt-Up Panel for the *Report of the Task Committee on Slender Walls*, adapted from (Simpson et al., 1982)

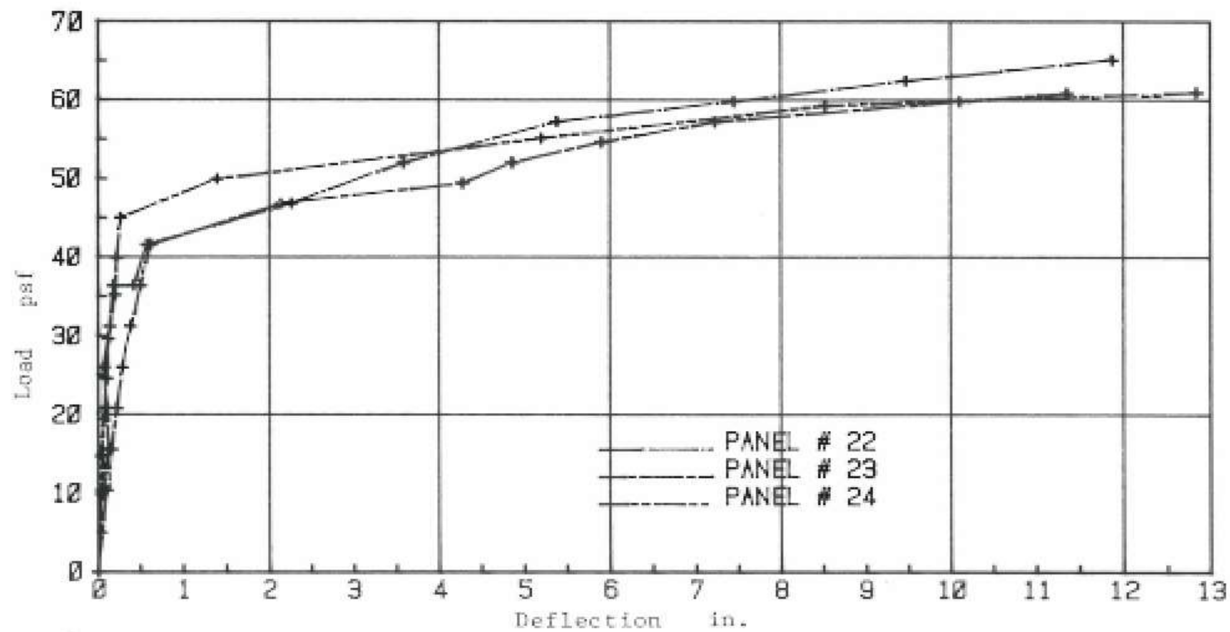

Figure 2-10: Load-Deflection Curves for 7.25" Concrete Tilt-Up Panels for the *Report of the Task Committee on Slender Walls*, adapted from (Simpson et al., 1982)

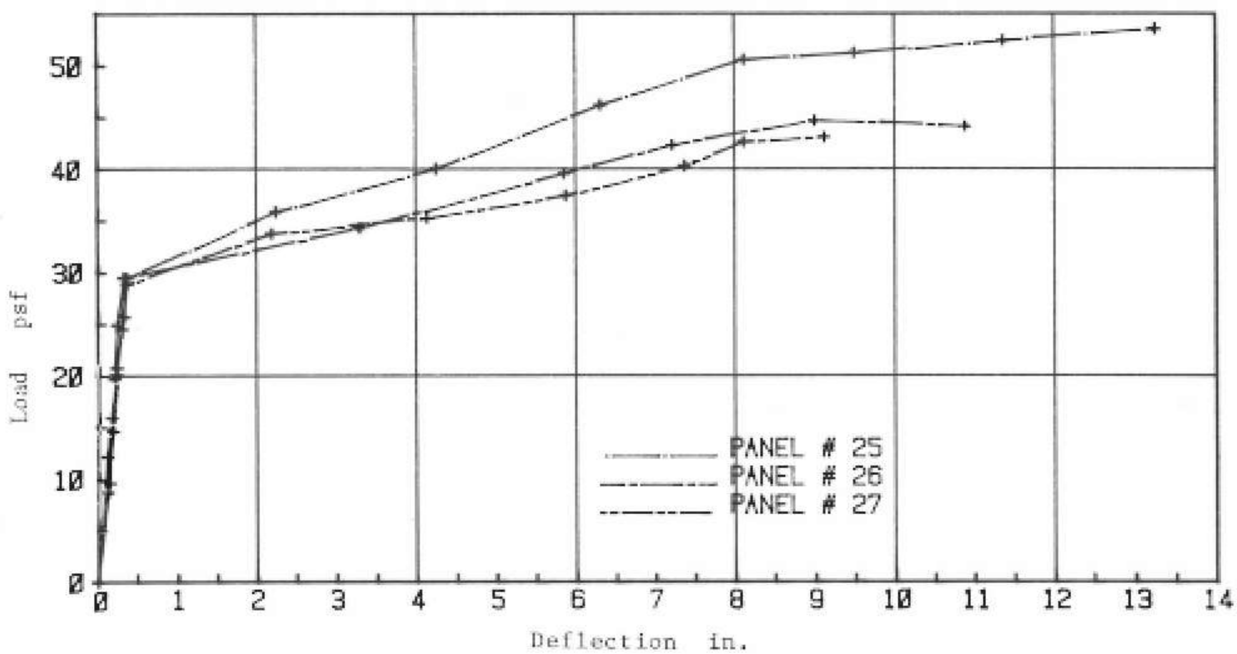

Figure 2-11: Load-Deflection Curves for 5.75" Concrete Tilt-Up Panels for the *Report of the Task Committee on Slender Walls*, adapted from (Simpson et al., 1982)

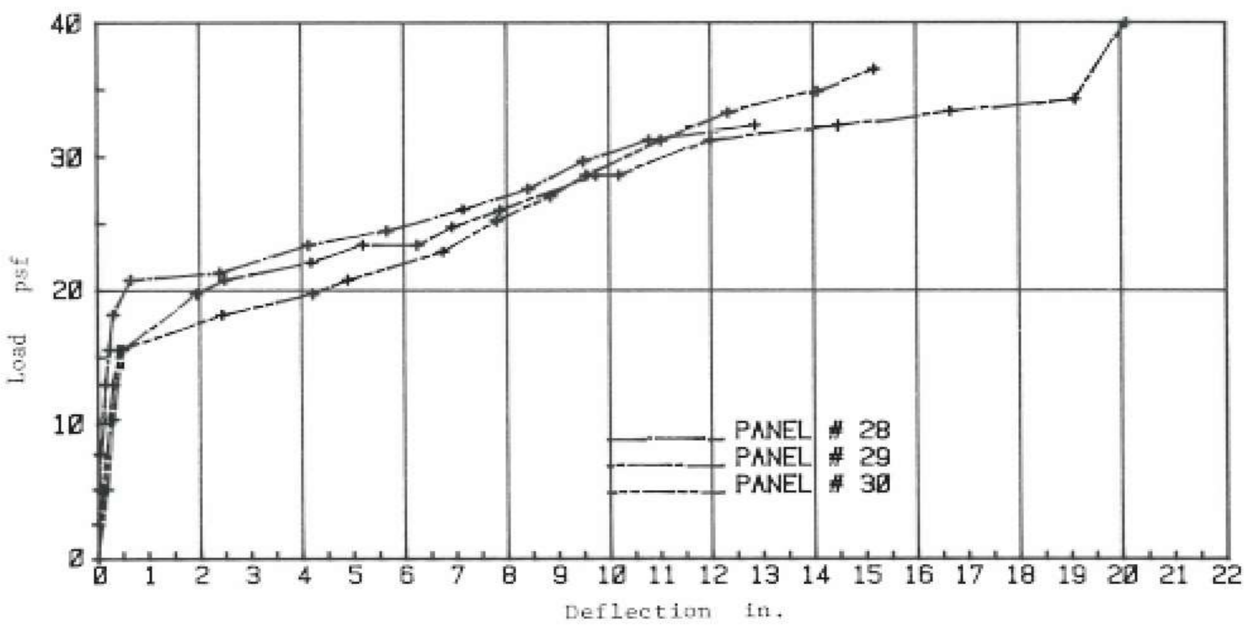

Figure 2-12: Load-Deflection Curves for 4.75" Concrete Tilt-Up Panels for the *Report of the Task Committee on Slender Walls*, adapted from (Simpson et al., 1982)

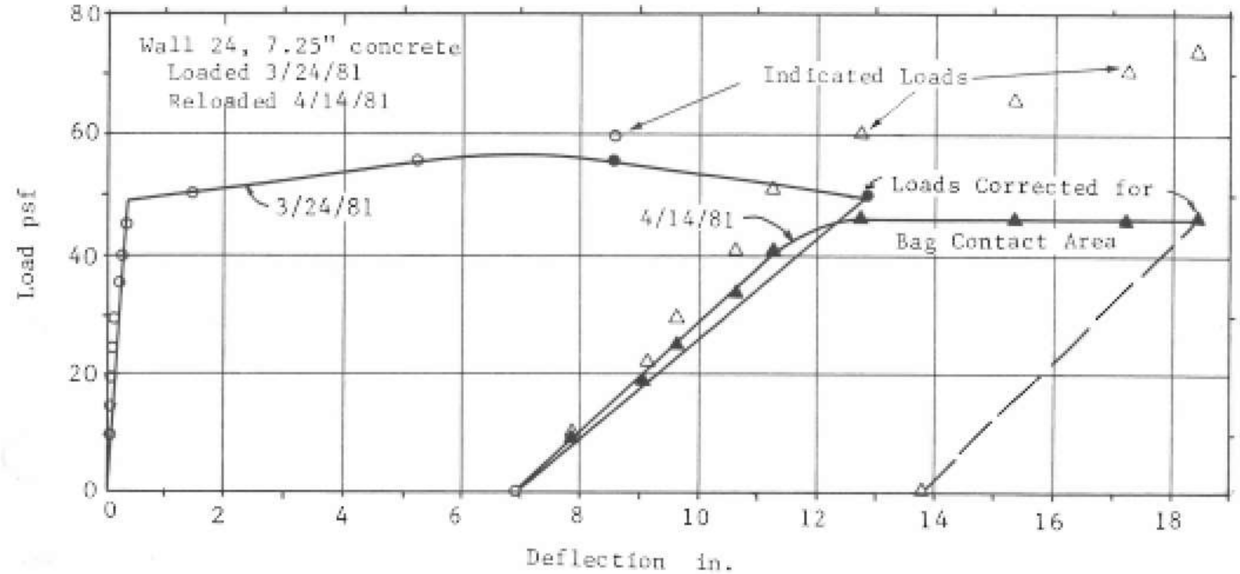

Figure 2-13: Loss of Contact Correction for Tilt-Up Panels for the *Report of the Task Committee on Slender Walls*, adapted from (Simpson et al., 1982)

No elastic or inelastic lateral instability of the wall panels was observed during the tests. The wall panels were able to resist lateral loading well beyond the deflection at which the steel yielded. The results from the load deflection measurements indicate that the wall panels can resist 50% to 90% of their weight laterally, depending on the h/t ratio (Figure 2-14). The *Report of the Task Committee on Slender Walls* also noted that lateral resistance was increasing even when deflections were very large and that this was likely due to strain hardening in the reinforcement.

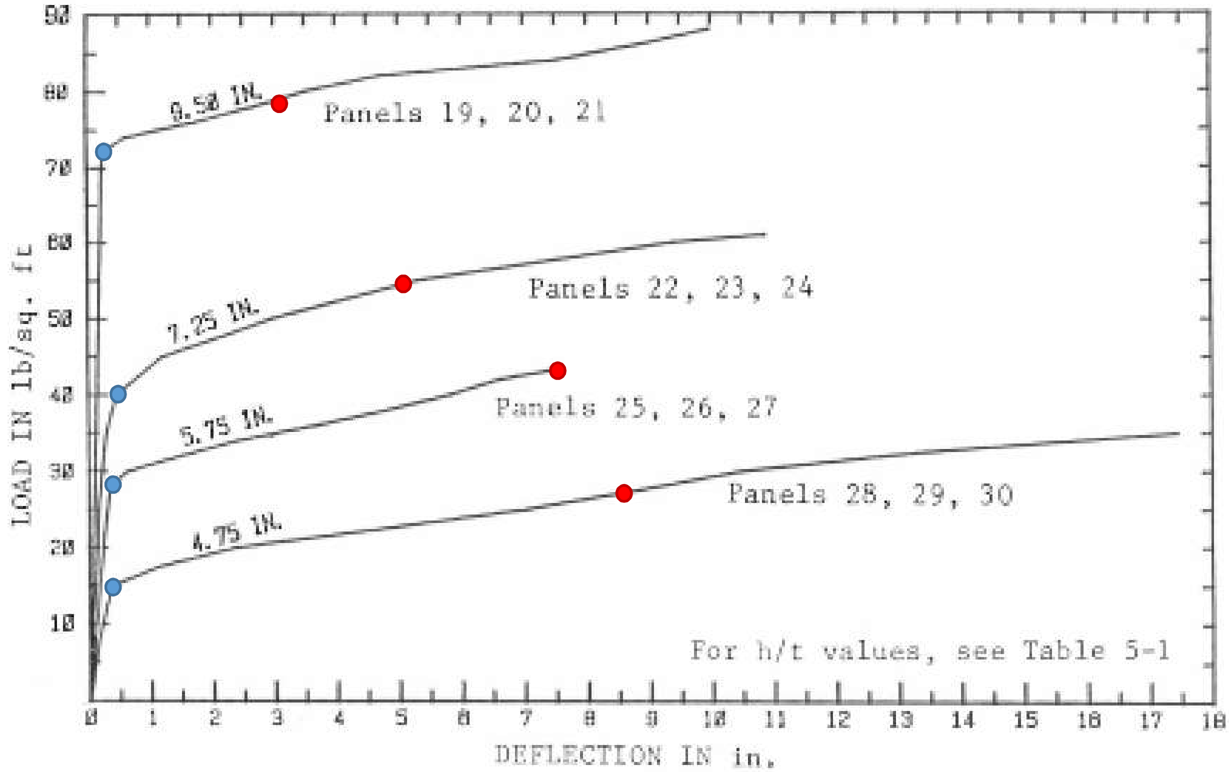

Figure 2-14: Load-Deflection Curves Slenderness Comparison for the *Report of the Task Committee on Slender Walls*, adapted from (Simpson et al., 1982)

The initial vertical incline shown in Figure 2-14 occurs due to the initial panel stiffness, E_cI_g, before the panels reached their cracking moment. The *Report of the Task Committee on Slender Walls* indicated that the tilt-up panels yielded at approximately 3" for the 9-1/2" panels, 5" for the 7-1/4" panels, 7-1/2" for the 5-3/4" panels, and 8-1/2" for the 4-3/4" panels. Panel yielding is shown in Figure 2-14 in red and panel cracking is shown in blue. Panel yielding occurs when the tilt-up panel has reached its nominal moment capacity. All of the wall panels experienced cracking due to the modulus of rupture at a deflection of less than ½". While the load at which the panels cracked increased with the panel thickness, the thinner panels experienced a larger increase in load capacity from cracking to yield when compared with the thicker panels. This is due to all panels using the same reinforcement, so the percentage of reinforcement in each panel was determined by the thickness, with the thinnest panels having the largest percentage of reinforcement. The steel ratios for the panels were 0.393%, 0.461%, 0.515%, and 0.696% for the 9.5”, 7.25”, 5.75”, and 4.75” thick panels, respectively.

The cracking load in the 9-1/2” panel was roughly 90% of the yield capacity, so the increase in capacity between cracking and yielding was 10% of the total yield capacity. In the 7-1/4” and 5-3/4” panels, the increase in capacity from cracking to yielding was 30%. This increase was 40% in the 4-3/4” panels. This further shows that the steel reinforcement is the controlling element in the overall panel performance, and the walls are governed by flexural tension behavior.

As mentioned previously, loss in contact between the air bladder and the wall panels occurred when some of the walls experienced large deflections at mid-point. The *Report of the Task Committee on Slender Walls* determined that this was not a serious concern to the integrity of the test since the loads below yield were unaffected and loads near the panel yield were only slightly affected. The separation distance in wall 21 (thickness of 9.5”) was 3”. For panels 22 through 30, floor positions were marked and the space between the wall and plywood was consistently near the 3” mark. Corrections were made to three of the wall panels, only one of which was a tilt-up panel (panel 29). The corrections are shown in Figure 2-15. The data from the contact area was used to calculate the resulting bending moment. Using the calculated bending moment, the pressure required to for equal moment at midspan for uniform load was determined to be 44.0 psf. The corrected moment and the moment determined from the 44.0 psf uniform load were compared for each foot of height of the panel, resulting in an average ratio of uniform load moment to corrected moment of 0.96. This difference was determined to be negligible.

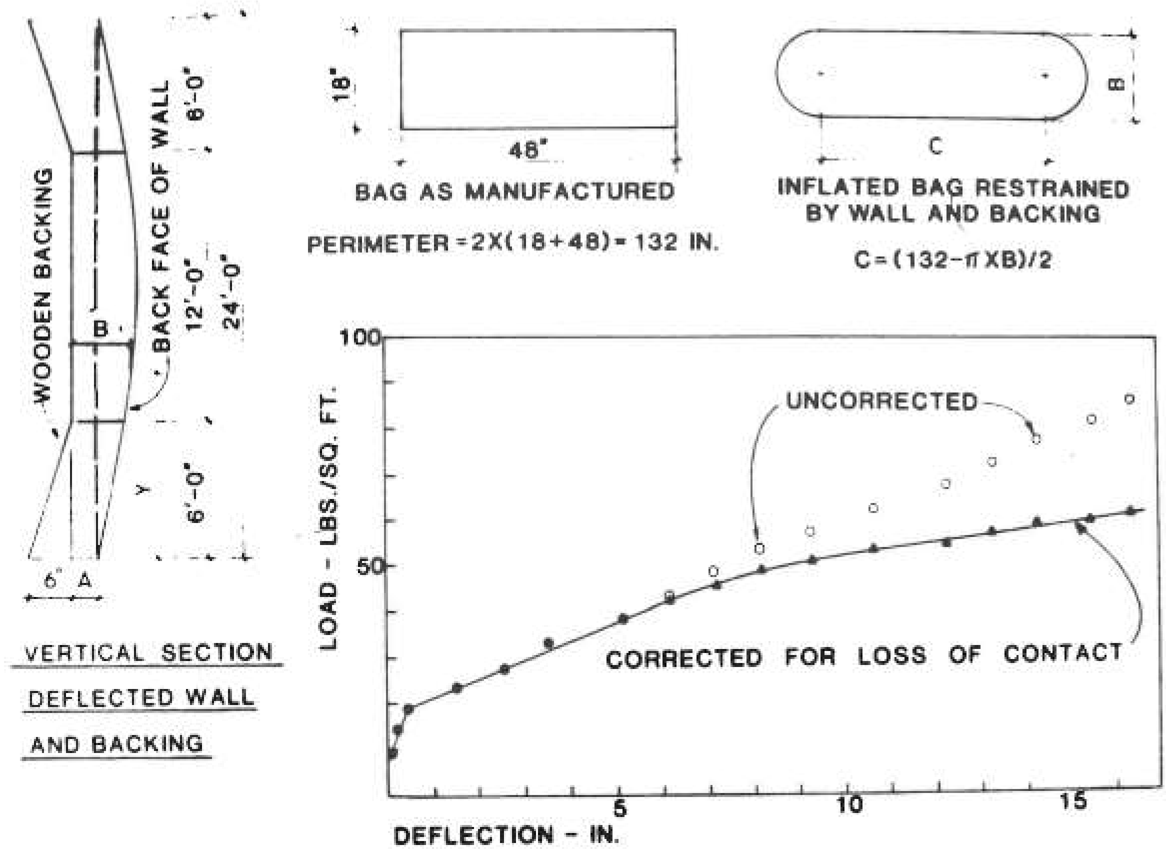

Figure 2-15: Correction for Loss of Contact Between Air Bladder and Wall Panels for the *Report of the Task Committee on Slender Walls*, adapted from (Simpson et al., 1982)

The report stated that crack spacing in reinforced concrete members decreases with increased applied load. The spacing of visible cracks remains constant once stress reaches its critical value. Average minimum crack spacing is larger than the panel thickness, but less than twice the panel thickness. The cracking patterns in one of the concrete tilt-up panels after major deflection are shown in Figure 2-16.

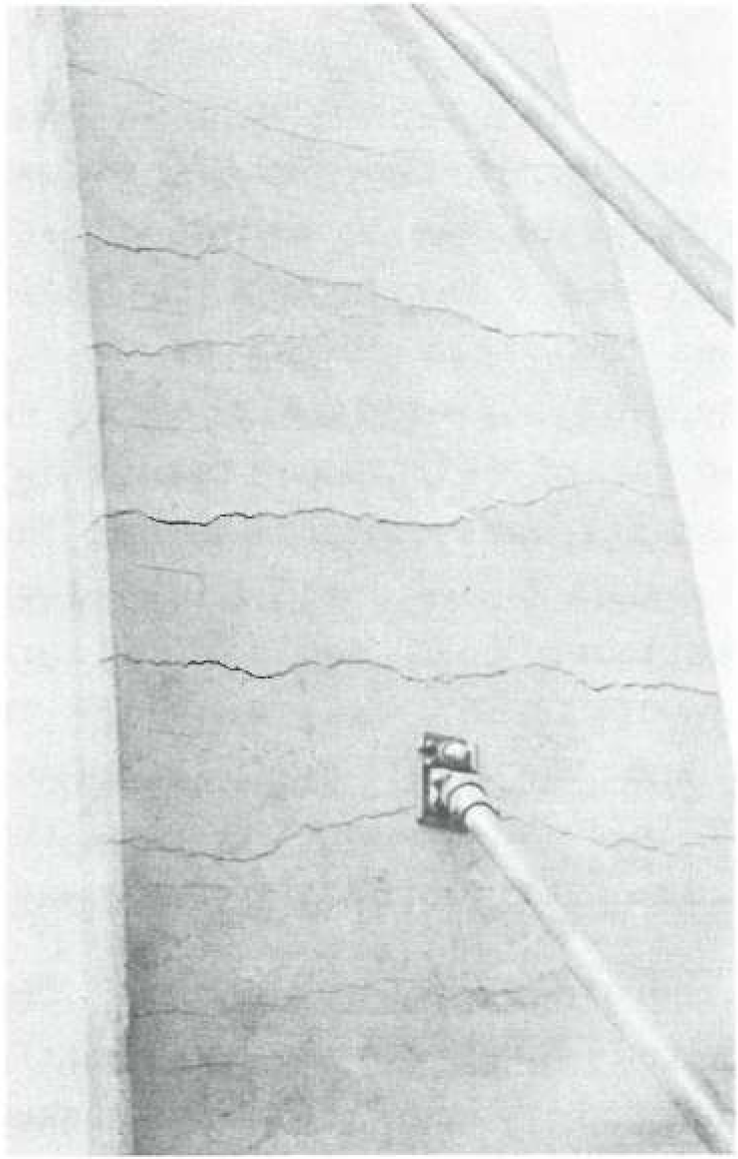

Figure 2-16: Cracking Patterns After Major Deflection for the *Report of the Task Committee on Slender Walls*, adapted from (Simpson et al., 1982)

Two panels (24 and 27) were tested with unloading and reloading. Panel 24 (thickness of 7-1/4") was loaded to a total midspan deflection of 13", or 6" beyond the steel reaching a yield stress of 70ksi. Pressure was released and a rebound of 6" was recorded, leaving a permanent set of 6-3/4". After twenty days, the wall was loaded once more, showing a deflection path showing a slightly steeper deflection path until yielding, where a shallower load deflection curve was recorded. The panel was loaded to a midspan deflection of 18". After the second loading, panel

24 rebounded 6”. Figure 2-17 describes the lateral deflection of the panel during these two tests. Panel 27 (thickness of 5-3/4”) was loaded to a total midspan deflection of 9” and a load of 43 lb, which was just beyond the calculated steel stress reaching yield. After the load was removed, the panel rebounded 5”, with a permanent set of 4”, even though the steel had barely yielded. Only two hours later, the panel was loaded to a lateral load of 40 psf, unloaded to 20 psf, and then loaded once more to the yield level. Once the wall panel had reached yield, it was loaded until a total midspan deflection of 16” was recorded when a lateral load of 45 psf was applied. Figure 2-18 shows a comparison between panels 24 and 27, demonstrating that the twenty-day period between loadings in panel 24 resulted in panel stiffening.

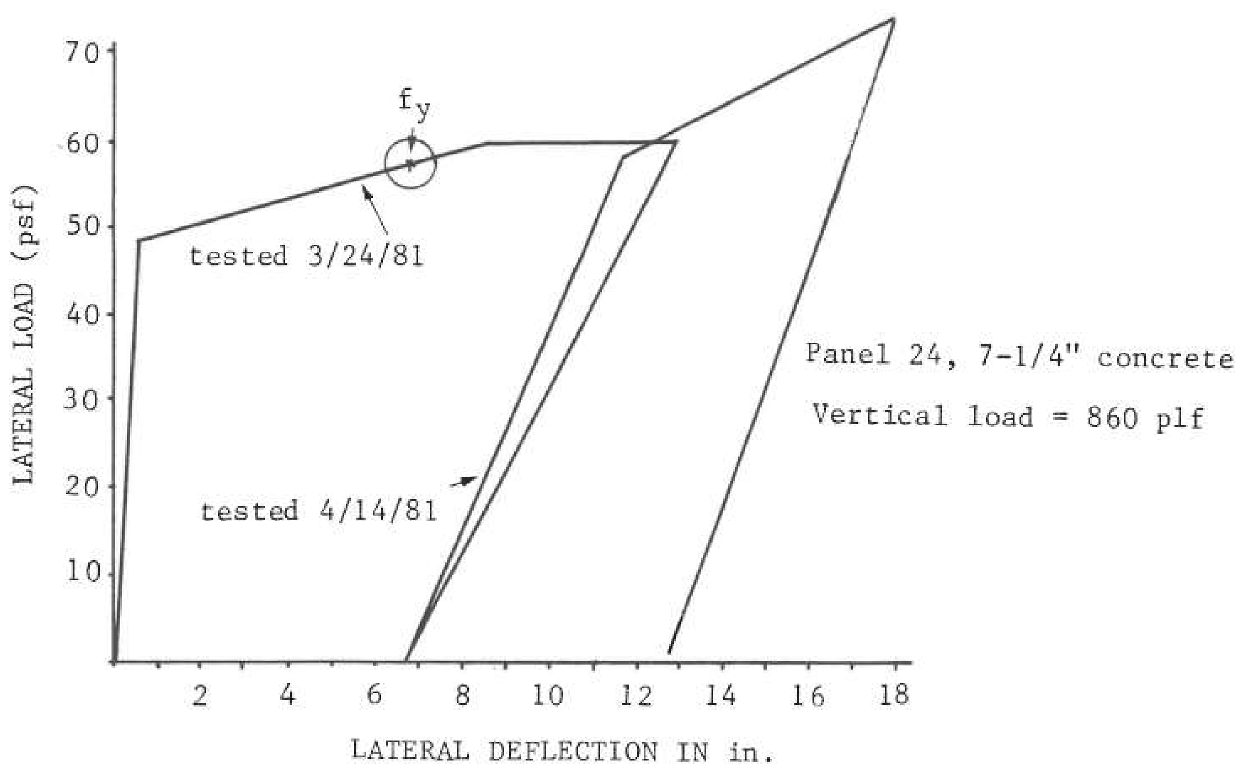

Figure 2-17: Load-Deflection Curves with Unloading and Rebound for the *Report of the Task Committee on Slender Walls*, adapted from (Simpson et al., 1982)

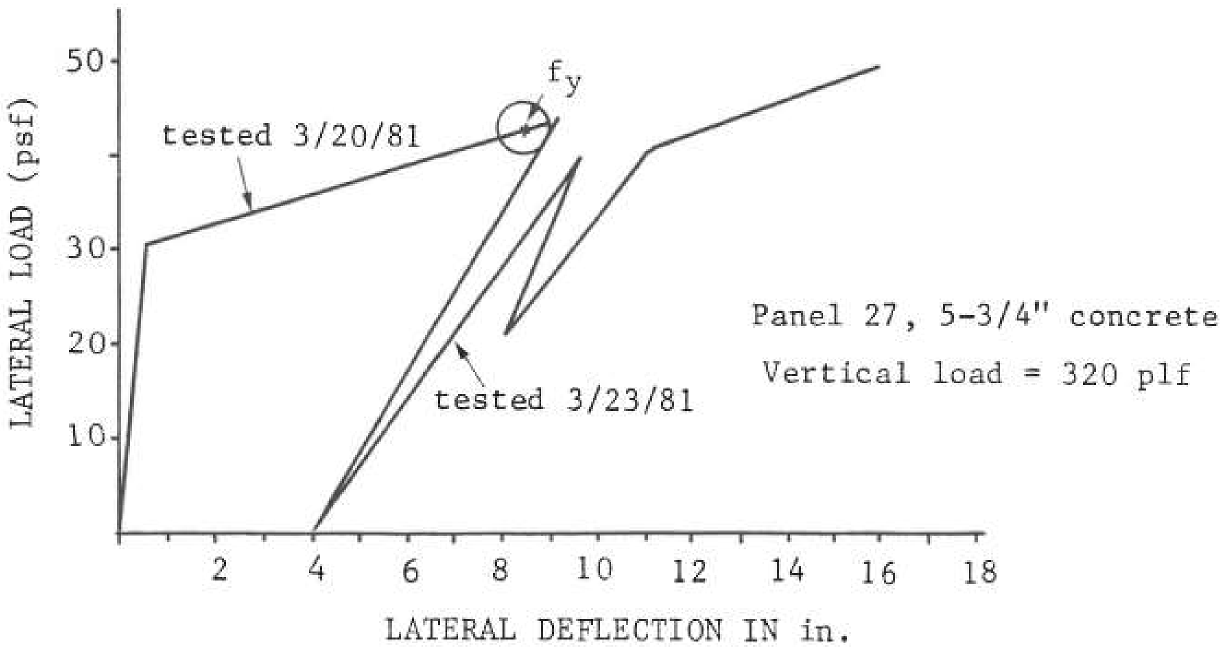

Figure 2-18: Load-Deflection Curves with Unloading and Rebound for the *Report of the Task Committee on Slender Walls*, adapted from (Simpson et al., 1982)

To determine the P-∆ moment, the roof load was multiplied by the midspan deflection and added to the weight of the wall above midspan times the midspan deflection. In order to analyze the impact of the P-∆ effect, the percent P-∆ moment was calculated by multiplying the P-∆ moment by 100 and dividing by the quantity of the applied lateral load times the panel height squared divided by 8 plus the roof load per foot times the load eccentricity divided by 2. These calculations are shown in Equations 2-4 and 2-5.

$$\boldsymbol{P\Delta\ Moment = Roof\ Load\ \times \Delta + Wall\,Weight\ Above\ \times \Delta} \tag{2-4}$$

$$\%\ \boldsymbol{P\Delta\ Moment} = \frac{\boldsymbol{P\Delta\ Moment \times 100}}{\frac{\boldsymbol{w\,h^2}}{\boldsymbol{8}}+\frac{\boldsymbol{P\,e}}{\boldsymbol{2}}} \tag{2-5}$$

The % P-∆ moment was plotted versus the normalized deflection for the 4.75" tilt-up wall panels as shown in Figure 2-19. For a typical wall, the horizontal deflection to height ratio never exceeds 0.01, resulting in the % P-∆ moment being less than 15%.

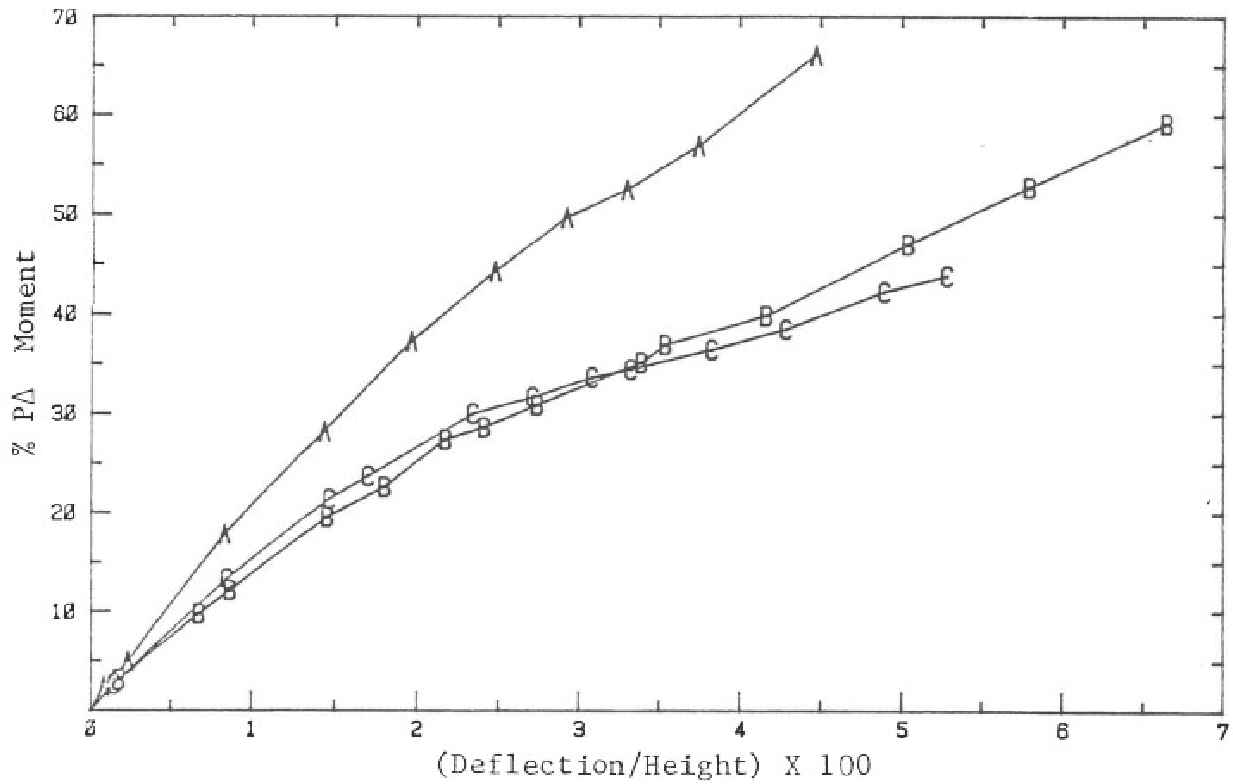

Figure 2-19: % P-∆ Moment Versus Normalized Deflection for 4.75" Tilt-Up Panels for the *Report of the Task Committee on Slender Walls*, adapted from (Simpson et al., 1982)

Interaction diagrams were formed for different wall panels that were tested. The diagrams relevant for this review are the 4.75" and 7.25" concrete tilt-up panel plots. The interaction diagram is displayed in Figure 2-20. The report also analyzes the interaction in the low axial load range, as shown in Figure 2-21. With low axial load, the moment is only slightly increased and is dependent on the amount and depth of the steel in the wall panel cross section.

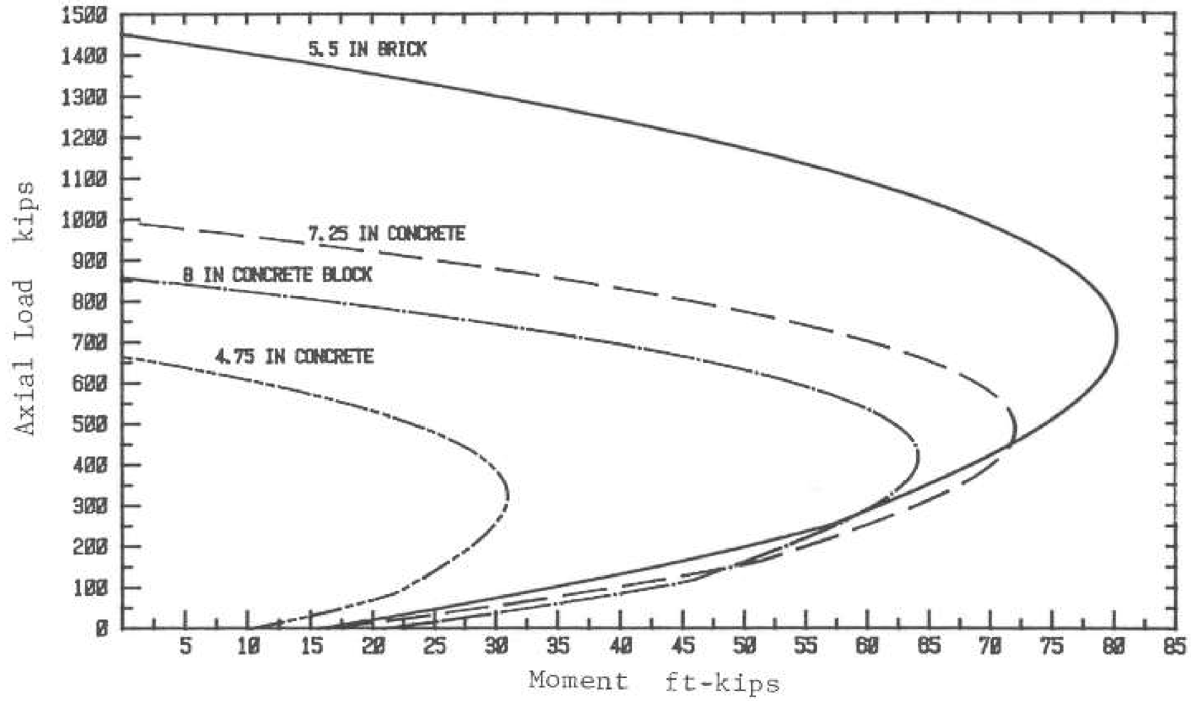

Figure 2-20: Interaction Diagram for the *Report of the Task Committee on Slender Walls*, adapted from (Simpson et al., 1982)

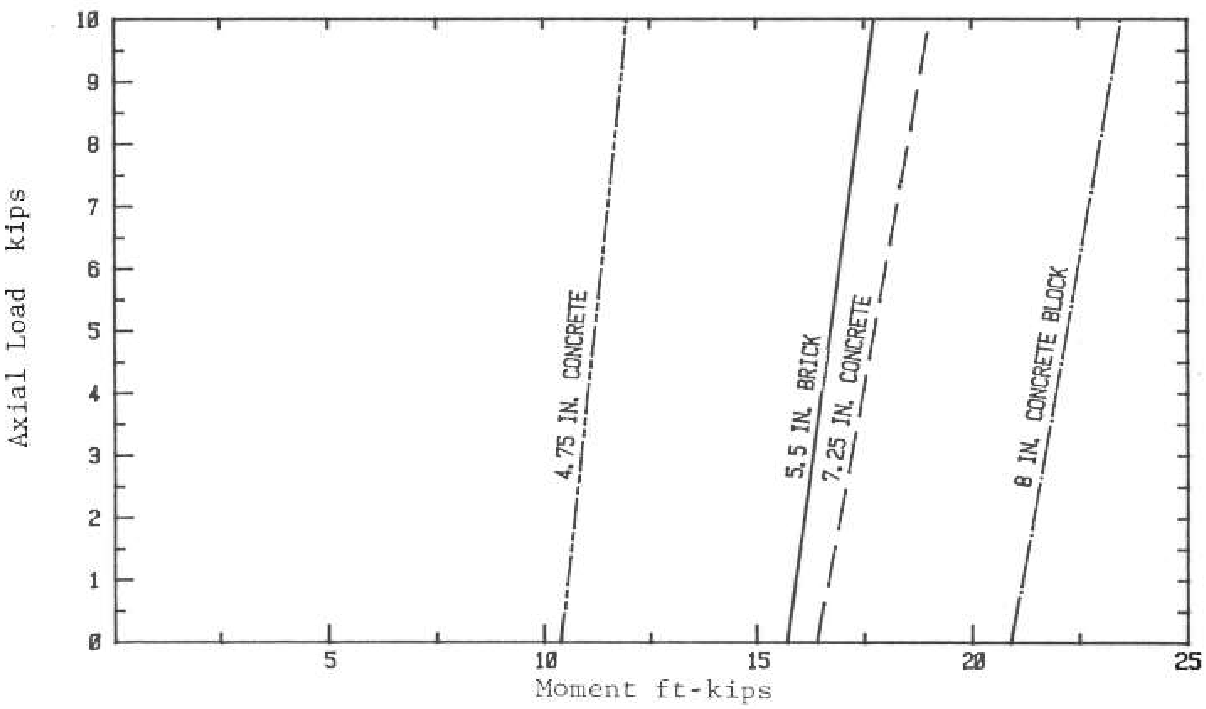

Figure 2-21: Low Axial Range Interaction Diagram for the *Report of the Task Committee on Slender Walls*, adapted from (Simpson et al., 1982)

The *Report of the Task Committee on Slender Walls* included a plot of axial load versus moment (Figure 2-22) for the 4.75" and 9.5" thick panels. Actual values of f'_c = 4 ksi and f_y = 70 ksi were used. The results from this data show that deflection controlled for the thin panels, while strength controlled for the thicker panels.

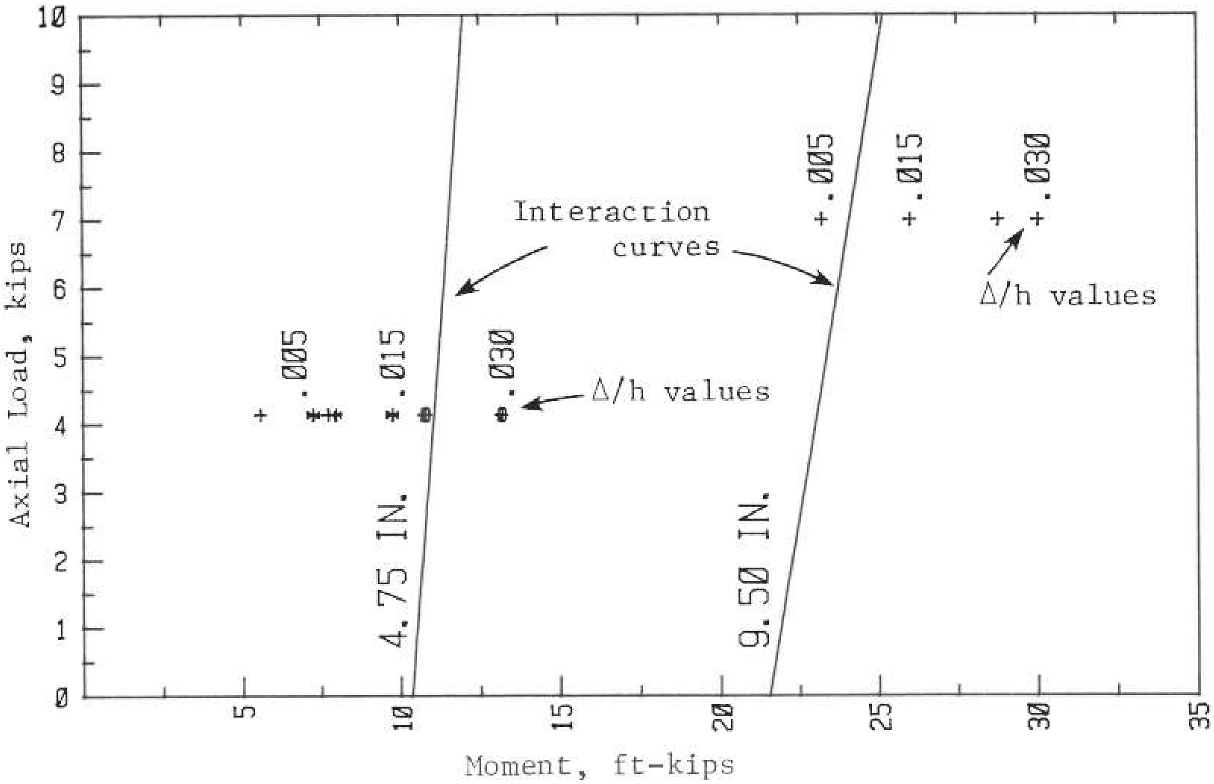

Figure 2-22: Axial Load Versus Moment Plot for the *Report of the Task Committee on Slender Walls*, adapted from (Simpson et al., 1982)

Flexural deflection can be predicted based on the relationship between moment and curvature. First, the interaction curve must be developed based on section properties. This is used to build a set of moment/curvature relationships for each point along the height of the wall with varying vertical load. Once this relationship is obtained, a moment of $wl^2/8 + Pe$ is applied, which results in a set of curvatures, which can be used to obtain initial deflections. With the initial deflections, the P-Δ moment can be calculated and added to the initial moment, resulting in a new set of curvatures. These are integrated and the process repeats until the values converge. The deflections obtained through this method are compared to the actual results in Figure 2-23 for the 9.5" thick panel.

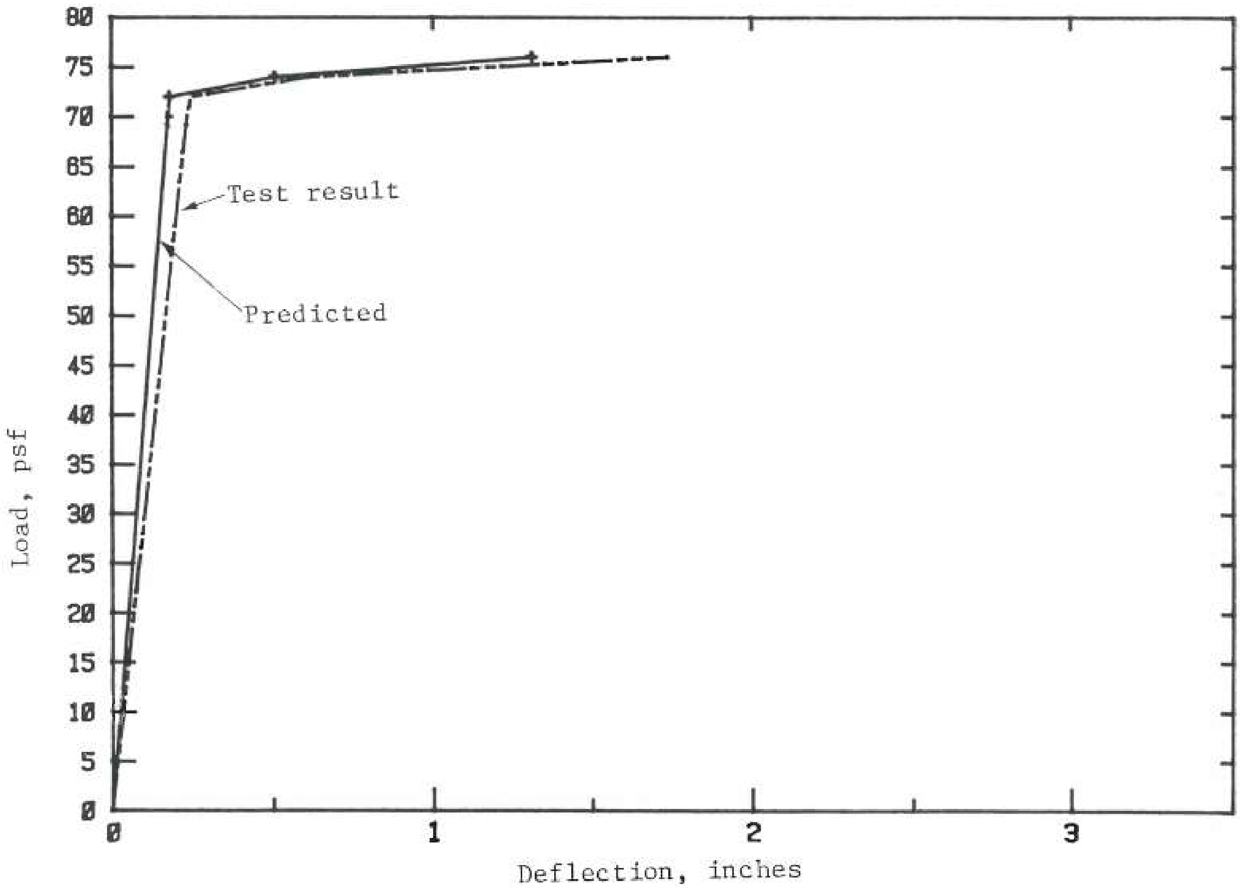

Figure 2-23: Calculated Deflections Compared to Test Results for 9.5" Tilt-Up Panel for the *Report of the Task Committee on Slender Walls*, adapted from (Simpson et al., 1982)

The results of the tests in the report established that the slender walls behaved similarly to shallow reinforced concrete beams subjected to a uniform load. The walls were flexible after cracking and the deflection curves were flat after yielding. The selection of the applied vertical loads for the tests was based on typical tributary design loads used in California. The self-weight of wall panels at the base are generally four to eight times larger than the roof load, so the secondary moment caused by the vertical load is primarily caused by the panel self-weight. The report found that roof load only contributes 12 to 25% to the secondary moment.

Before the panel yields, the relationship between the mid-height deflection and lateral load applied is bilinear (Figure 2-24). Before cracking, the response is a steep, straight line. After cracking, the relationship is a curve until the cracking pattern has stabilized, which results in a low-slope or straight-line response.

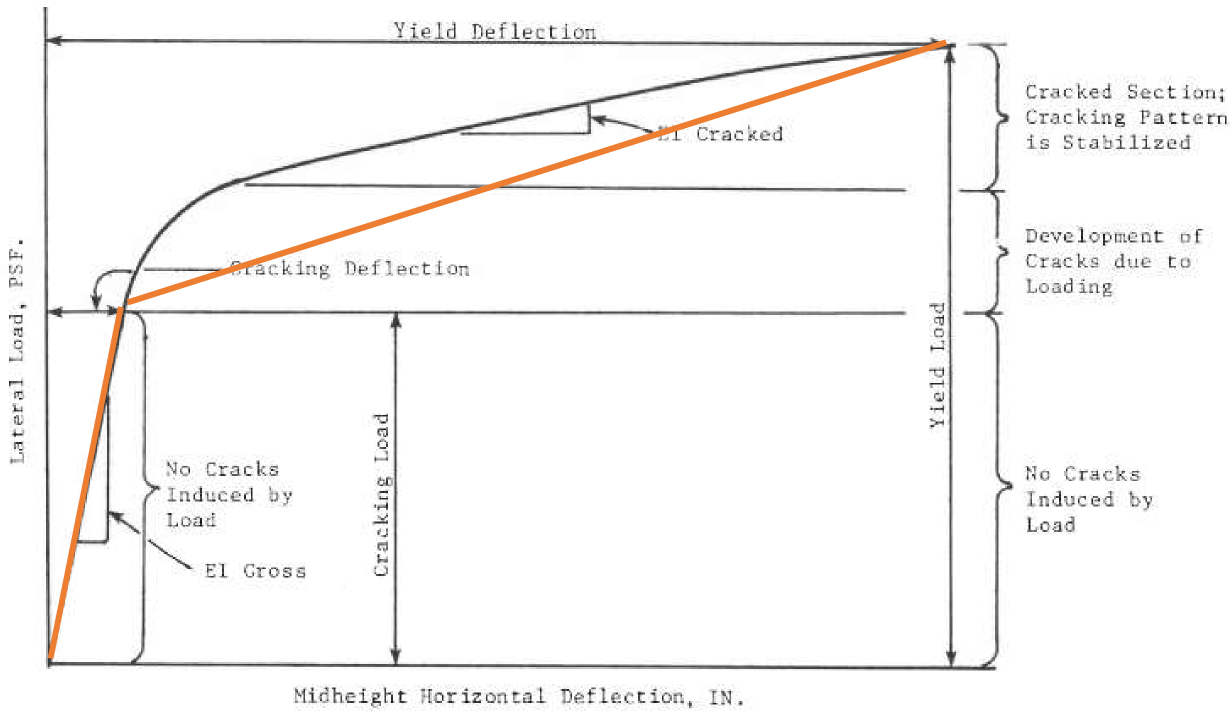

Figure 2-24: Bilinear Relationship for the *Report of the Task Committee on Slender Walls*, adapted from (Simpson et al., 1982)

The variables in panel design are the wall panel height, wall panel thickness, and amount of vertical reinforcement. First, the wall height is selected for function and architectural design. Next, the width is selected to meet the prescribed height-to-thickness ratio. The amount of vertical reinforcement is selected based on strength requirements. Deflection criteria must also be considered, particularly for thin panels.

Load combinations at the time of the test report were as follows:

$$\boldsymbol{U = 0.75(1.4D + 1.7L + 1.87E)} \quad (2\text{-}6)$$

$$\boldsymbol{U = 0.75(1.4D + 1.7L + 1.7W)} \quad (2\text{-}7)$$

$$\boldsymbol{U = 0.9D + 1.43E} \tag{2-8}$$

$$\boldsymbol{U = 0.9D + 1.3W} \tag{2-9}$$

These are the load factors that were used for the design of elements subjected to seismic or wind forces. There were other load combinations that were used for shear elements that weren't expected to undergo significant lateral loading.

2.3 Design Criteria for Slender Tilt-Up Panels

Kripanarayanan (1994) provided a design aid for slender tilt-up load-bearing walls with slenderness ratios $20 < \frac{kl_u}{h} \leq 50$ and thicknesses varying from 5 ½ to 7 ½ inches. It should be noted that the design recommendations given do not include stresses induced in the wall panels during the lifting and tilting process. The yield strength of the reinforcement is assumed to be 60 ksi. The compressive strength of the concrete is assumed as less than or equal to 4,000 psi and the concrete weight is assumed as 150 pcf. The wall panel is considered as hinged along its loaded edges, free along its vertical edges, initially straight, and laterally restrained at the top of the panel. The equations of equilibrium at a typical section of the wall panel are given as

$$\boldsymbol{\Sigma F = 0, F_1 + F_2 - F_3 = P} \tag{2-10}$$

$$\boldsymbol{\Sigma M = 0, T_1 + T_2 - T_3 = M} \tag{2-11}$$

where F_1 is the net force in the reinforcement, F_2 is the force in the concrete, F_3 is the force for the concrete section displaced by the steel in compression regions, and P is the applied axial load at the section. T_1 is the net bending moment of the reinforcement about the centroidal axis, T_2 is the bending moment of the concrete forces about the centroidal axis, T_3 is the bending moment of the force F_3 about the centroidal axis, and M is the applied bending moment at the section.

The transverse loads used in Kripanarayanan's design were 0, 15, 30, and 45 psf. The influence of creep on the slender wall panels can be approximated with

$$\boldsymbol{e_a = \beta C_t h/20}$$

(2-12)

where e_a is the additional end eccentricity due to creep (inches), β is the ratio of sustained design load to total design load, C_t is the creep coefficient (between 1 and 2), and h is the overall panel thickness (inches). It should be noted that Equation 2-12 does not account for the slenderness ratio but provides an adequate approximation for evaluating sustained load effects on slender walls.

Kripanarayanan provides design aids in the form of tables and load-moment interaction diagrams. While these design aids have been created for use with normal weight concrete (150 pcf), the values may be adjusted using a reduction factor, x, calculated as

$$\boldsymbol{x = \frac{Load\ capacity\ with\ w \leq 150\ pcf}{Load\ capacity\ with\ w = 150\ pcf}} \tag{2-13}$$

$$\boldsymbol{for\ \frac{l_u}{h} > 30: \quad x = 1 - (\frac{l_u}{h} - 30)(1 - \frac{(w-115)}{35})/38}$$

(2-14)

$$\boldsymbol{for\ \frac{l_u}{h} \leq 30: \quad x = 1.00} \tag{2-15}$$

where the use of this reduction factor is limited to panels with eccentricities less than h/3.

A more recent design guide for slender tilt-up wall panels is provided by ACI Committee 551 (2015). This guide, provided by the American Concrete Institute, was the primary reference for the calculations performed in this report's parametric study. This guide, in accordance with

ACI 318 code, provides the following equations for the design moment strength, applied moment, and applied deflection.

$$\boldsymbol{\varphi M_n \geq M_u} \tag{2-16}$$

$$\boldsymbol{M_u = M_{ua} + P_u \Delta_u} \tag{2-17}$$

$$\Delta_{\boldsymbol{u}} = \frac{\boldsymbol{5M_u l_c^2}}{\boldsymbol{0.75(48E_c I_{cr})}} \tag{2-18}$$

The applied moment, M_u, is calculated either through iterations of deflections, or with Equation 2-19, where the cracked moment of inertia, I_{cr}, is given in Equation 2-20.

$$\boldsymbol{M_u = \frac{M_{ua}}{1 - \frac{5P_u l_c^2}{0.75(48E_c I_{cr})}}} \tag{2-19}$$

$$\boldsymbol{I_{cr} = \frac{E_s}{E_c}\left[A_s + \frac{P_u}{f_y}\left(\frac{h}{2d}\right)\right](d-c)^2 + \frac{bc^3}{3}} \tag{2-20}$$

The 0.75 factor reduces the calculated bending stiffness to more accurately match test data by accounting for varied material properties and differences in construction. This factor is a requirement for compliance with ACI 318. It should be noted that I_{cr} can only be calculated as shown in Equation 2-19 if the vertical stress, P_u/A_g, does not exceed a limit of $0.06f'_c$. The strength reduction factor, φ, is given by ACI 318 as 0.9 for tension-controlled members.

The design guide also provides recommended design procedures. For a solid panel without openings, the panel geometry must first be determined, as well as the loading conditions for applied axial and out-of-plane lateral loads. Next, a panel thickness is to be assumed. For a single layer of reinforcement, a minimum thickness of $l_c/50$ is recommended. For two layers of reinforcement, a minimum thickness of $l_c/65$ is recommended. Once the thickness is assumed, the reinforcement should be selected, and the panel should be analyzed for each applicable load combination. This process is often iterative, where adjustments may be made to the thickness and reinforcement.

P-Δ effects, or secondary effects, are an important consideration in the design and analysis of slender wall panels. P-Δ effects occur when an axial load is applied to a member with a deflected shape. The eccentricity of the axial forces in the member cause additional moment. The ACI 551 design guide provides Figure 2-25, which displays the impact of secondary effects. The moment caused by secondary effects is greatest at midspan for pin-pin members.

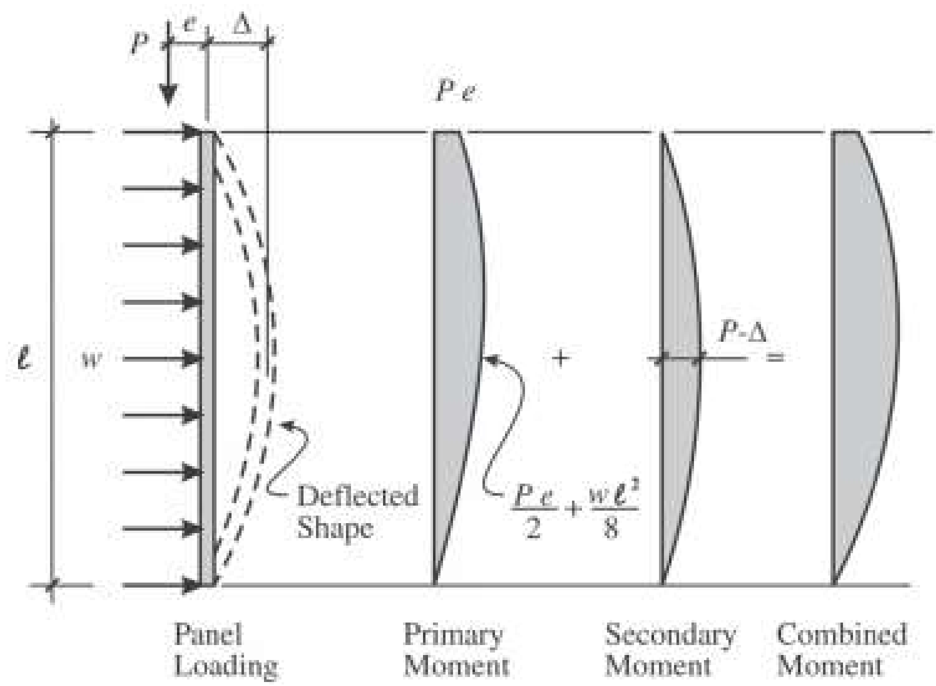

Figure 2-25: P-Δ effects

The design of columns using lightweight concrete is essentially the same as for normal weight concrete. The reduced modulus should be used in the code sections in which slenderness effects are considered. Extensive tests (Pfeifer 1968; Washa and Fluck 1952) comparing the time-dependent behavior of lightweight and normal weight columns developed the following:

a) Instantaneous shortening caused by initial loading can be accurately predicted by elastic theory. Such shortening of a lightweight concrete column will be greater than that of a comparable normal weight column due to the lower modulus of elasticity of lightweight concrete.

b) Time-dependent shortening of lightweight and normal weight concrete may differ when small unreinforced specimens are compared. These differences, however, are minimized when large reinforced concrete columns are tested as both increasing size and amount of longitudinal reinforcement reduces time-dependent shortening. Measured timed dependent shortening was compared with those predicted by theory, and satisfactory correlations were found

c) Measured ultimate strengths were compared with theory and good correlations were found. Both concrete type and previous loading had no effect on this correlation.

Items (a) and (c) are applied in the parametric study of this thesis.

Chapter 3 - Parametric Study

3.1 Building Conditions

In order to compare this parametric study with the Report of the Task Committee on Slender Walls (Simpson et al., 1982), the building conditions were selected to match those used in the test report. Each wall panel had a height of 24'-8", with a bearing elevation of 24'-0". The width of each panel was 4'-0", and pin supports were used.

While the test report varied the axial load for three of the twelve panels by applying 860 plf in panels 24, 25, and 26, an axial load of 320 plf was used in the majority of the tested panels. This parametric study applied an axial load of 320 plf to each panel to most accurately represent the test report. The lateral load for each panel is applied in 5 psf increments until the panels analyzed achieve similar deflection to the maximum deflection given by the test report. To match the eccentricities of the applied axial load used in the report, Equation 3-1 was used.

$$\boldsymbol{e_{cc} = 3.5\ in + \frac{t}{2}} \tag{3-1}$$

3.2 Panel Designation

The panels analyzed in this parametric study will be designated using the naming convention shown in Figure 3-1. For example, a panel with a thickness of 4.75", a modulus of rupture K value of 7.5, and a concrete weight of 90 pcf (λ=.75) would be described as Panel 4.75-7.5-.75. The normal weight panels which are intended to represent the same conditions as the test report panels are the first four panels shown in Table 3-1.

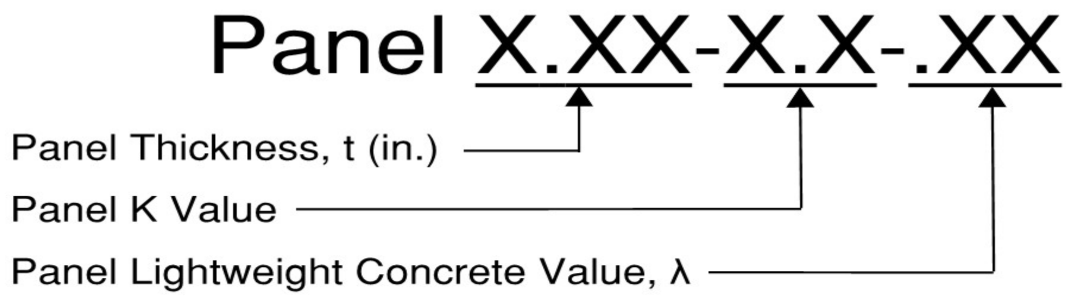

Figure 3-1: Panel Designation

3.3 Panel Parameters

Many of the panel properties were also chosen to represent the panels which were tested in the Report of the Task Committee on Slender Walls (Simpson et al., 1982). The four panel thicknesses that were selected were 4.75", 5.75", 7.25", and 9.5". All four thicknesses used four #4 bars in one layer for vertical reinforcement. While the thicker panels would likely use 2 layers of steel and a larger quantity than four #4 bars due to code requirements and economic design, four #4 bars were used for slenderness comparisons and to match the slender wall test report. Since horizontal reinforcement does not influence the lateral deflection and applied moment, it was not considered. The steel yield stress f_y and modulus of elasticity E_s chosen were 70 ksi and 28,600 ksi respectively, matching the tested values reported by Twining Laboratories in the test report.

The panels were analyzed with a lightweight concrete modification factor λ of 0.75, 0.8, and 0.85 for each panel thickness. 0.75 was chosen as it is the lower bound of λ and is used for all-lightweight concrete with fine and coarse aggregates complying with ASTM C330. 0.8 was chosen to represent lightweight, fine blend concrete with fine aggregates complying to a combination of ASTM C330 and C33. 0.85 was chosen for sand-lightweight concrete with fine aggregates complying with ASTM C33 (ACI Committee 318, 2019). The most common unit weight of lightweight concrete is 110 to 115 pcf (Martin et al., 2013), which corresponds to a lightweight concrete modification factor of approximately 0.85.

The K factor used in the modulus of rupture f_r was varied between values of 5, 6.7, and 7.5 for each panel thickness. 7.5 was selected as it is the current K value recommended by ACI 318 for the calculation of the modulus of rupture (ACI Committee 318, 2019). 5 was selected as it was the K value used in the design examples given in the Report of the Task Committee on Slender Walls and was determined by the committee to be the best fit to the deflections seen in the panel testing (Simpson et al., 1982). 6.7 was selected as an intermediate value for comparison purposes. It should be noted that there has been debate over the calculation of the modulus of rupture. Abi-Nader (2009) states that ACI Committee 435 suggests that the modulus of rupture K value varies from 7.5 to 12, while ACI Committee 330, the Florida State Road Department, and the Portland Cement Association recommend entirely different equations for the modulus of rupture. It is clear that more testing should be done to determine a standardized method to calculate the modulus of rupture, so this report will focus on analyzing the impact that varying the K value has on panel deflection.

The 28-day specified concrete compressive strength f'_c was 4,009 psi. The modulus of elasticity was calculated using the ACI 318 equation shown in Equation 3-2 (ACI Committee 318, 2019). The concrete weight w_c was selected based on the various values for λ using Equation 3-3 (Graybeal & Greene, 2015). 90 pcf was used for $\lambda = 0.75$, 105 pcf for $\lambda = 0.8$, and 115 pcf for $\lambda = 0.85$. To best represent the test report panels, the d value was taken as an average of the d_{avg} values from the three panels of each thickness. The panel parameters which vary between each panel are given in Table 3-1.

$$\boldsymbol{E_c = w_c^{1.5} 33\sqrt{f'_c}} \tag{3-2}$$

$$\mathbf{0.75 \leq \boldsymbol{\lambda} = 7.5\boldsymbol{w_c} \leq 1.0} \tag{3-3}$$

Table 3-1: Panel Parameters

Panel Designation	t (in.)	K factor	λ	w_c (pcf)	E_c (ksi)	f_r (psi)	d (in.)
4.75-5-1.0	4.75	5	1	150	3225	316.6	2.63
5.75-5-1.0	5.75			150	3225	316.6	3.35
7.25-5-1.0	7.25			150	3225	316.6	3.97
9.5-5-1.0	9.5			150	3225	316.6	4.66
4.75-5-.75	4.75	5	0.75	90	1784.0	237.4	2.63
4.75-5-.8			0.8	105	2248.1	253.3	
4.75-5-.85			0.85	115	2576.8	269.1	
4.75-6.7-.75		6.7	0.75	90	1784.0	318.2	
4.75-6.7-.8			0.8	105	2248.1	339.4	
4.75-6.7-.85			0.85	115	2576.8	360.6	
4.75-7.5-.75		7.5	0.75	90	1784.0	356.2	
4.75-7.5-.8			0.8	105	2248.1	379.9	
4.75-7.5-.85			0.85	115	2576.8	403.6	
5.75-5-.75	5.75	5	0.75	90	1784.0	237.4	3.35
5.75-5-.8			0.8	105	2248.1	253.3	
5.75-5-.85			0.85	115	2576.8	269.1	
5.75-6.7-.75		6.7	0.75	90	1784.0	318.2	
5.75-6.7-.8			0.8	105	2248.1	339.4	
5.75-6.7-.85			0.85	115	2576.8	360.6	
5.75-7.5-.75		7.5	0.75	90	1784.0	356.2	
5.75-7.5-.8			0.8	105	2248.1	379.9	
5.75-7.5-.85			0.85	115	2576.8	403.6	
7.25-5-.75	7.25	5	0.75	90	1784.0	237.4	3.97
7.25-5-.8			0.8	105	2248.1	253.3	
7.25-5-.85			0.85	115	2576.8	269.1	
7.25-6.7-.75		6.7	0.75	90	1784.0	318.2	
7.25-6.7-.8			0.8	105	2248.1	339.4	
7.25-6.7-.85			0.85	115	2576.8	360.6	
7.25-7.5-.75		7.5	0.75	90	1784.0	356.2	
7.25-7.5-.8			0.8	105	2248.1	379.9	
7.25-7.5-.85			0.85	115	2576.8	403.6	
9.5-5-.75	9.5	5	0.75	90	1784.0	237.4	4.66
9.5-5-.8			0.8	105	2248.1	253.3	
9.5-5-.85			0.85	115	2576.8	269.1	
9.5-6.7-.75		6.7	0.75	90	1784.0	318.2	
9.5-6.7-.8			0.8	105	2248.1	339.4	
9.5-6.7-.85			0.85	115	2576.8	360.6	
9.5-7.5-.75		7.5	0.75	90	1784.0	356.2	
9.5-7.5-.8			0.8	105	2248.1	379.9	
9.5-7.5-.85			0.85	115	2576.8	403.6	

3.4 Parametric Study Methods

The parametric study made analyzed each panel with three ASCE 7-16 (2017) load and resistance factor design load combinations, as well as the ACI 318 (2019) recommended service load combination, all of which are shown below. While there are other load combinations that should typically be considered in design, it was determined that these four load combinations would govern for the purposes of this study.

$$\mathbf{1.2}\boldsymbol{D} + \mathbf{1.6}\boldsymbol{L_r} + \mathbf{0.5}\boldsymbol{W} \quad (3\text{-}4)$$

$$\mathbf{1.2}\boldsymbol{D} + \mathbf{0.5}\boldsymbol{L_r} + \mathbf{1.0}\boldsymbol{W} \quad (3\text{-}5)$$

$$\mathbf{0.9}\boldsymbol{D} + \mathbf{1.0}\boldsymbol{W}$$

(3-6)

$$\mathbf{1.0}\boldsymbol{D} + \mathbf{0.5}\boldsymbol{L} + \boldsymbol{W_a} \quad (3\text{-}7)$$

Following the guide published by ACI Committee 551 (2015) and in accordance with ACI 318-19 (2019), A_{se} (Equation 3-8) was used in the calculation of I_{cr} as the vertical stress, P_u/A_g, did not exceed the limit of $0.06f'_c$ for any of the panels. The depth of the equivalent stress block a and the distance from the extreme fiber to the neutral axis c were calculated with Equations 3-9 and 3-10.

$$\boldsymbol{A_{se}} = \boldsymbol{A_s} + \frac{\boldsymbol{P_{um}}}{\boldsymbol{f_y}}\left(\frac{\boldsymbol{h}}{\mathbf{2}\boldsymbol{d}}\right) \quad (3\text{-}8)$$

$$\boldsymbol{a} = \frac{\boldsymbol{A_{se}f_y}}{\mathbf{0.85}\boldsymbol{f'_c b}} \quad (3\text{-}9)$$

$$\boldsymbol{c} = \frac{\boldsymbol{a}}{\mathbf{0.85}} \quad (3\text{-}10)$$

The cracking moment M_{cr}, the applied moment at midspan without $P - \Delta$ effects M_{ua}, and the effective moment of inertia I_e were calculated using Equations 3-11, 3-12, and 3-13 in accordance with ACI 318 (2019). The modulus of rupture f_r, used in the calculation of the cracking moment, was calculated using Equation 3-14.

$$\boldsymbol{M_{cr}} = \frac{\boldsymbol{f_r I_g}}{\boldsymbol{y_t}} \tag{3-11}$$

$$\boldsymbol{M_{ua}} = \frac{\boldsymbol{w_u l_c}}{\boldsymbol{8}} + \frac{\boldsymbol{P_{ua} e_{cc}}}{\boldsymbol{2}} \tag{3-12}$$

$$\boldsymbol{I_e} = \left(\frac{\boldsymbol{M_{cr}}}{\boldsymbol{M_a}}\right)^{\boldsymbol{3}} \boldsymbol{I_g} + \left[\boldsymbol{1} - \left(\frac{\boldsymbol{M_{cr}}}{\boldsymbol{M_a}}\right)^{\boldsymbol{3}}\right] \boldsymbol{I_{cr}} \tag{3-13}$$

$$\boldsymbol{f_r} = \boldsymbol{K\lambda\sqrt{f'_c}} \tag{3-14}$$

The maximum applied moment M_u, including $P - \Delta$ effects, was calculated with Equation 3-15, where K_b is defined in Equation 3-16. The gross moment of inertia I_g was used when $M_a \leq M_{cr}$, and the effective moment of inertia I_e was used in Equation 3-16 when $M_a > M_{cr}$. The resulting deflection Δ_u was calculated using Equation 3-17.

$$\boldsymbol{M_u} = \frac{\boldsymbol{M_{ua}}}{\left(\boldsymbol{1} - \frac{\boldsymbol{P_{um}}}{\boldsymbol{0.75 K_b}}\right)} \tag{3-15}$$

$$\boldsymbol{K_b} = \frac{\boldsymbol{48 E_c I_e}}{\boldsymbol{5 l_c^2}} \tag{3-16}$$

$$\Delta_{\boldsymbol{u}} = \frac{\boldsymbol{M_u}}{\boldsymbol{0.75 K_b}} \tag{3-17}$$

The calculation of the service level deflection Δ_s, which is the primary variable that was researched in this study, was calculated using Equations 3-18 through 3-21 in accordance with ACI 318-19 (2019). Equation 3-18 gives the out-of-plane deflection corresponding to the cracking moment Δ_{cr}. The applied service moment without $P - \Delta$ effects M_{sa} is given in Equation 3-19. The service level deflection was calculated using Equation 3-20. The original test data collected from the Report of the Task Committee on Slender Walls (Simpson et al.,

1982) was reevaluated, and it was determined that the out-of-plane deflections increase much more rapidly once the concrete exceeds its cracking moment. To account for this, a linear interpolation between the deflections at the cracking moment and the nominal moment is used. This linear interpolation is shown in the second portion of Equation 3-20. The committee found that using a K value of 5 in the modulus of rupture equation best represented the deflection curves from their testing. The $(2/3)$ factors in Equation 3-20 adjust the K factor in the modulus of rupture from the code value of 7.5 to 5. Since this parametric study tested different values of K, the $(2/3)$ factors were removed in the calculations. Removing the (2/3) factors in this equation means that a K value of 5 in this report correlates to a K value of 7.5 using standard ACI 318 code. Once the first service level deflection had been calculated, Equation 3-21 was used to determine the applied service moment including $P-\Delta$ effects M_a. Equations 3-20 and 3-21 were then iterated six times to approximate the service level deflection in the panel.

$$\Delta_{cr}=\frac{5M_{cr}l_c^2}{48E_cI_g} \tag{3-18}$$

$$M_{sa}=\frac{w_sl_c^2}{8}+\frac{P_ae_{cc}}{2} \tag{3-19}$$

$$\Delta_s=\frac{M_{sa}}{M_{cr}}\Delta_{cr}\ for\ M_a<\left(\frac{2}{3}\right)M_{cr} \tag{3-20}$$

$$\Delta_s=\left(\frac{2}{3}\right)\Delta_{cr}+\frac{M_a-(2/3)M_{cr}}{M_n-(2/3)M_{cr}}\left[\Delta_n-\left(\frac{2}{3}\right)\Delta_{cr}\right]\ for\ M_a>\left(\frac{2}{3}\right)M_{cr}$$

$$M_a=M_{sa}+P_{sm}\Delta_s \tag{3-21}$$

3.5 Comparison with Test Report

The parametric study analyzed one normal weight concrete tilt-up wall panel for each of the panel thicknesses researched in the Report of the Task Committee on Slender Walls (Simpson et al., 1982). The results of the parametric study for each of the four panel thicknesses, performed using ACI 318 code, are shown in Figures 3-1, 3-2, 3-3, and 3-4. Included in these figures are lines displaying the lateral load and deflections at the panel nominal moment capacity. As shown by the graphs, the code equations appear to match the actual deflections for panels with a high slenderness ratio. In the 7.25” and 9.5” panels, however, the calculated deflections appear to be overly conservative.

It should be noted that a portion of the test report panels have differing variables that were not accounted for in this parametric study. Panels 24 and 27 (7.25” and 5.75” respectively) were loaded and unloaded in order to test rebound. The rebound curves (discussed in chapter 3 of this report) were not included in the graphs shown in Figures 3-3 and 3-4, so this had no impact on the accuracy of the parametric study. Another variable that was adjusted in the test report was the axial load which was applied to panels 24, 25, and 26. The applied axial load for these panels was increased from 320 plf to 860 plf. This was not accounted for in this parametric study, as the majority of the test report panels were loaded with 320 plf axially. Additionally, the difference in deflection due to secondary moments in these three panels was minimal. For true comparison between the test report panels and the parametric study, however, these three panels should be neglected.

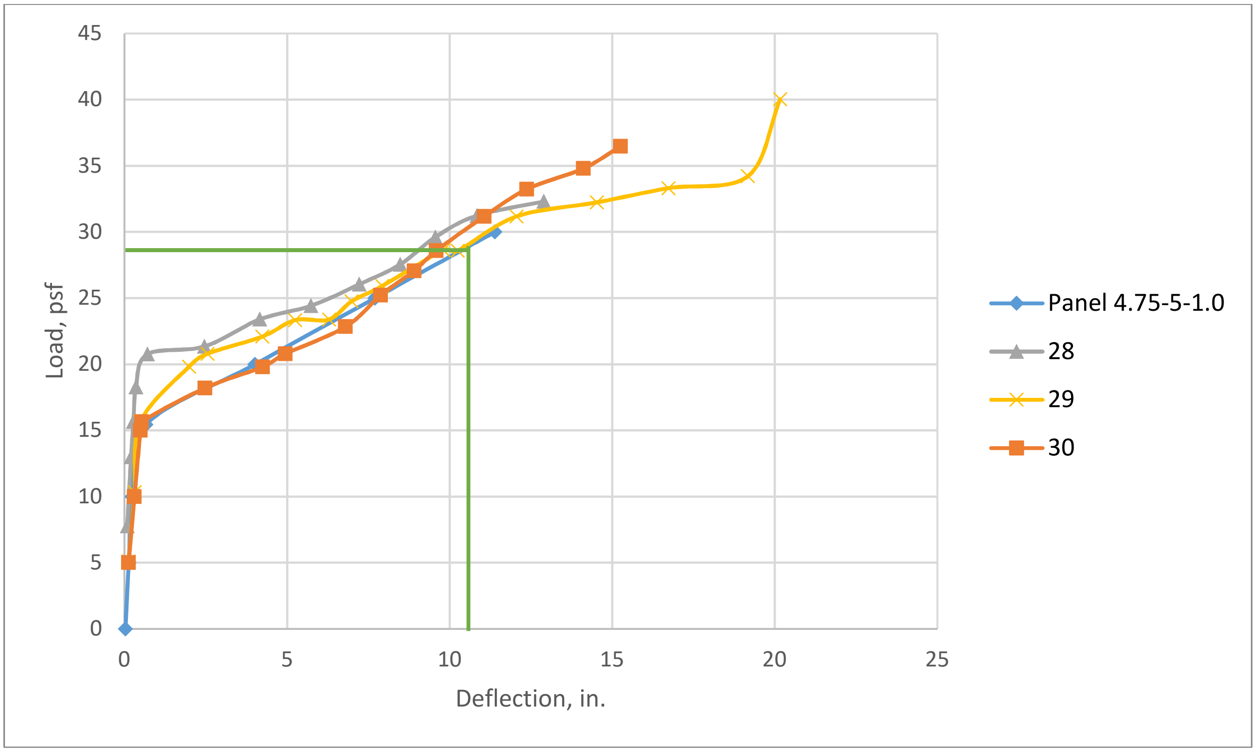

Figure 3-2: Deflection Curve – 4.75" Panels

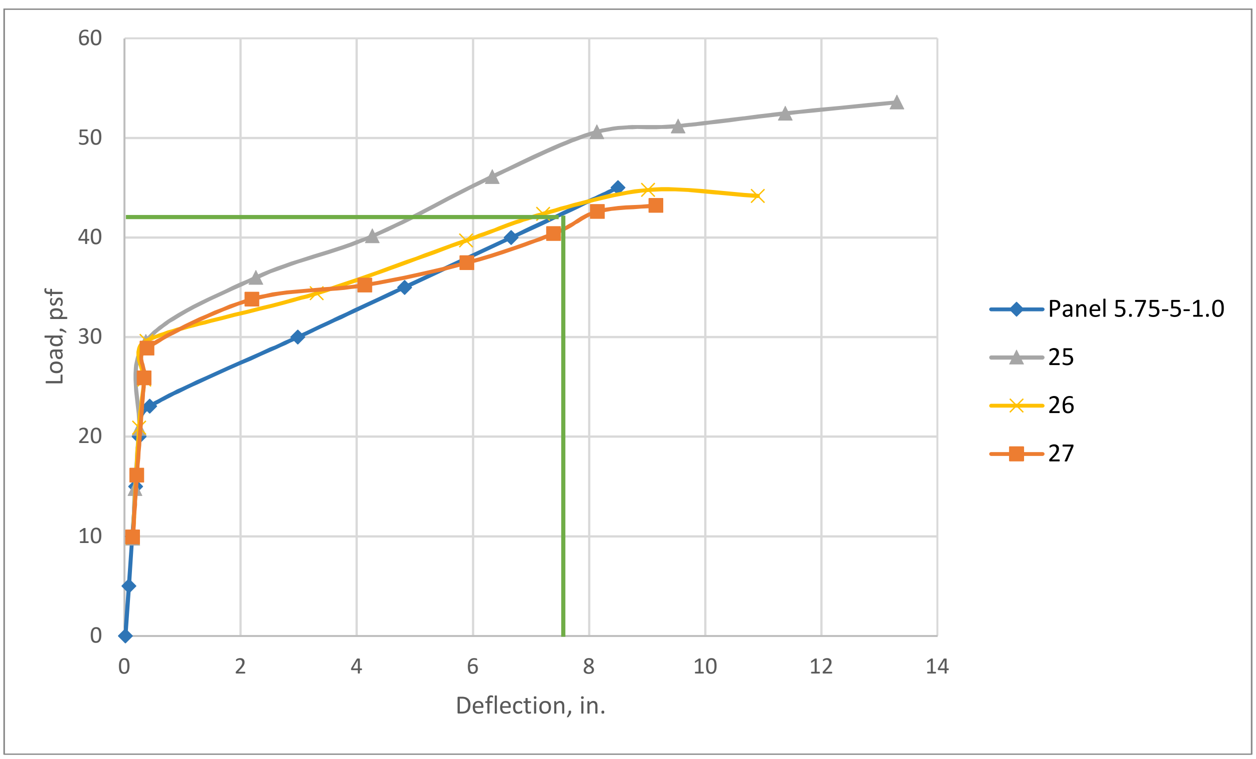

Figure 3-3: Deflection Curve – 5.75" Panels

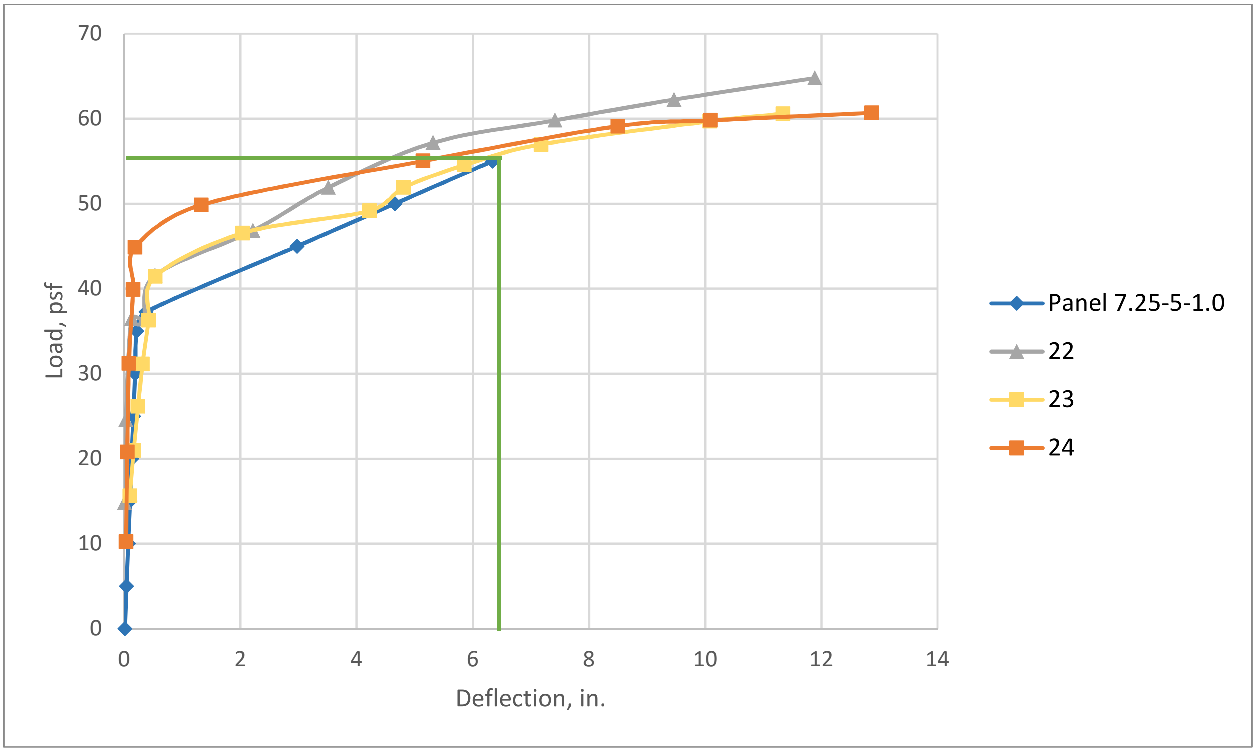

Figure 3-4: Deflection Curve – 7.25" Panels

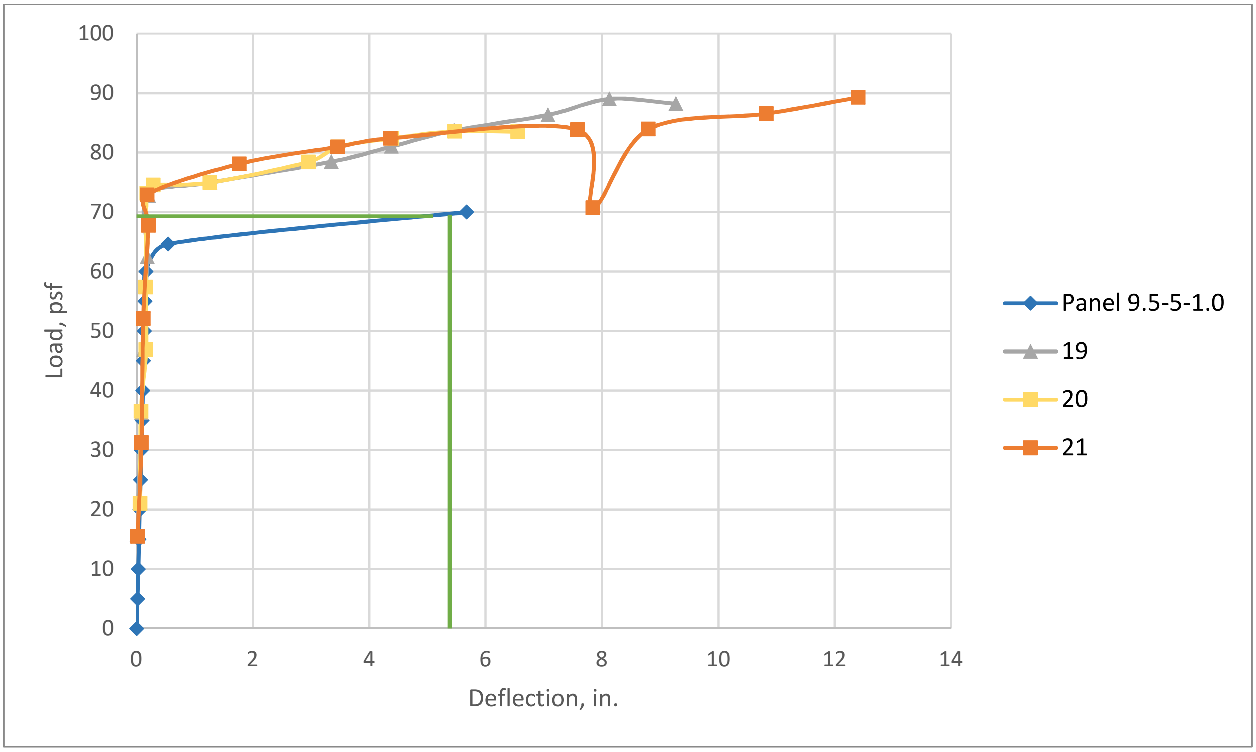

Figure 3-5: Deflection Curve – 9.5" Panels

3.6 Slenderness Ratio Comparison

In order to show the impact that the slenderness ratio has on slender lightweight concrete tilt-up panels, a comparison was done between the four different panel thicknesses. The panels used in this comparison were selected based on the extreme values of K and λ, where K was set to either 5 or 7.5, and λ was set to either 0.75 or 0.85. Graphs of these results are shown in Figures 3-6, 3-7, 3-8, and 3-9.

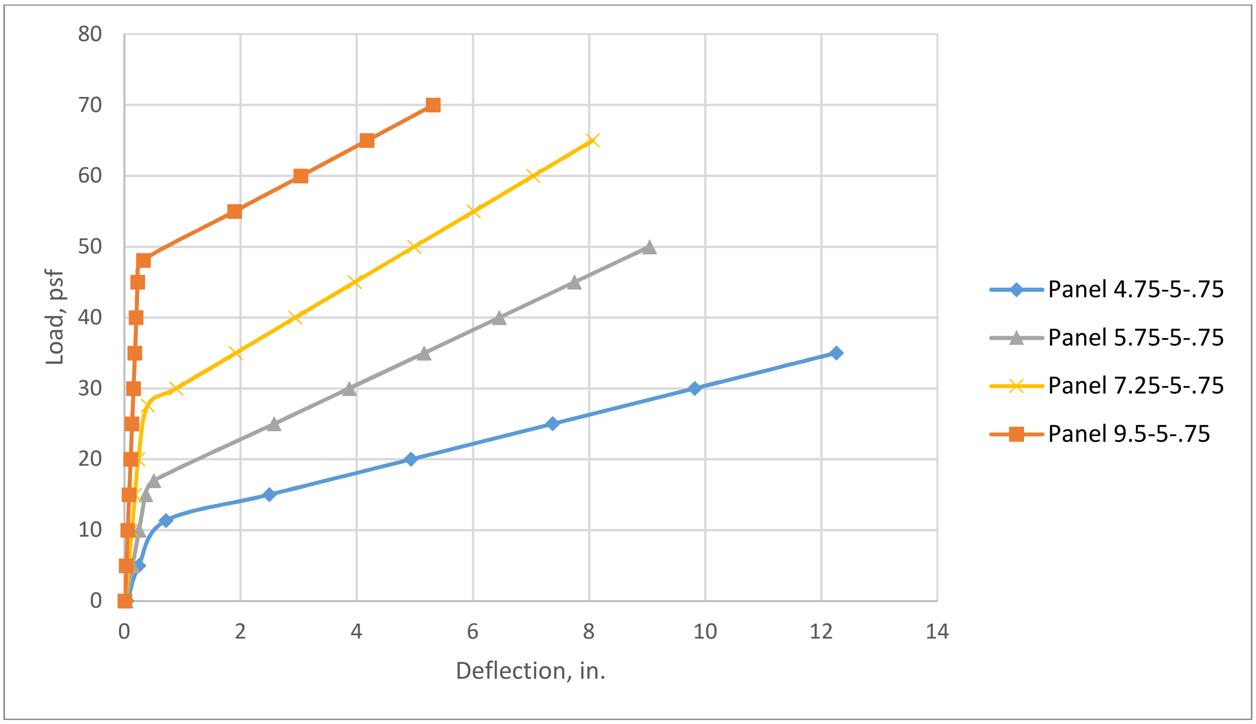

Figure 3-6: Slenderness Comparison – K = 5, λ = 0.75

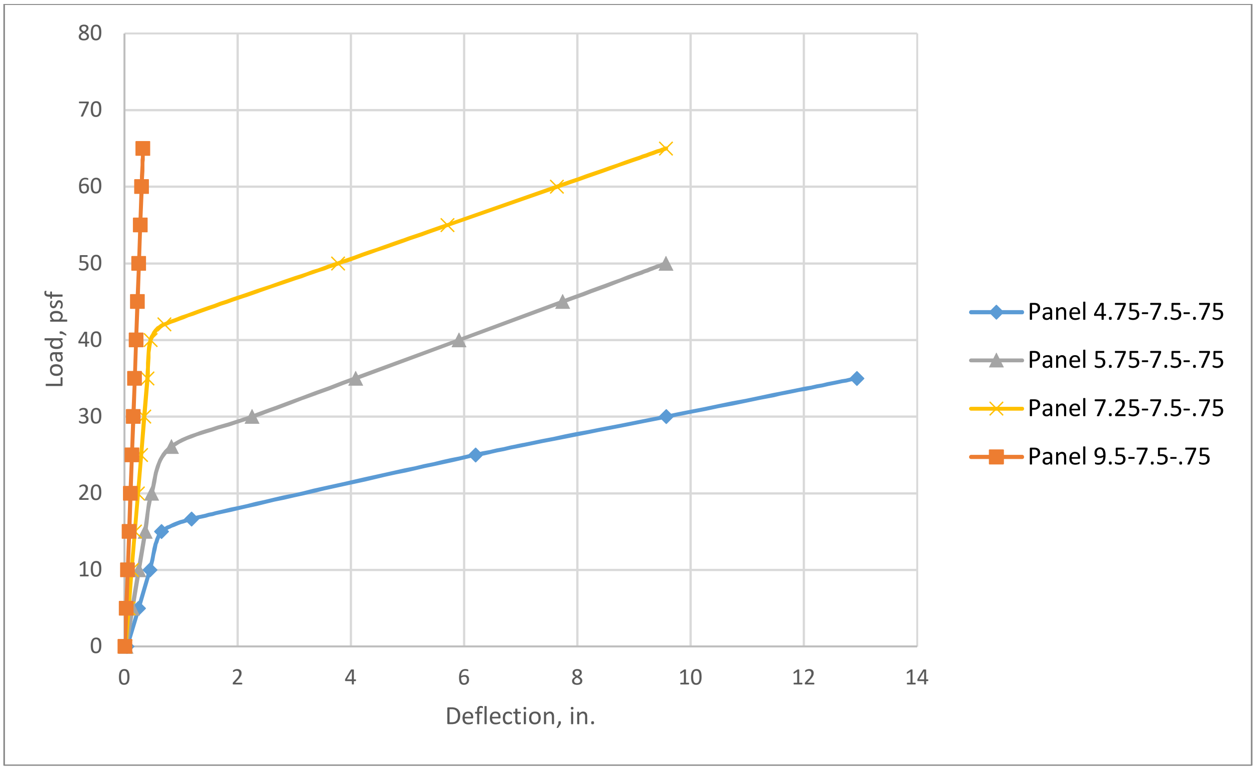

Figure 3-7: Slenderness Comparison – K = 7.5, λ = 0.75

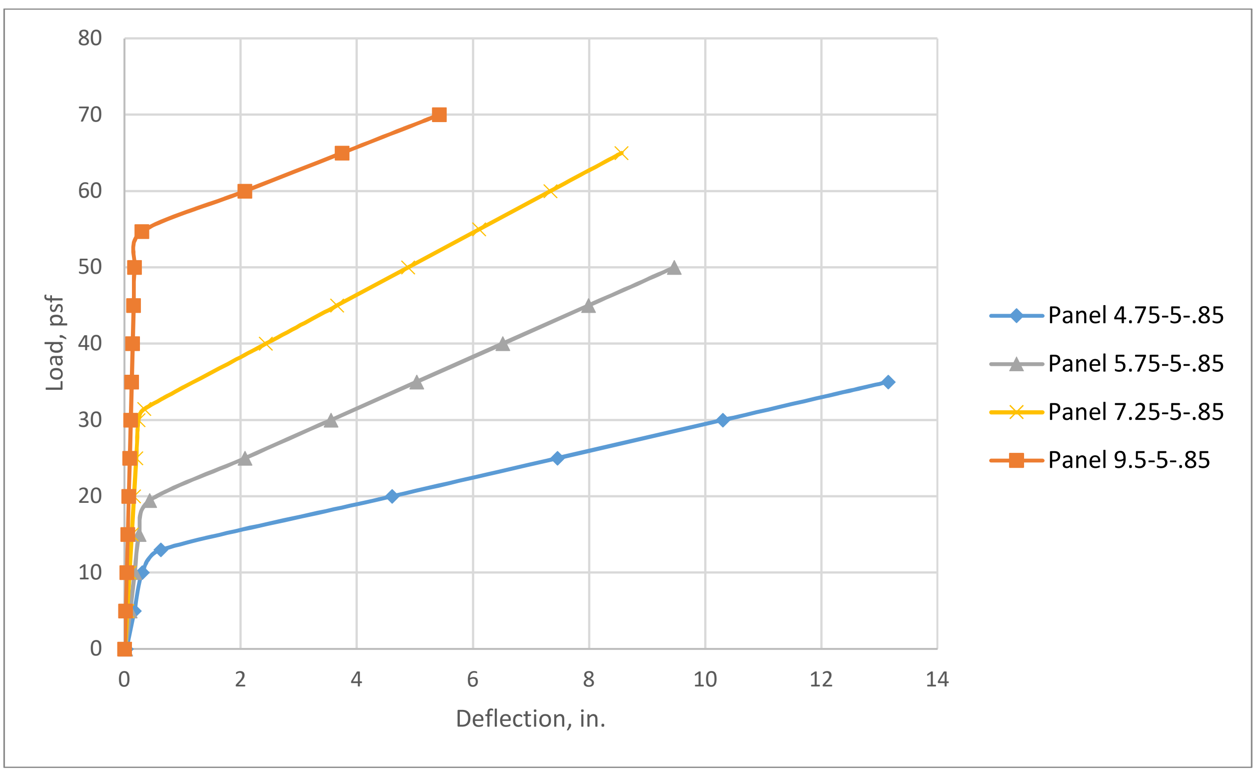

Figure 3-8: Slenderness Comparison – K = 5, λ = 0.85

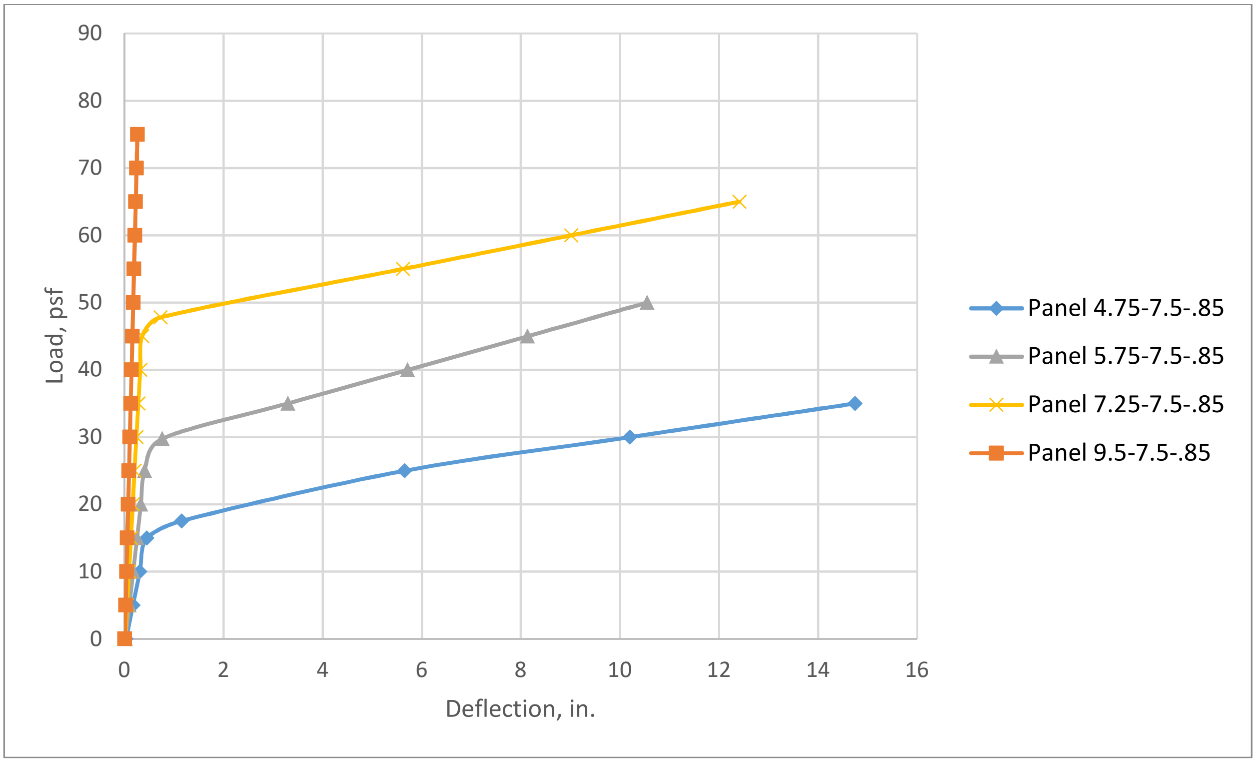

Figure 3-9: Slenderness Comparison – K = 7.5, λ = 0.85

The linear interpolation used for the calculation of service level deflections has certain limitations. For panels that with a nominal moment that is smaller than the cracking moment, the calculations are limited to the first portion of Equation 3-20. Linear interpolation at any lateral loads that are larger than the cracking moment in these panels will yield negative deflections. Panel 9.5-7.5-.85 in Figure 3-9 is an example of a panel affected by this limitation. Most tilt-up panels in design applications will not have a larger cracking moment than their nominal moment, so this limitation should rarely impact tilt-up design.

Table 3-2 displays the % decrease in deflection for each panel in comparison to the 4.75" panel with the same values of K and λ at three given loads. The three lateral loads chosen for comparison were 15, 25, and 35 psf, which were selected to stay below the nominal moment in all of the analyzed panels.

Table 3-2: Impact of Slenderness Ratio on Deflection

Panel Designation	Slenderness Ratio (h/t)	Lateral Load (psf)	Deflection (in.)	% Decrease
Panel 4.75-5-.75	60.63	15	2.495	-
		25	7.377	-
		35	12.259	-
Panel 5.75-5-.75	50.09	15	0.288	88.46%
		25	2.331	68.40%
		35	5.108	58.33%
Panel 7.25-5-.75	39.72	15	0.182	92.71%
		25	0.344	95.34%
		35	1.916	84.37%
Panel 9.5-5-.75	30.32	15	0.081	96.75%
		25	0.130	98.24%
		35	0.180	98.53%
Panel 4.75-7.5-.75	60.63	15	0.651	-
		25	6.202	-
		35	12.933	-
Panel 5.75-7.5-.75	50.09	15	0.364	44.09%
		25	0.764	87.68%
		35	4.081	68.45%
Panel 7.25-7.5-.75	39.72	15	0.182	72.04%
		25	0.293	95.28%
		35	0.404	96.88%
Panel 9.5-7.5-.75	30.32	15	0.081	87.56%
		25	0.130	97.90%
		35	0.180	98.61%
Panel 4.75-5-.85	60.63	15	1.762	-
		25	7.459	-
		35	13.156	-
Panel 5.75-5-.85	50.09	15	0.251	85.75%
		25	2.075	72.18%
		35	5.033	61.74%
Panel 7.25-5-.85	39.72	15	0.125	92.91%
		25	0.202	97.29%
		35	1.210	90.80%
Panel 9.5-5-.85	30.32	15	0.056	96.82%
		25	0.090	98.79%
		35	0.124	99.06%
Panel 4.75-7.5-.85	60.63	15	0.447	-
		25	5.655	-
		35	14.745	-
Panel 5.75-7.5-.85	50.09	15	0.251	43.85%
		25	0.406	92.82%
		35	3.296	77.65%
Panel 7.25-7.5-.85	39.72	15	0.125	72.04%
		25	0.202	96.43%
		35	0.279	98.11%
Panel 9.5-7.5-.85	30.32	15	0.056	87.47%
		25	0.090	98.41%
		35	0.124	99.16%

As expected, decreasing the slenderness ratio by increasing the panel width (with height held constant) yields a large reduction in the deflection at a given load. The 5.75” panel with a slenderness ratio of approximately 50 experienced a deflection reduction of 44-93% in comparison to the 4.75” panels. The 7.25” panel with a slenderness ratio of approximately 40 experienced a deflection reduction of 72-98% in comparison to the 4.75” panels. The 9.5” panel with a slenderness ratio of approximately 30 experienced a deflection reduction of 87-99% in comparison to the 4.75” panels. While the lateral loads selected influence these results due to the thinner panels reaching their cracking moment at much lower lateral loads, it is still apparent that lower slenderness ratios greatly increase the stability of the panel.

A comparison between the slenderness ratios, the cracking moment of inertia I_{cr}, the cracking moment M_{cr}, and the lateral load at which the concrete cracks of the same panels in table 3-2 is shown in Table 3-3. The results of this comparison clearly show that the cracking moment greatly increases as the slenderness ratio decreases. The cracking moments of the 5.75” panels are 46.6% larger than that of the 4.75” panels. The cracking moments of the 7.25” panels are 134.0% larger than that of the 4.75” panels. The cracking moments of the 9.5” panels are 400.1% larger than that of the 4.75” panels. This greatly increases the panel stability by increasing the lateral load required to crack the concrete in the panels.

The cracking moment is so much larger in panels with lower slenderness ratios primarily due to the gross moment of inertia. As shown in Table 3-3, the gross moment of inertia increases much more than the cracking moment of inertia as slenderness ratios decrease. This leads to the cracking moment increasing much more dramatically than the nominal moment, making the first portion of the bilinear equation (prior to cracking) sustain even more load than the second portion (between cracking and panel yielding).

Table 3-3: Impact of Slenderness Ratio on Cracking Moment

Panel Designation	(h/t)	I_g (in^4)	I_{cr} (in^4)	M_{cr} (K-ft)
Panel 4.75-5-.75	60.63	428.688	67.410	3.571
Panel 5.75-5-.75	50.09	760.438	117.702	5.234
Panel 7.25-5-.75	39.72	1524.313	174.590	8.320
Panel 9.5-5-.75	30.32	3429.500	253.896	14.286
Panel 4.75-7.5-.75	60.63	428.688	67.410	5.357
Panel 5.75-7.5-.75	50.09	760.438	117.702	7.850
Panel 7.25-7.5-.75	39.72	1524.313	174.590	12.480
Panel 9.5-7.5-.75	30.32	3429.500	253.896	21.429
Panel 4.75-5-.85	60.63	428.688	47.343	4.048
Panel 5.75-5-.85	50.09	760.438	82.512	5.931
Panel 7.25-5-.85	39.72	1524.313	122.584	9.430
Panel 9.5-5-.85	30.32	3429.500	179.016	16.191
Panel 4.75-7.5-.85	60.63	428.688	47.343	6.071
Panel 5.75-7.5-.85	50.09	760.438	82.512	8.897
Panel 7.25-7.5-.85	39.72	1524.313	122.584	14.144
Panel 9.5-7.5-.85	30.32	3429.500	179.016	24.286

3.7 Lightweight Concrete Results

Three primary factors were adjusted in the parametric study to analyze the differences between lightweight and normal weight concrete in the tilt-up panels: the concrete weight w_c, the K factor used in the modulus of rupture, and the lightweight concrete factor λ. Since the concrete weight was adjusted based on the lightweight concrete factor (see section 3.3), the results have been separated into two categories: panels with varied values for λ and w_c, and panels with varied values for the K factor.

For analysis of the impact of the lightweight concrete factor, panels with a K value of 5 were selected for direct comparison with the Report of the Task Committee on Slender Walls (Simpson et al., 1982). These panels correlate directly to current ACI 318 (2019) code recommendations, as a K value of 5 equates to a K value of 7.5 due to the adjustments that were made to Equation 3-19. The graphs displaying this comparison are shown in Figures 3-10, 3-11, 3-12, and 3-13.

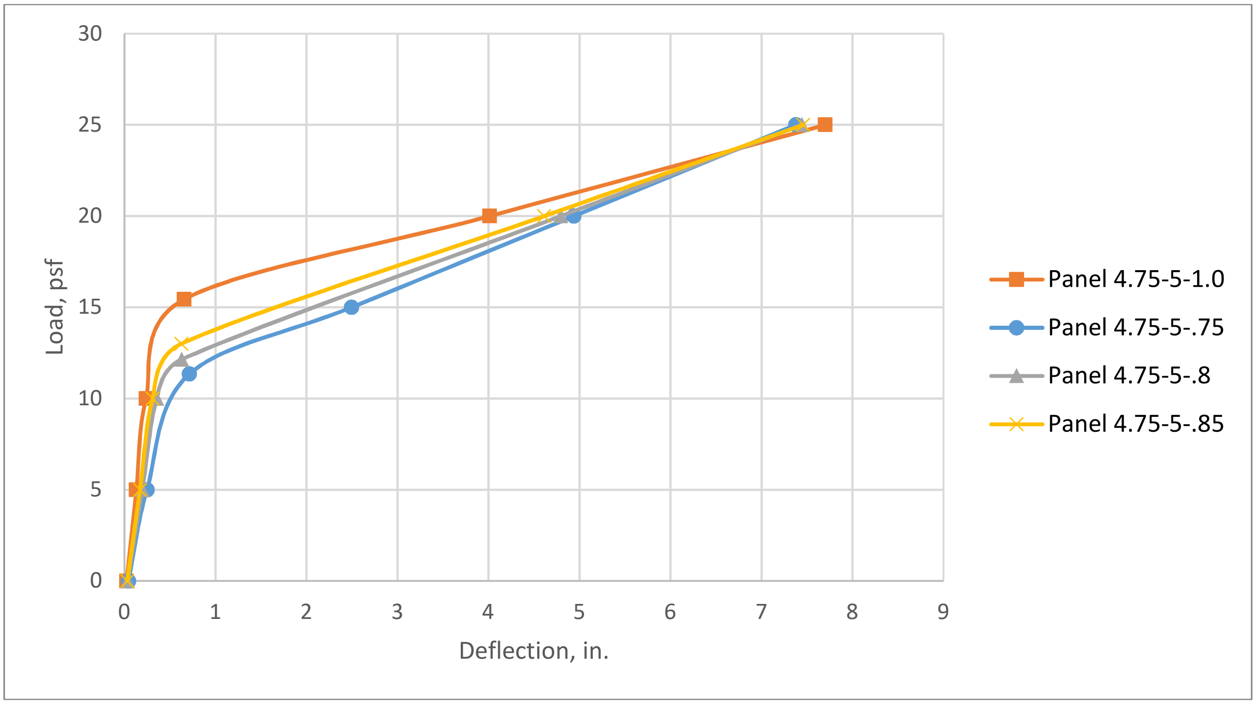

Figure: 3-10 4.75" Deflection Curve – K = 5, λ Varies

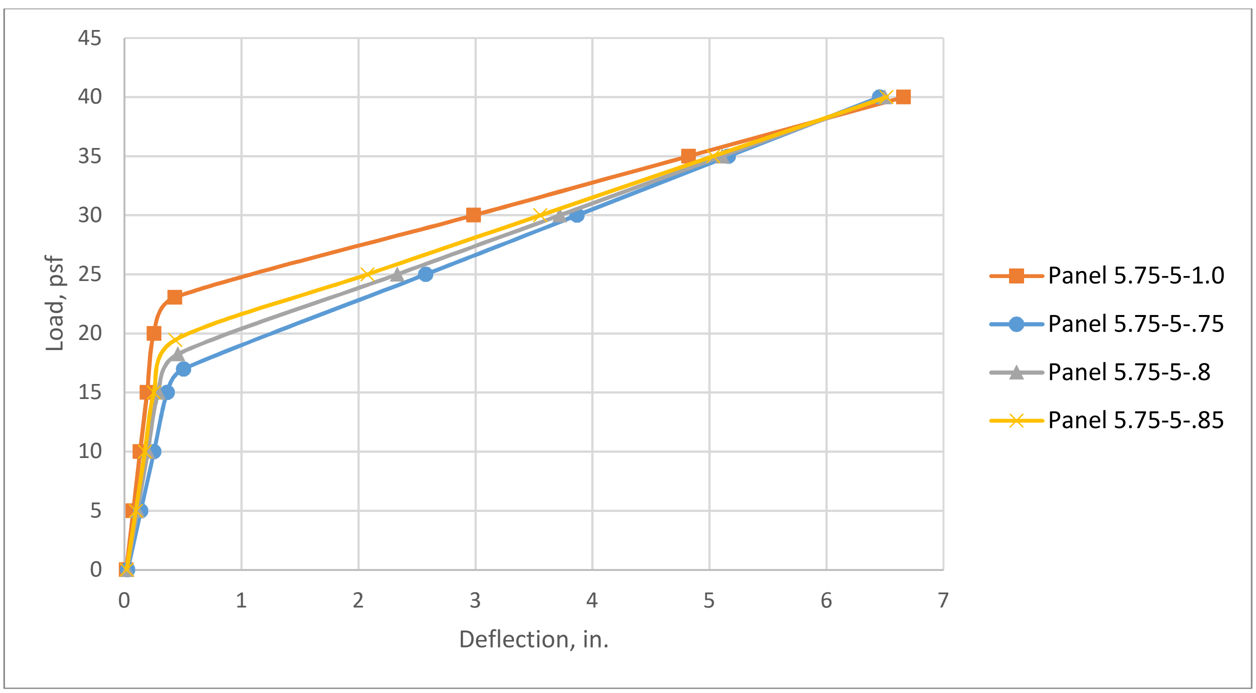

Figure: 3-11 5.75" Deflection Curve – K = 5, λ Varies

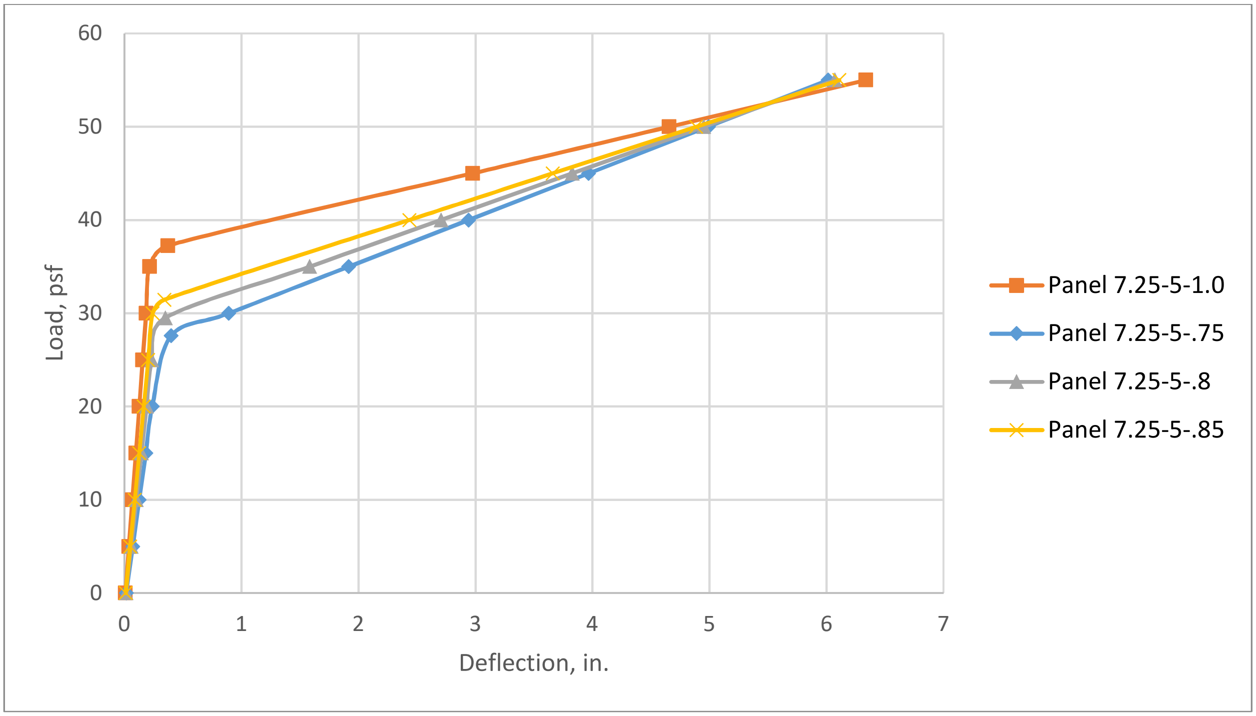

Figure: 3-12 7.25” Deflection Curve – K = 5, λ Varies

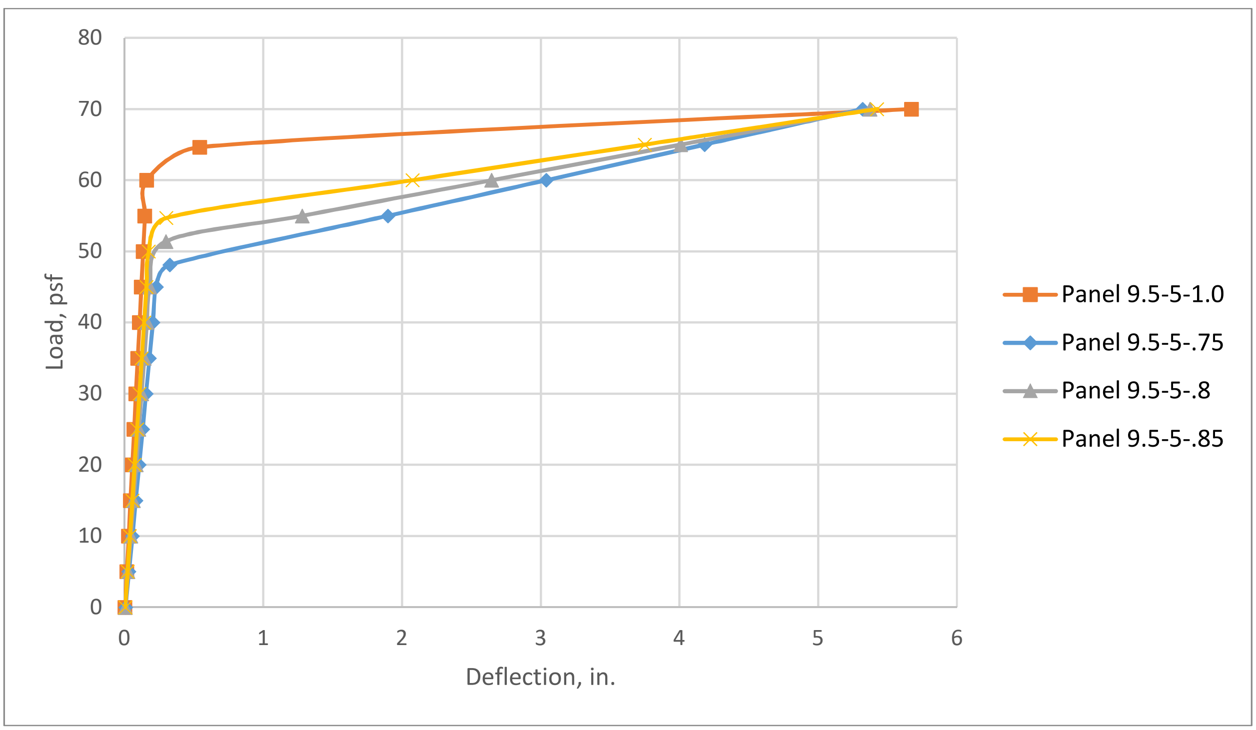

Figure: 3-13 9.5” Deflection Curve – K = 5, λ Varies

As the panels approach their nominal moment, the panels intersect near their nominal moment capacity. This suggests that stability might govern for the deflection in the panels as panels approach yielding. Near the nominal capacity, or panel yielding, the panel stiffness has a very small impact on the deflections compared to near panel cracking.

The results of this comparison at two selected lateral loads are shown in Table 3-4. The two loads selected for this analysis were chosen as a load that resulted in approximately the cracking moment and an arbitrary load past the cracking moment and before the lines converged. Table 3-4 was used in conjunction with Figures 3-9 through 3-13 to most effectively convey the results of the study.

Table 3-4: Impact of Lightweight Concrete Factor λ on Deflection

Panel Designation	Lateral Load (psf)	Deflection (in.)	% Increase
Panel 4.75-5-1.0	15.45	0.657	-
	20.00	4.014	-
Panel 4.75-5-.85	13.00	0.623	-5.2%
	20.00	4.611	14.9%
Panel 4.75-5-.8	12.15	0.628	-4.4%
	20.00	4.793	19.4%
Panel 4.75-5-.75	11.35	0.713	8.5%
	20.00	4.936	23.0%
Panel 5.75-5-1.0	23.05	0.432	-
	30.00	2.985	-
Panel 5.75-5-.85	19.45	0.433	0.2%
	30.00	3.554	19.1%
Panel 5.75-5-.8	18.25	0.456	5.6%
	30.00	3.720	24.6%
Panel 5.75-5-.75	17.00	0.506	17.1%
	30.00	3.868	29.6%
Panel 7.25-5-1.0	37.25	0.369	-
	45.00	2.975	-
Panel 7.25-5-.85	31.45	0.340	-7.9%
	45.00	3.660	23.0%
Panel 7.25-5-.8	29.50	0.348	-5.7%
	45.00	3.827	28.6%
Panel 7.25-5-.75	27.60	0.399	8.1%
	45.00	3.966	33.3%
Panel 9.5-5-1.0	64.65	0.544	-
	65.00	0.880	-
Panel 9.5-5-.85	54.70	0.302	-44.5%
	65.00	3.751	326.3%
Panel 9.5-5-.8	51.40	0.298	-45.2%
	65.00	4.009	355.6%
Panel 9.5-5-.75	48.10	0.326	-40.1%
	65.00	4.181	375.1%

The decrease in deflections at the cracking moment for some of the panels can be attributed to the normal weight panels having such larger cracking moments. For comparison purposes, the following discussion will focus on the arbitrary loads between the cracking moment and the nominal moment, which compares deflection at the same load for each panel thickness.

As shown in the table, the increase in deflection from normal weight (λ = 1.0) to lightweight concrete (λ = 0.85, 0.8, 0.75) can be sizeable. Deflections were increased considerably as the lightweight concrete factors decreased within the same panel thickness at loads before the panel yielded. While this was the case for smaller loads, as the load increased, the impact was lessened. This shows that the ACI 318 (2019) linear interpolation used assumes that stability will govern at loads near panel yielding. For the loads that result in deflections before the panel has yielded, the deflections in slender tilt-up wall panels increase as the aggregate density is decreased. A lower density aggregate is accounted for in design through λ, which results in larger deflections at all applied lateral loads.

Adil Nassar recorded the splitting tensile strength f_{ct} of lightweight and normal weight concrete girders during testing (2002). Four of his test specimens used 800 lbs of lightweight coarse aggregate with 1419 lbs of natural sand while another test specimen used 1873 lbs of normal weight coarse aggregate with 1208 lbs of natural sand. All other components of the concrete mix were held constant. The results of the splitting tensile strength test yielded a strength of 537 psi for the four lightweight specimens and 845 psi for the normal weight specimen.

ACI 318 (2019) permits the substitution of $f_{ct}/6.7$ for $\lambda\sqrt{f'_c}$ in the modulus of rupture equation (equation 3-14). Using this substitution in equation 3-14 gives a modulus of rupture of 601 psi for the lightweight mix and 946 psi for the normal weight mix. Proportionally, the lightweight girders had a modulus of rupture that was 63.6% smaller than the normal weight girder. If these values were to be used to calculate the cracking moment M_{cr} with Equation 3-11, the lightweight girders would reach their cracking moment well before the normal weight girders. This would lead to larger deflections in the lightweight girders under loading conditions that would induce bending, and implies that using lightweight concrete in place of normal weight concrete would increase deflections through the lightweight concrete factor λ.

The next analysis involved panels with varied K values and constant λ. Two sets of λ were used: one set with $\lambda = 0.75$ to represent all-lightweight concrete with fine and coarse aggregates complying with ASTM C330 per ACI 318 (ACI Committee 318, 2019) and the other set with $\lambda = 1.0$ (normal weight concrete) for a direct comparison with the Report of the Task Committee on Slender Walls (Simpson et al., 1982). The first set of data examined was the lightweight concrete comparison with $\lambda = 0.75$. Graphs displaying these results for each panel thickness are shown in Figures 3-14 through 3-21.

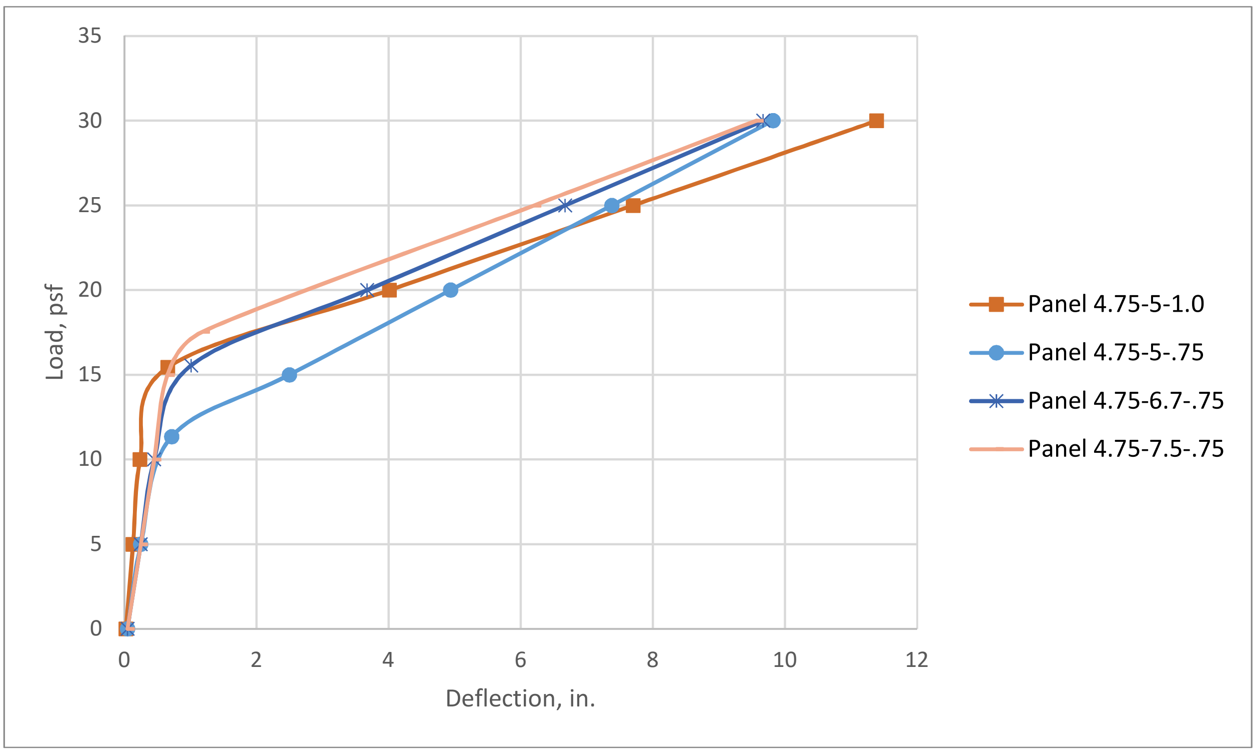

Figure 3-14: 4.75” Deflection Curve – K Varies, λ = 0.75

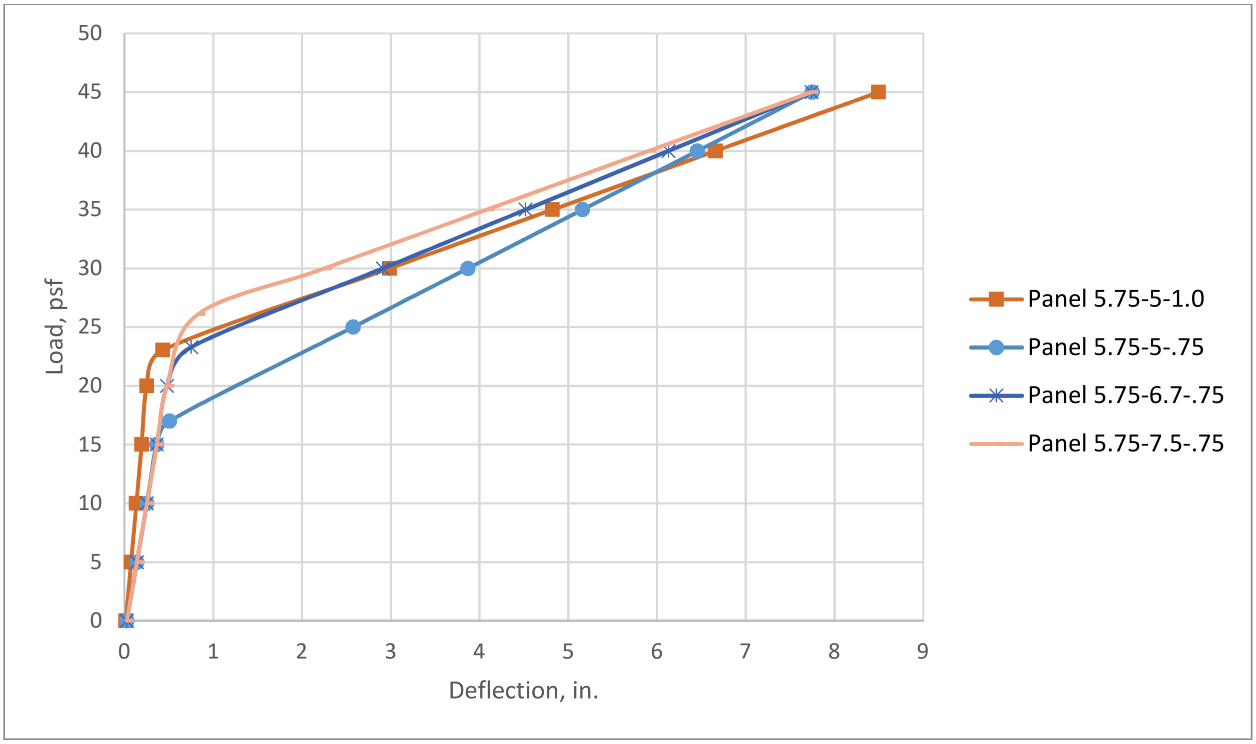

Figure: 3-15 5.75" Deflection Curve – K Varies, λ = 0.75

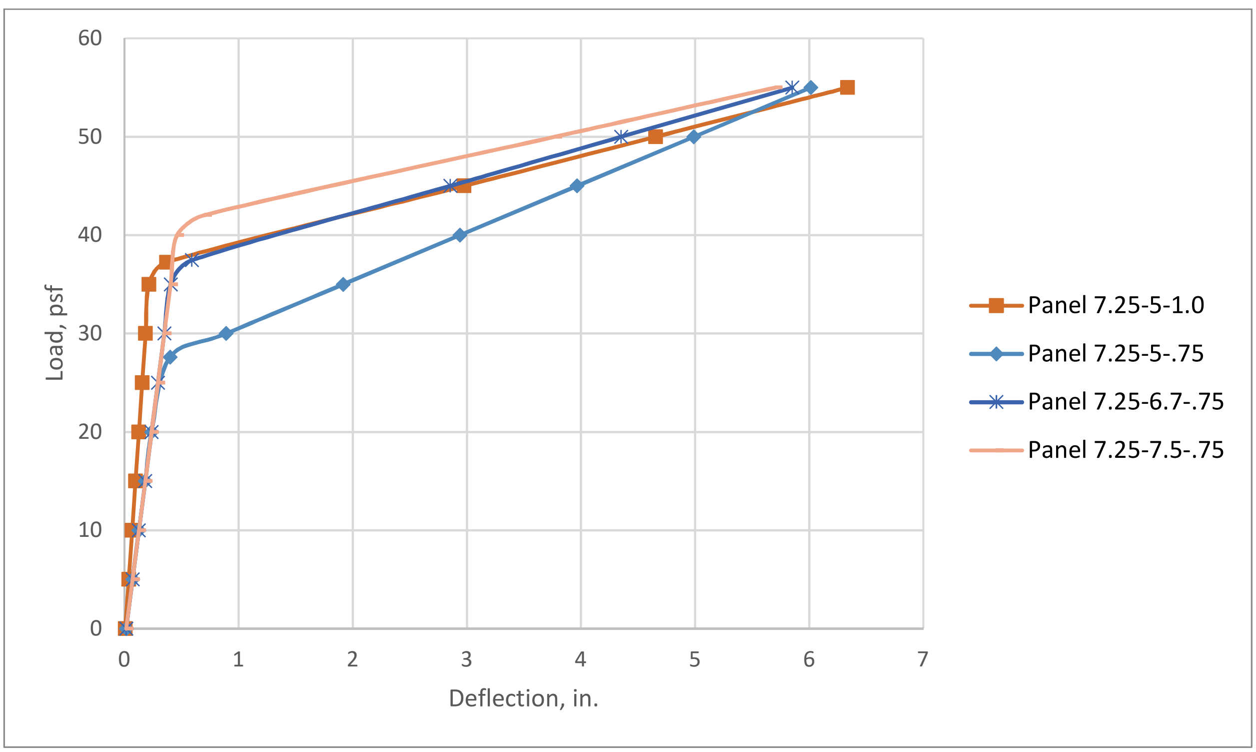

Figure: 3-16 7.25" Deflection Curve – K Varies, λ = 0.75

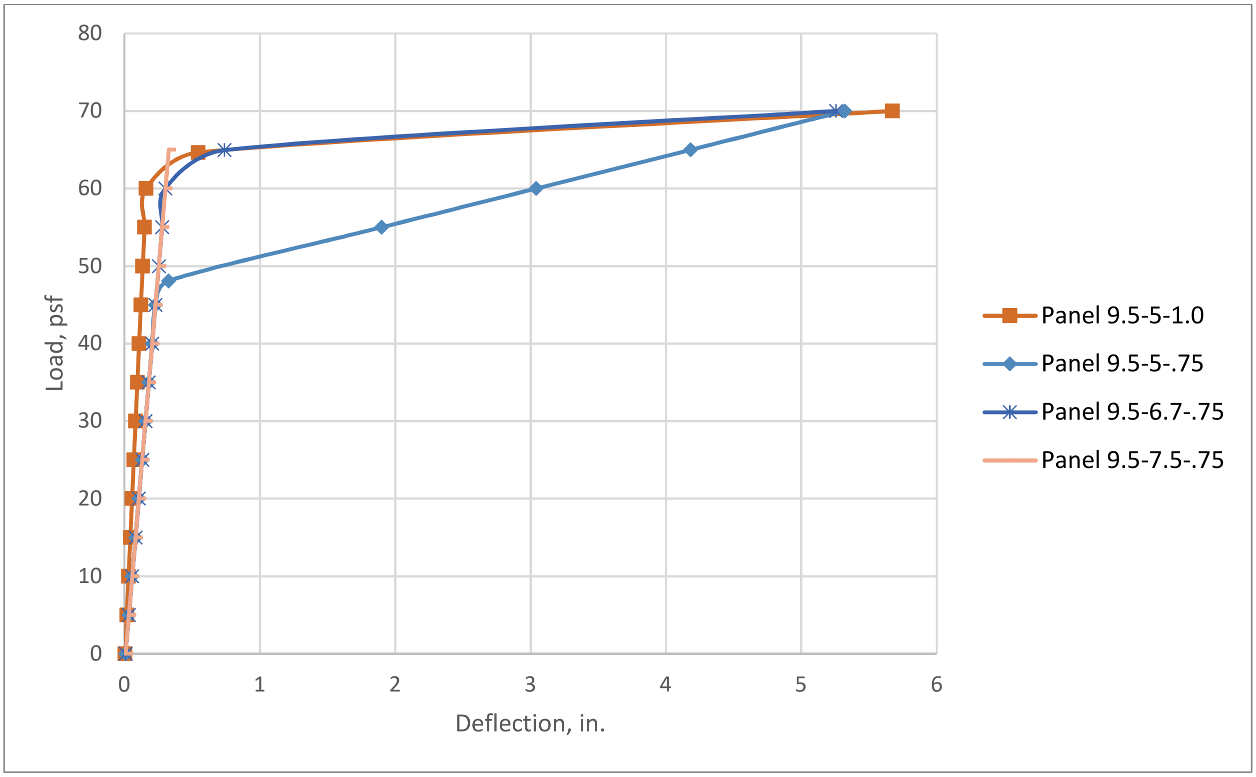

Figure: 3-17 9.5" Deflection Curve – K Varies, λ = 0.75

These results at two selected lateral loads are shown in Table 3-5. These two lateral loads were selected similarly to the loads in Table 3-4 where the first was a load that resulted in the cracking moment, and the second was a load occurring past the cracking moment and before the curves intersected at the nominal moment capacity. Figures 3-14 through 3-17 include the parametric study deflections for the slender wall test report panels (normal weight) for reference. Since these panels have a lightweight concrete modification factor of 1.0, they were not used in this comparison. To show the relationship between deflection and the K factor in lightweight concrete, Table 3-5 relates the deflection of panels with K factors of 7.5 and 6.7 to panels with a K factor of 5.

Table 3-5: Impact of K Factor on Deflection

Panel Designation	Lateral Load (psf)	Deflection (in.)	% Decrease
Panel 4.75-5-.75	11.35	0.713	-
	20.00	4.936	-
Panel 4.75-6.7-.75	15.55	1.008	-41.4%
	20.00	3.675	25.5%
Panel 4.75-7.5-.75	17.55	1.187	-66.5%
	20.00	2.836	42.5%
Panel 5.75-5-.75	17.00	0.506	-
	30.00	3.868	-
Panel 5.75-6.7-.75	23.30	0.751	-48.4%
	30.00	2.909	24.8%
Panel 5.75-7.5-.75	26.10	0.828	-63.6%
	30.00	2.253	41.8%
Panel 7.25-5-.75	27.60	0.399	-
	45.00	2.941	-
Panel 7.25-6.7-.75	37.45	0.591	-48.1%
	45.00	2.854	3.0%
Panel 7.25-7.5-.75	42.05	0.704	-76.4%
	45.00	1.843	37.3%
Panel 9.5-5-.75	48.10	0.326	-
	65.00	4.181	-
Panel 9.5-6.7-.75	64.95	0.737	-126.1%
	65.00	0.782	81.3%
Panel 9.5-7.5-.75	72.90	-	-
	65.00	-	-

The decrease in deflections at the cracking moment for some of the panels can be attributed to the panels with larger K values having such larger cracking moments. For comparison purposes, the following discussion will focus on the arbitrary loads between the cracking moment and the nominal moment, which compares deflection at the same load for each panel thickness. Additionally, Panel 9.5-7.5-.75 had a cracking moment that was larger than its nominal moment. The bilinear equation for service level deflection is limited by the nominal moment capacity. This would be unlikely to occur in actual design, so this panel will be disregarded in the following comparison.

These results show that the K factor used in the modulus of rupture has a significant impact on the deflection in slender tilt-up panels. The linear interpolation again yields deflections that converge near the nominal moment capacity, as the panel stiffness has less of an impact.

The K factor has a larger impact on the deflection than the lightweight concrete factor. Numerically, lowering the K factor from 7.5 to 5 in the modulus of rupture (Equation 3-14) results in a 66.7% reduction in f_r, while lowering λ from 1.0 to 0.75 results in a 75% reduction.

The second set of panels with varied K values analyzed in this parametric study are normal weight panels (λ = 1.0). While the focus of this report is on lightweight concrete panels, this set of data is provided for comparison to the Report of the Task Committee on Slender Walls (Simpson et al., 1982) since no tests have been performed on deflection in lightweight slender tilt-up wall panels. This comparison is shown in Figures 3-18 through 3-21.

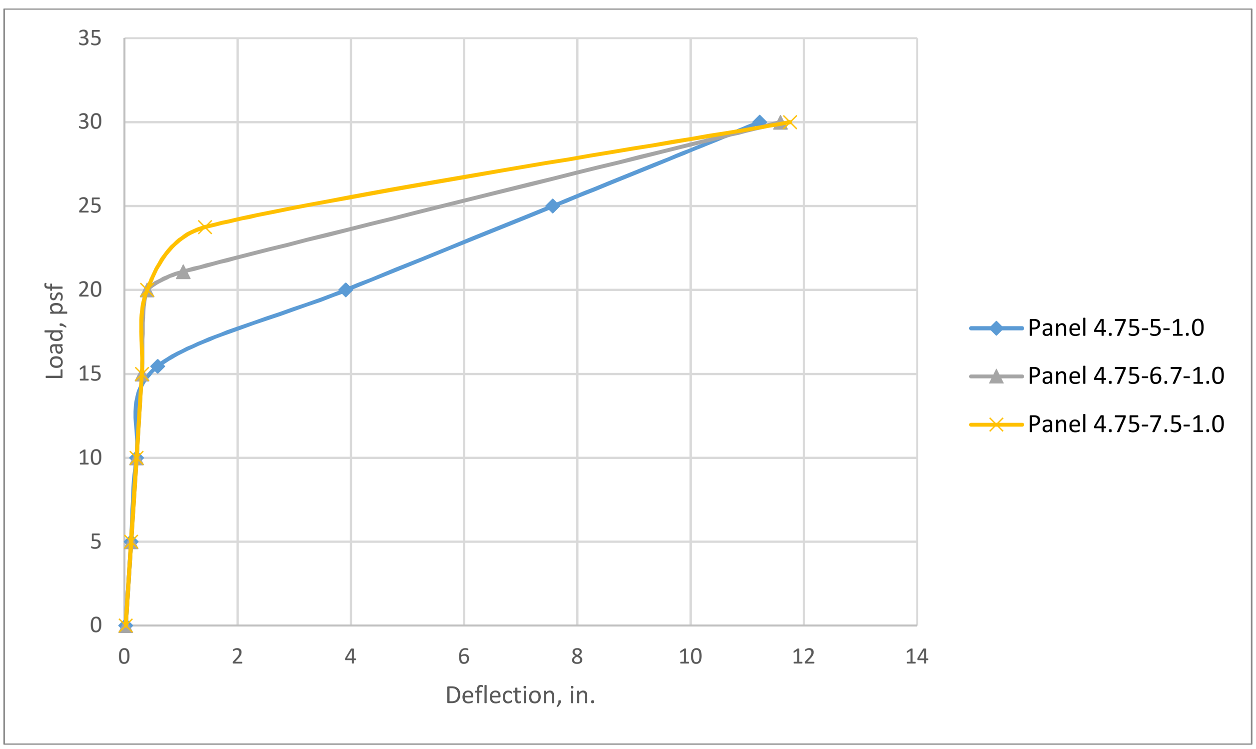

Figure 3-18: 4.75” Deflection Curve – K Varies, λ = 1.0

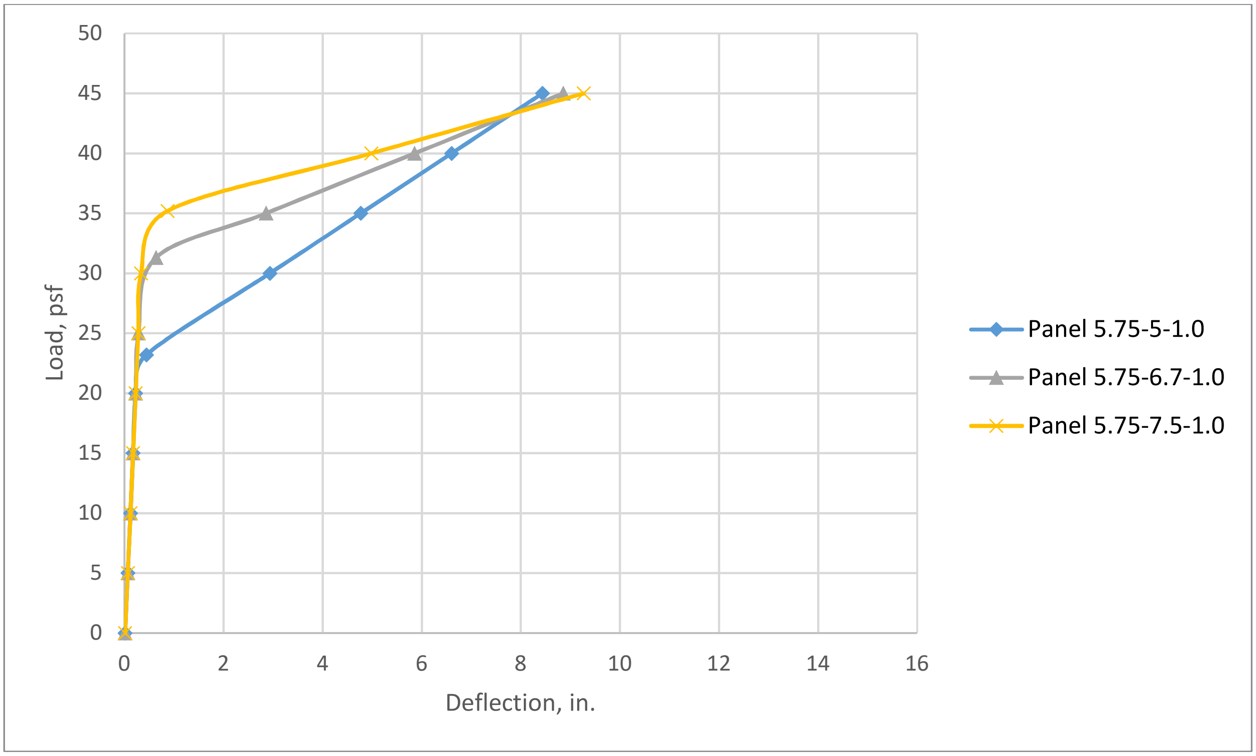

Figure 3-19: 5.75” Deflection Curve – K Varies, λ = 1.0

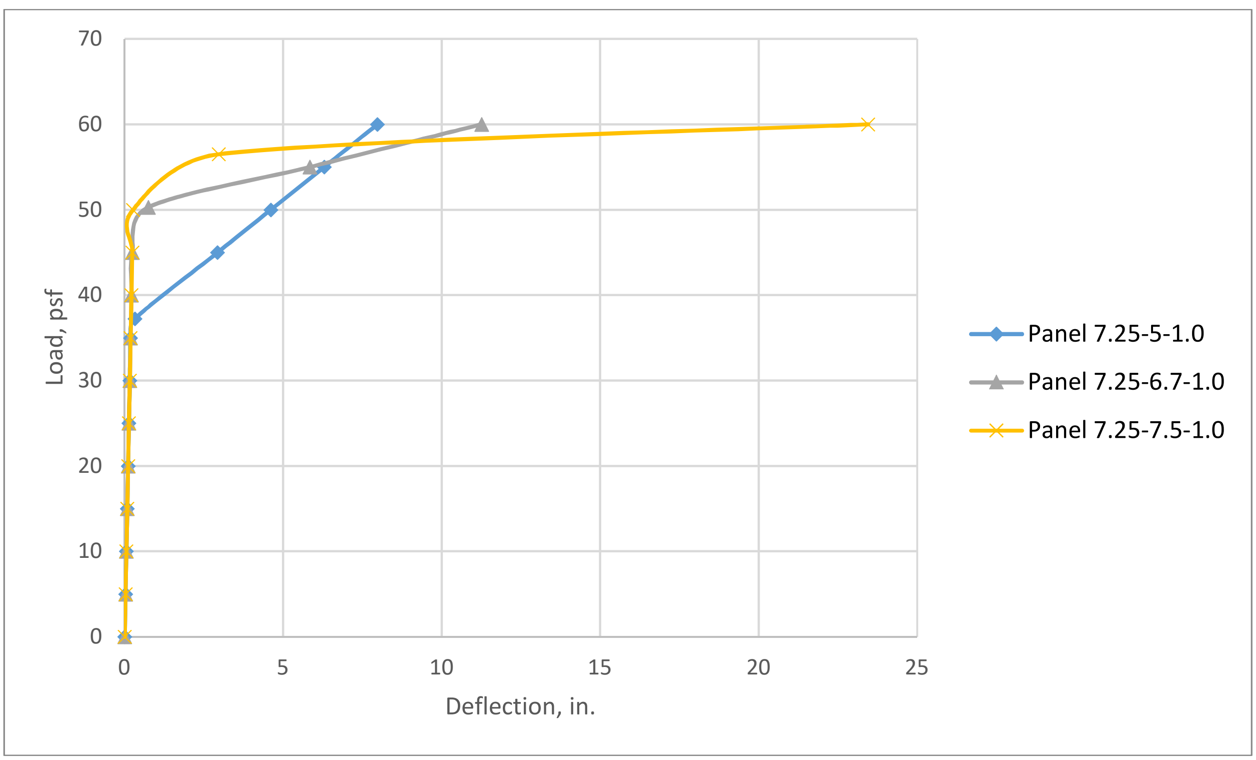

Figure 3-20: 7.25” Deflection Curve – K Varies, λ = 1.0

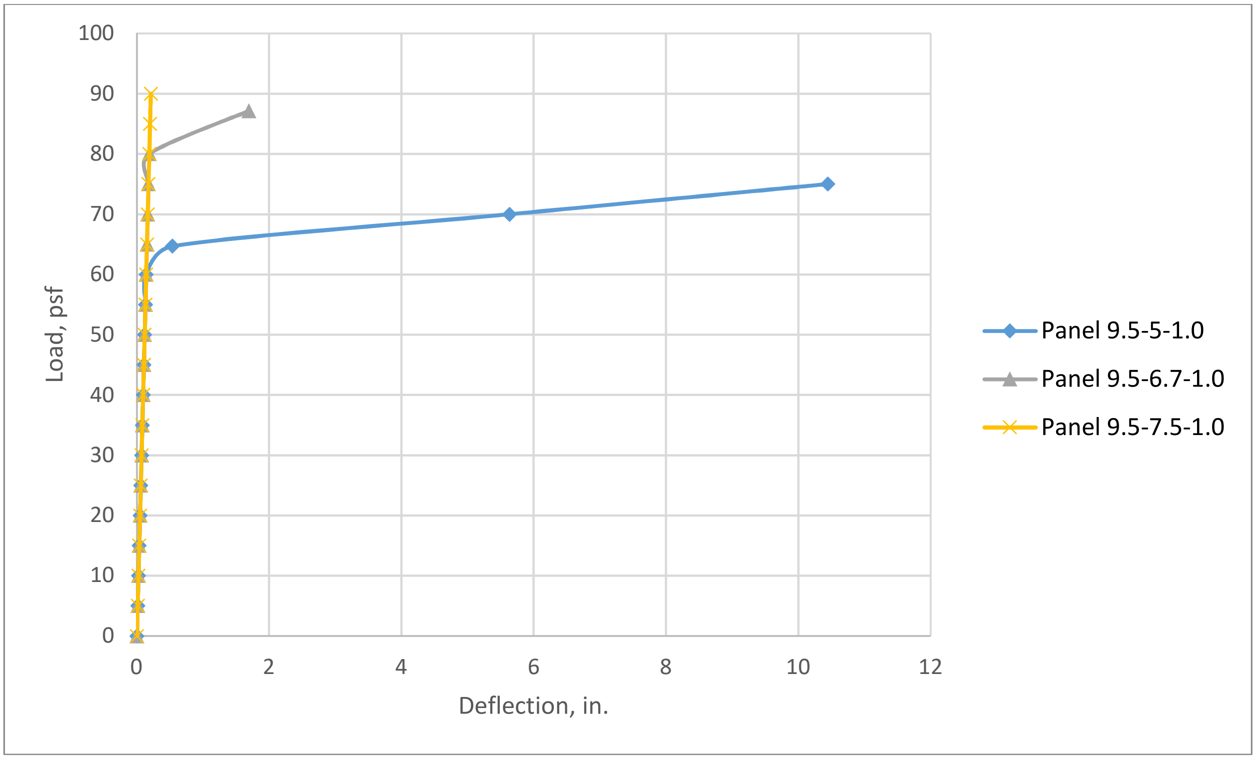

Figure 3-21: 9.5” Deflection Curve – K Varies, λ = 1.0

Examination of these figures reveals the similar behavior to Figures 3-14 through 3-17: as the K factor is reduced, the deflection at an applied lateral load is generally increased. Once again, the deflection curves intersect near the panel nominal moment capacity. Panel 9.5-7.5-1.0 was limited by having a cracking moment larger than the nominal moment, as discussed in section 3.6.

Additionally, this comparison shows that the K factor used in the modulus of rupture has no impact on the deflection for lateral loads that result in a moment lower than the cracking moment of the panel. Table 3-6 shows that the service level deflection calculated in accordance with ACI 318 code (2019) is the same for panels of the same thickness at lateral loads below the panel cracking moment. The lateral load displayed for each panel thickness was selected as a load roughly halfway between the cracking moment M_{cr} and an applied lateral load of 0.

Table 3-6: Deflection with Varied K Factor Below Cracking Moment

Panel Designation	K Factor	Lateral Load (psf)	Deflection (in)
Panel 4.75-5-1.0	5	10	0.21097
Panel 4.75-6.7-1.0	6.7	10	0.21097
Panel 4.75-7.5-1.0	7.5	10	0.21097
Panel 5.75-5-1.0	5	15	0.17214
Panel 5.75-6.7-1.0	6.7	15	0.17214
Panel 5.75-7.5-1.0	7.5	15	0.17214
Panel 7.25-5-1.0	5	20	0.11247
Panel 7.25-6.7-1.0	6.7	20	0.11247
Panel 7.25-7.5-1.0	7.5	20	0.11247
Panel 9.5-5-1.0	5	30	0.07264
Panel 9.5-6.7-1.0	6.7	30	0.07264
Panel 9.5-7.5-1.0	7.5	30	0.07264

The service level deflection at lateral loads resulting in moments less than the cracking moment is calculated using the gross moment of inertia I_g. I_g is determined based solely on geometric properties and is not influenced by the modulus of rupture. Once the concrete has cracked, however, the cracking moment M_{cr} is used in the deflection calculation (Equation 3-20). The cracking moment incorporates the modulus of rupture f_r, which is partially determined with the K factor. Therefore, until the concrete has cracked, the K factor has no influence on the deflection based on the code equations.

The lightweight concrete facto λ r acts similarly, but since λ is determined based on the weight of the concrete w_c, there will still be an effect in the deflection at lateral loads before the concrete has cracked. The concrete weight determines the modulus of elasticity (Equation 2-1), which influences the deflection in the concrete at any applied lateral loading through the deflection corresponding to the cracking moment (Equation 3-18). While this will affect the deflections at these lateral loads, the impact will be minor. This is shown in Figures 3-10 through 3-13.

Chapter 4 - Other Considerations

There are many factors that influence the selection of lightweight or normal weight concrete in the design of tilt-up slender wall panels. This chapter will discuss the cost implications, fireproof ratings, and sustainability of using lightweight concrete in place of normal weight concrete. Other important considerations such as panel weight and panel reinforcement differences are covered in Chapter 5 through design examples.

4.1 Cost Implications

Often one of the most important considerations in the eyes of contractors, design engineers, and building owners is the cost considerations of the type of concrete used in tilt-up wall panels. In a Structure Magazine article (Martin, Zimmer, Bolduc, & Hopps, 2013) the cost of lightweight concrete was compared to the cost of normal weight concrete. This article stated that common pricing for lightweight concrete is $135 per cubic yard. Compared to a price of $105 per cubic yard for normal weight concrete, this is almost a 130% increase in material cost.

While material cost of lightweight concrete may seem expensive, utilizing lightweight concrete can offer savings in other aspects of the construction process. Due to the reduced weight of lightweight concrete, less volume of concrete and structural steel is often required to support the structure. The Structure Magazine article (Martin et al., 2013) performed a comparison of a multiuse composite structural steel building. The comparison considered two buildings which were identical except for normal weight concrete used in system A and lightweight concrete in system B. System A, which used normal weight concrete, was estimated to cost $14.35 per square foot. As a result of less steel, concrete, and shear studs required, system B utilizing lightweight concrete was estimated to cost $11.53 per square foot.

This example demonstrates that even with an increase in material cost per cubic yard, using lightweight concrete often offsets this by reducing the overall cost of the structure. Tilt-up projects in particular can have even more cost benefit for using lightweight concrete. Reduced weight in the wall panels results in lifting advantages and smaller footings.

Two benefits involving the lifting process when utilizing lightweight concrete panels are using a lower capacity crane and having larger panels. For panels of similar size, a lightweight panel will weigh roughly 60% to 77% the weight of a normal weight panel. Since the costs of the crane rental can be one of the most expensive factors in the construction of tilt-up panels, using a lower capacity crane is an effective way to reduce construction costs. It is important, however, for contractors and designers to include the water weight of the panel at the time of the lift. Since lightweight panels can have water absorption of up to 25% in some cases, the weight of the wet concrete can increase the panel weight. This can also impact the construction schedule, as architectural finishes cannot be applied while the concrete is still wet.

Additionally, tilt-up panel size is limited by the weight of the panel. Generally, 80-ton capacity cranes are used for lifting tilt-up panels. The largest panel that can be safely lifted by an 80-ton crane is a 40-ton panel, or 80,000 lbs (Ward, 2011). As an example, a 40-ton normal weight panel with a thickness of 8 inches would have 800 square feet of wall surface area. With lightweight concrete, the surface area of the same weight and thickness panel is increased to 1,040 square feet for 115 pcf concrete and 1,333 square feet for 90 pcf concrete.

Reduced panel weight also results in smaller footings to support the structure. Typical tilt-up structures are supported by spread footings (continuous) as the foundation system. Footing size and reinforcement are designed by the engineer with the primary considerations being soil bearing capacity and the structural weight (Ward, 2011). Since lightweight panels reduce the panel weight by 60% to 77%, a much smaller load is applied to the footing, resulting in a reduction in footing size and required reinforcement. This reduction leads to further material cost savings in lightweight tilt-up design.

4.2 Fireproof Rating

Another consideration in the design of any structural system is its fire resistance properties. Concrete in general is one of the most effective construction materials for fire resistance (Ward, 2011). Lightweight concrete is particularly effective in fire resistance due to the low-density aggregates used in the mix. The International Building Code (IBC) lists fire resistance ratings for concrete walls based on the aggregates and wall thickness (International Code Council, 2015). Table 4-1 displays the minimum finish (face-to-face) wall thicknesses of normal weight concrete (siliceous and carbonate aggregates) and lightweight concrete (sand-lightweight and lightweight) to achieve the listed fire ratings.

Table 4-1: IBC Rated Fire Resistance Periods for Concrete Walls

Concrete Material		Minimum Finish Wall Thickness (inches)			
		1 Hour	**2 Hour**	**3 Hour**	**4 Hour**
Normal Weight	Siliceous Aggregate	3.5	5	6.2	7
	Carbonate Aggregate	3.2	4.6	5.7	6.6
	Average	**3.35**	**4.8**	**5.95**	**6.8**
Lightweight	Sand-Lightweight	2.7	3.8	4.6	5.4
	Lightweight	2.5	3.6	4.4	5.1
	Average	**2.6**	**3.7**	**4.5**	**5.25**

Compared to lightweight concrete, normal weight concrete requires 0.75 to 1.55 inches of additional wall thickness to achieve the same fire resistance rating. The fire resistance properties of lightweight concrete offer an advantage in thinner wall panel thickness required to meet code.

4.3 Sustainability

Lightweight concrete offers some sustainability benefits due to the ability to use recycled materials and renewable materials as aggregates. Typical normal weight concrete aggregates are considered a non-renewable resource, and 30 million tons of natural aggregate are consumed yearly. At this rate, it is estimated that the natural aggregate supply will be exhausted in 20 years (Park, Kim, Roh, & Kim, 2019). Due to this rapidly declining supply, researchers are looking into viable alternatives to traditional natural aggregates.

Lightweight concrete can make use of renewable natural aggregates. Date palm seeds have been researched as an alternative to river-sourced aggregate (Almograbi, 2010). Date palm seeds can be used as lightweight concrete aggregate once harvested, cleaned, and dried. While the strength of concrete using this aggregate has yet to be tested, Almograbi performed tests on durability under various conditions. These tests showed similar results to traditional lightweight concrete in water permeability, water absorption, and sorptivity. While testing on strength capacity of date palm seeds and other renewable aggregates needs further study, it is a promising substitute for traditional, non-renewable aggregates.

Another potential replacement for non-renewable aggregates is recycled aggregates. One recyclable resource that has been studied is waste polystyrene (Herki, Safary, & Khalid, 2016). Using waste polystyrene has two environmental benefits: it replaces traditional, non-renewable aggregate in concrete and reduces landfill waste. Compared to normal weight concrete, mixes containing 20%, 40%, and 60% waste polystyrene had a reduction in density of 11%, 17%, and 30% respectively. This study performed cube tests on both normal weight concrete with traditional aggregates and lightweight concrete with waste polystyrene aggregate. The cube tests revealed that the 20%, 40%, and 60% waste polystyrene concrete mixes had a 28-day compressive strength reduction of 34%, 51%, and 67% respectively. Strength reduction is typically expected in lower density concrete and is partially offset by reduced structural weight. The sample mixes containing the waste polystyrene also failed with more ductile behavior than the brittle compressive failure that is typically seen in concrete. This added ductility allowed the lightweight samples to retain the load after failure. The final test performed in the study was on water absorption. The normal weight concrete had an absorption rate of 4.65% while the samples with waste polystyrene had a slightly increased absorption rate of 4.97% to 6.06%. The increase in water absorption is primarily due to shrinkage in the polystyrene particles. Overall, waste polystyrene showed potential as a viable replacement to non-renewable aggregates.

While recycled aggregates solve the solution of limited natural aggregate supply, some negative impacts on the environment have been observed. A study performed by Lukic, Malesev, Radonjanin, and Milovanovic (2013) compared the environmental effects of recycled lightweight aggregates and normal weight aggregates using the following four metrics: global warming, eutrophication, acidification, and photochemical ozone creation. First, the study analyzed the environmental impacts involved in the production of both normal weight aggregates and recycled lightweight aggregates. The results of this study are shown in Table 4-2.

Table 4-2: Average Increase in Environmental Impact of Recycled Aggregate Production

	Global Warming	Eutrophication	Acidification	Photochemical Ozone Creation
Production	62.35%	87.25%	121.00%	48.15%

The production of recycled aggregates resulted in an increase in environmental impact in all four metrics that were researched. The study attributed the increase to using more cement with the recycled aggregate mix to achieve the same strength as the normal weight mix as well as the more involved production required for the recycled aggregates. After researching production environmental impacts, the study analyzed the impacts involved in transportation. The influence of transport on the environmental impact for the four metrics is shown in Table 4-3.

Table 4-3: Average Influence of Transportation on Environment Impact

Aggregate	Global Warming	Eutrophication	Acidification	Photochemical Ozone Creation
Recycled	6.35%	20.55%	8.60%	8.60%
Normal	10.65%	40.75%	19.90%	13.50%

The study concluded that the transportation of normal weight concrete was a much larger percentage of its environmental impact in comparison to the recycled aggregate lightweight concrete. Since the recycled aggregate concrete is a lower density, the impact of transportation on the environment is less than the more dense normal weight concrete.

Since recycled aggregates are relatively new to the construction industry, the production process is less refined than normal weight concrete. While the production of recycled aggregates will likely always require more processing than the non-renewable normal weight aggregates, the process could potentially be refined further. Developments in the production process could result in more efficient methods with less environmental impact. Until further advances are made, however, natural renewable aggregates appear to be the most promising substitution for non-renewable aggregates.

Chapter 5 - Design Examples

Two design problems were analyzed for comparison following the Design Guide for Tilt Up Concrete Panels (ACI Committee 551, 2015) in accordance with ACI 318 code (2019). The purpose of these design examples is to communicate the design process of slender tilt-up wall panels and convey differences between normal weight and lightweight panels of a typical design size. The first problem was be designed as a normal weight concrete tilt-up panel, while the second was designed as a lightweight concrete tilt-up panel.

Both problems were designed with one layer of reinforcement located in the center of the panel. Horizontal reinforcement was not considered as it does not impact the moments and deflections resulting from out-of-plane wind loads. The same panel size, applied loads, and all mechanical properties that are not influenced by lightweight concrete were used in both design examples. These values are listed in Table 5-1. The panels in both problems have no openings and support loads from three roof joists with an eccentricity of 3 inches. A figure displaying the design panel for both problems is shown in Figure 5-1. ACI 318 (2019) references are shown in the design problems. Equations 3-4 through 3-7 were used as the load combinations.

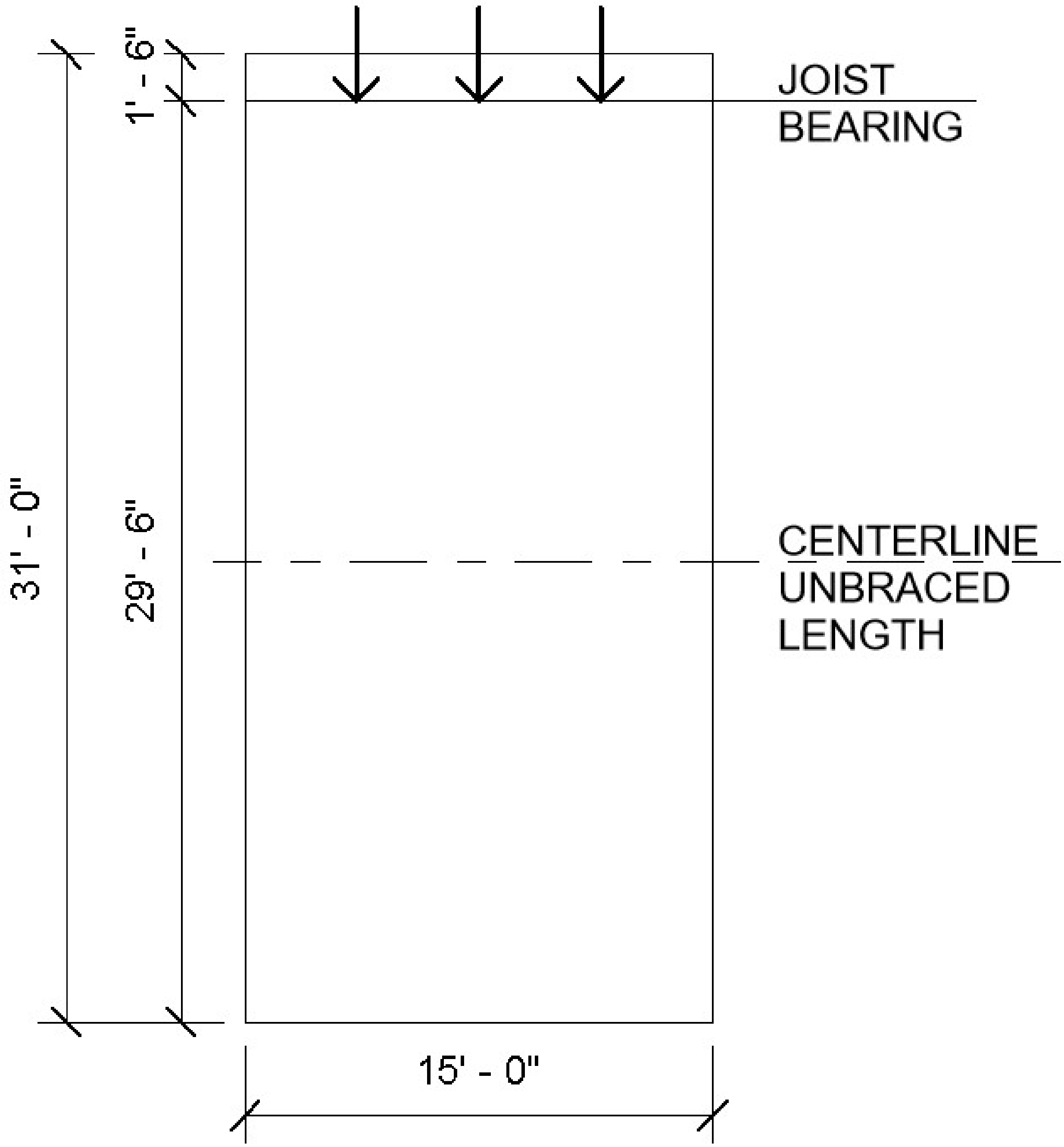

Figure 5-1: Tilt-Up Wall Panel without Openings

Table 5-1: Panel Dimensions, Applied Loads, and Mechanical Properties

Panel Dimensions			
Panel Thickness	$h=$	6.25	in.
Panel Height	$l_{total}=$	31	ft.
Panel Width	$l_w=$	15	ft.
Joist Bearing Height	$l_c=$	29.5	ft.
Load Eccentricity	$e_{cc}=$	3	in.
Applied Loads			
Axial Dead Load	$D=$	2.4	K
Axial Roof Live Load	$L_r=$	2.5	K
Wind Load	$W=$	27.2	lb/ft^2
Mechanical Properties			
28-Day Compressive Strength	$f'_c=$	4,000	psi
Steel Yield Stress	$f_y=$	60,000	psi
Steel Modulus of Elasticity	$E_s=$	29,000	ksi

5.1 Design Example 1 – Normal Weight Slender Tilt-Up Wall Panel

Mechanical Properties

$w_c = 150\ pcf$

$E_c = 57{,}000\sqrt{f'_c} = 57{,}000\sqrt{4{,}000\ psi} = 3{,}605\ ksi$ (19.2.2.1.b)

$n = \frac{E_s}{E_c} = \frac{29{,}000\ ksi}{3{,}605\ ksi} = 8.044$

$f_r = 7.5\lambda\sqrt{f'_c} = 7.5(1.0)\sqrt{4{,}000\ psi} = 474\ psi$ (19.2.3.1)

Load Determination and Load Cases

$P_{DL} = 3(2.4\ K) = 7.2\ K$

$P_{LL} = 3(2.5\ K) = 7.5\ K$

The weight of the wall panel above the centerline of the unbraced length:

$\left(\frac{6.25\ in}{12\ in/ft}\right) 150\ psf(15\ ft)\left(\frac{29.5\ ft}{2} + 1.5\ ft\right)\left(\frac{1\ K}{1000\ lb}\right) = 19.0\ K$

Strength Determination – Load Case 1

Assume 16 No. 6 bars

$A_s = 7.0\ in^2$

$P_{ua} = 1.2(7.2\ K) + 1.6(7.5\ K) = 20.6\ K$

$P_{um} = 20.6\ K + 1.2(19.0\ K) = 43.4\ K$

$w_u = 0.5(15\ ft)(27.2\ psf) = 204\ plf = 0.204\ klf$

Check vertical stress at mid-height of panel

$\frac{P_{um}}{A_g} = \frac{43.4\ K\ (1000\ lb/1\ K)}{6.25\ in(15\ ft)(12\ in/ft)} = 38.6\ psi < 0.06f'_c = 240\ psi$ (11.8.1.1)

Check design moment strength

$A_{se} = A_s + \frac{P_{um}}{f_y}\left(\frac{h}{2d}\right) = 7.0\ in^2 + \frac{43.4\ K}{60\ ksi}\left(\frac{6.25\ in}{2(3.13\ in)}\right) = 7.72\ in^2$ (R11.8.3.1)

$a = \frac{A_{se}f_y}{0.85f'_cb} = \frac{7.72\ in^2(60\ ksi)}{0.85(4\ ksi)(15\ ft)(12\ in/ft)} = 0.757\ in$

$c = \frac{a}{0.85} = \frac{0.757}{0.85} = 0.891\ in$ (22.2.2.4.1)

$\frac{c}{d} = \frac{0.891}{3.13} = 0.285 < 0.375\ \rightarrow Tension\ Controlled$ (R21.2.2)

$I_{cr} = nA_{se}(d-c)^2 + \frac{l_wc^3}{3}$ (11.8.3.1c)

$= 8.044(7.72\ in^2)(3.13\ in - 0.891\ in)^2 + \frac{15\ ft\left(12\frac{in}{ft}\right)(0.891)^3}{3} = 353\ in^4$

$M_{cr} = \frac{f_rI_g}{y_t} = f_rS = f_r\left(\frac{1}{6}bt^2\right) = 0.474\ ksi\left(\frac{1}{6}\right)(15\ ft)(6.25\ in^2) = 46.3\ K\ ft$ (24.2.3.5)

$\phi M_n = \phi A_{se}f_y\left(d - \frac{a}{2}\right)$

$= 0.9(7.72\ in^2)(60\ ksi)\left(3.13\ in - \frac{0.757\ in}{2}\right) = 46.3\ K\ ft$

Check minimum reinforcement:

$\phi M_n \geq M_{cr}$ (11.8.1.1)

$\rho = \frac{A_s}{bh} = \frac{7.0\ in^2}{15\ ft(12\ in/ft)(6.25\ in)} = 0.00622 > \rho_l = 0.0015$ (11.6.1)

Check applied moment:

$$K_b = \frac{48E_cI_{cr}}{5l_c^2} = \frac{48(3605\ ksi)(353\ in^4)}{5[29.5\ ft(12\ in/ft)]^2} = 97.4\ K$$

$$M_{ua} = \frac{w_ul_c^2}{8} + \frac{P_{ua}e_{cc}}{2} = \frac{0.204\ klf(29.5\ ft)^2}{8} + \frac{20.6\ K(3\ in)}{2(12\ in/ft)} = 24.8\ K\ ft$$

$$M_u = \frac{M_{ua}}{\left(1 - \frac{Pum}{0.75K_b}\right)} = \frac{24.8\ K\ ft}{\left[1 - \frac{43.4\ K}{0.75(97.4\ K)}\right]} = 61.2\ K\ ft < \phi M_n \qquad (11.8.3.1d)$$

$$\Delta_u = \frac{M_u}{0.75\ \ {}_b} = \frac{61.2\ K\ ft(12\ in/ft)}{0.75(97.4\ K)} = 10.0\ in \qquad (11.8.3.1b)$$

Strength Determination – Load Case 2

$P_{ua} = 12.4\ K$

$P_{um} = 35.2\ K$

$w_u = 0.408\ klf$

$\frac{P_{um}}{A_g} = 31.3\ psi < 0.06f'_c = 240\ psi$

$A_{se} = 7.59\ in^2$

$a = 0.744\ in$

$c = 0.875\ in$

$\frac{c}{d} = 0.280 < 0.375\ \rightarrow Tension\ Controlled$

$I_{cr} = 349\ in^4$

$M_{cr} = 46.3\ K\ ft$

$\phi M_n = 94.0\ K\ ft > M_{cr}$

$K_b = 96.4\ K$

$M_{ua} = 45.9\ K\ ft$

$M_u = 89.5\ K\ ft < \phi M_n$

$\Delta_u = 14.8\ in$

Strength Determination – Load Case 3

$P_{ua} = 6.48\ K$

$P_{um} = 23.6\ K$

$w_u = 0.408\ klf$

$\frac{P_{um}}{A_g} = 21.0\ psi < 0.06f'_c = 240\ psi$

$A_{se} = 7.39\ in^2$

$a = 0.725\ in$

$c = 0.853\ in$

$\frac{c}{d} = 0.273 < 0.375\ \rightarrow Tension\ Controlled$

$I_{cr} = 344\ in^4$

$M_{cr} = 46.3\ K\ ft$

$\phi M_n = 91.9\ K\ ft > M_{cr}$

$K_b = 95.1\ K$

$M_{ua} = 45.2\ K\ ft$

$M_u = 67.5\ K\ ft < \phi M_n$

$\Delta_u = 11.4\ in$

Service Deflection

$\Delta_{allowable} = \frac{l_c}{150} = 2.36\ in$ (11.8.1.1)

$\Delta_{cr} = \frac{5M_{cr}l_c^2}{48E_cI_g} = 0.550\ in$ (11.8.4.3a)

$M_{sa} = \frac{w_s l_c^2}{8} + \frac{P_a e_{cc}}{2} = \frac{0.6(27.2\ psf)(15.0\ ft)(29.5\ ft)^2}{8(1000\ lb/K)} + \frac{7.2\ K(3\ in)}{2(12\ in/ft)} = 27.5\ in$

Using M_{sa} to find the initial deflection:

$\Delta_s = \frac{M_{sa}}{M_{cr}}\Delta_{cr} = \frac{27.5\ K\ ft}{46.3\ K\ ft}(0.550\ in) = 0.327\ in$ (11.8.4.1)

$M_a = M_{sa} + P_{sm}\Delta_s = 27.5\ K\ ft + 26.2\ K(0.327\ in)$

$= 28.2\ K\ ft < (2/3)M_{cr} = 30.9\ K\ ft$ (11.8.4.2a)

Iterating Δ_s to determine M_a:

$M_a = 28.26\ K\ ft$

$$\Delta_s = \frac{M_a}{M_{cr}}\Delta_{cr} = \frac{28.26\ K\ ft}{46.3\ K\ ft}(0.550\ in) = 0.335\ in$$

5.2 Design Example 2 – Lightweight Slender Tilt-Up Wall Panel

Mechanical Properties

$$w_c = 100\ pcf$$

$$E_c = w_c^{1.5}33\sqrt{f'_c} = (100\ pcf)^{1.5}33\sqrt{4{,}000\ psi} = 2{,}087\ ksi \qquad (19.2.2.1.b)$$

$$n = \frac{E_s}{E_c} = \frac{29{,}000\ ksi}{2{,}087\ ksi} = 13.896$$

$$\lambda = 0.0075w_c = 0..75(100\ pcf) = 0.75 \qquad (19.2.4.1a)$$

$$f_r = 7.5\lambda\sqrt{f'_c} = 7.5(.75)\sqrt{4{,}000\ psi} = 356\ psi \qquad (19.2.3.1)$$

Load Determination and Load Cases

$$P_{DL} = 3(2.4\ K) = 7.2\ K$$

$$P_{LL} = 3(2.5\ K) = 7.5\ K$$

The weight of the wall panel above the centerline of the unbraced length:

$$\left(\frac{6.25\ in}{12\ in/ft}\right)100\ psf(15\ ft)\left(\frac{29.5\ ft}{2} + 1.5\ ft\right)\left(\frac{1\ K}{1000\ lb}\right) = 12.7\ K$$

Strength Determination – Load Case 1

Assume 14 No. 6 bars

$$A_s = 6.125\ in^2$$

$$P_{ua} = 1.2(7.2\ K) + 1.6(7.5\ K) = 20.6\ K$$

$P_{um} = 20.6\ K + 1.2(12.7\ K) = 35.8\ K$

$w_u = 0.5(15\ ft)(27.2\ psf) = 204\ plf = 0.204\ klf$

Check vertical stress at mid-height of panel

$\frac{P_{um}}{A_g} = \frac{35.8\ K\ (1000\ lb/1\ K)}{6.25\ in(15\ ft)(12\ in/ft)} = 31.8\ psi < 0.06f'_c = 240\ psi$ (11.8.1.1)

Check design moment strength

$A_{se} = A_s + \frac{P_{um}}{f_y}\left(\frac{h}{2d}\right) = 6.125\ in^2 + \frac{35.8\ K}{60\ ksi}\left(\frac{6.25\ in}{2(3.13\ in)}\right) = 6.72\ in^2$ (R11.8.3.1)

$a = \frac{A_{se}f_y}{0.85f'_c b} = \frac{6.72\ in^2(60\ ksi)}{0.85(4\ ksi)(15\ ft)(12\ in/ft)} = 0.659\ in$

$c = \frac{a}{0.85} = \frac{0.659}{0.85} = 0.775\ in$ (22.2.2.4.1)

$\frac{c}{d} = \frac{0.775}{3.13} = 0.248 < 0.375\ \rightarrow Tension\ Controlled$ (R21.2.2)

$I_{cr} = nA_{se}(d-c)^2 + \frac{l_w c^3}{3}$ (11.8.3.1c)

$= 13.896(6.72\ in^2)(3.13\ in - 0.775\ in)^2 + \frac{15\ ft\left(12\frac{in}{ft}\right)(0.775)^3}{3} = 546\ in^4$

$M_{cr} = \frac{f_r I_g}{y_t} = f_r S = f_r\left(\frac{1}{6}bt^2\right) = 0.356\ ksi\left(\frac{1}{6}\right)(15\ ft)(6.25\ in^2) = 34.7\ K\ ft$ (24.2.3.5)

$\phi M_n = \phi A_{se} f_y\left(d - \frac{a}{2}\right)$

$= 0.9(6.72\ in^2)(60\ ksi)\left(3.13\ in - \frac{0.659\ in}{2}\right) = 84.7\ K\ ft$

Check minimum reinforcement:

$\phi M_n \geq M_{cr}$ (11.8.1.1)

$\rho = \frac{A_s}{bh} = \frac{6.125\ in^2}{15\ ft(12\ in/ft)(6.25\ in)} = 0.00544 > \rho_l = 0.0015$ (11.6.1)

Check applied moment:

$K_b = \frac{48\ \ _cI_{cr}}{5l_c^2} = \frac{48(2087\ ksi)(546\ in^4)}{5[29.5\ ft(12\ in/ft)]^2} = 87.3\ K$

$M_{ua} = \frac{w_u l_c^2}{8} + \frac{P_{ua}e_{cc}}{2} = \frac{0.204\ klf(29.5\ ft)^2}{8} + \frac{20.6\ K(3\ in)}{2(12\ in/ft)} = 24.8\ K\ ft$

$M_u = \frac{M_{ua}}{\left(1 - \frac{P_{um}}{0.75\ \ _b}\right)} = \frac{24.8\ K\ ft}{\left[1 - \frac{35.8\ K}{0.75(87.3\ K)}\right]} = 54.8\ K\ ft < \phi M_n$ (11.8.3.1d)

$\Delta_u = \frac{M_u}{0.75 K_b} = \frac{54.8\ K\ ft(12\ in/ft)}{0.75(87.3\ K)} = 10.0\ in$ (11.8.3.1b)

Strength Determination – Load Case 2

$P_{ua} = 12.4\ K$

$P_{um} = 27.6\ K$

$w_u = 0.408\ klf$

$\frac{P_{um}}{A_g} = 24.6\ psi < 0.06f'_c = 240\ psi$

$A_{se} = 6.58\ in^2$

$a = 0.646\ in$

$c = 0.759\ in$

$\frac{c}{d} = 0.243 < 0.375\ \rightarrow Tension\ Controlled$

$I_{cr} = 540\ in^4$

$M_{cr} = 34.7\ K\ ft$

$\phi M_n = 83.2\ K\ ft > M_{cr}$

$K_b = 86.4\ K$

$M_{ua} = 45.9\ K\ ft$

$M_u = 80.1\ K\ ft < \phi M_n$

$\Delta_u = 14.8\ in$

<u>Strength Determination – Load Case 3</u>

$P_{ua} = 6.5\ K$

$P_{um} = 17.9\ K$

$w_u = 0.408\ klf$

$\frac{P_{um}}{A_g} = 15.9\ psi < 0.06f'_c = 240\ psi$

$A_{se} = 6.42\ in^2$

$a = 0.630\ in$

$c = 0.741\ in$

$\frac{c}{d} = 0.237 < 0.375\ \rightarrow Tension\ Controlled$

$I_{cr} = 534\ in^4$

$M_{cr} = 34.7\ K\ ft$

$\phi M_n = 81.4\ K\ ft > M_{cr}$

$K_b = 85.4\ K$

$M_{ua} = 45.2\ K\ ft$

$M_u = 62.7\ K\ ft < \phi M_n$

$\Delta_u = 11.8\ in$

Service Deflection

$$\Delta_{allowable} = \frac{l_c}{150} = 2.36\ in \tag{11.8.1.1}$$

$$\Delta_{cr} = \frac{5M_{cr}l_c^2}{48E_cI_g} = 0.712\ in \tag{11.8.4.3a}$$

$$M_{sa} = \frac{w_s l_c^2}{8} + \frac{P_a e_{cc}}{2} = \frac{0.6(27.2\ psf)(15.0\ ft)(29.5\ ft)^2}{8(1000\ lb/K)} + \frac{7.2\ K(3\ in)}{2(12\ in/ft)} = 27.5\ k\ ft$$

The concrete has cracked since M_{sa} > (2/3) M_{cr}, equation 11.8.4.2b must be used. Iterating Δ_s to determine M_a:

$$M_a = 30.5\ K\ ft$$

$$\Delta_s = \left(\frac{2}{3}\right)\Delta_{cr} + \frac{M_a-(2/3)M_{cr}}{M_n-(2/3)M_{cr}}\left[\Delta_n - \left(\frac{2}{3}\right)\Delta_{cr}\right] = 1.815\ in \tag{11.8.4.2b}$$

5.3 Design Example Comparison

A comparison of the two design examples in sections 5.1 and 5.2 shows that a lightweight slender tilt-up wall panel will both weigh less and use less reinforcement than a normal weight panel, assuming all other variables are held constant. Table 5-2 displays the reinforcement used, the density, the total weight, the cracking moment, and the service deflection for both panels.

Table 5-2: Comparison of Design Examples

	Design Example 1	Design Example 2
Vertical Reinforcement	16 no. 6 bars	14 no. 6 bars
Area of Steel	7 in^2	6.125 in^2
Concrete Density	150 pcf	100 pcf
Total Panel Weight	36.3 K	24.2 K
Cracking Moment	46.3 K-ft	34.7 K-ft
Service Deflection	0.335 in	1.815 in

The lightweight panel had an increase in deflection and a reduced cracking moment. The lightweight panel had a total panel weight that was 66.7% smaller than the normal weight panel total weight, which was a contributing factor to the adequate design despite the smaller cracking moment. Additionally, the lightweight panel utilized 12.5% less steel than the normal weight panel. Figure 5-2 displays the load-deflection curves for these two panels.

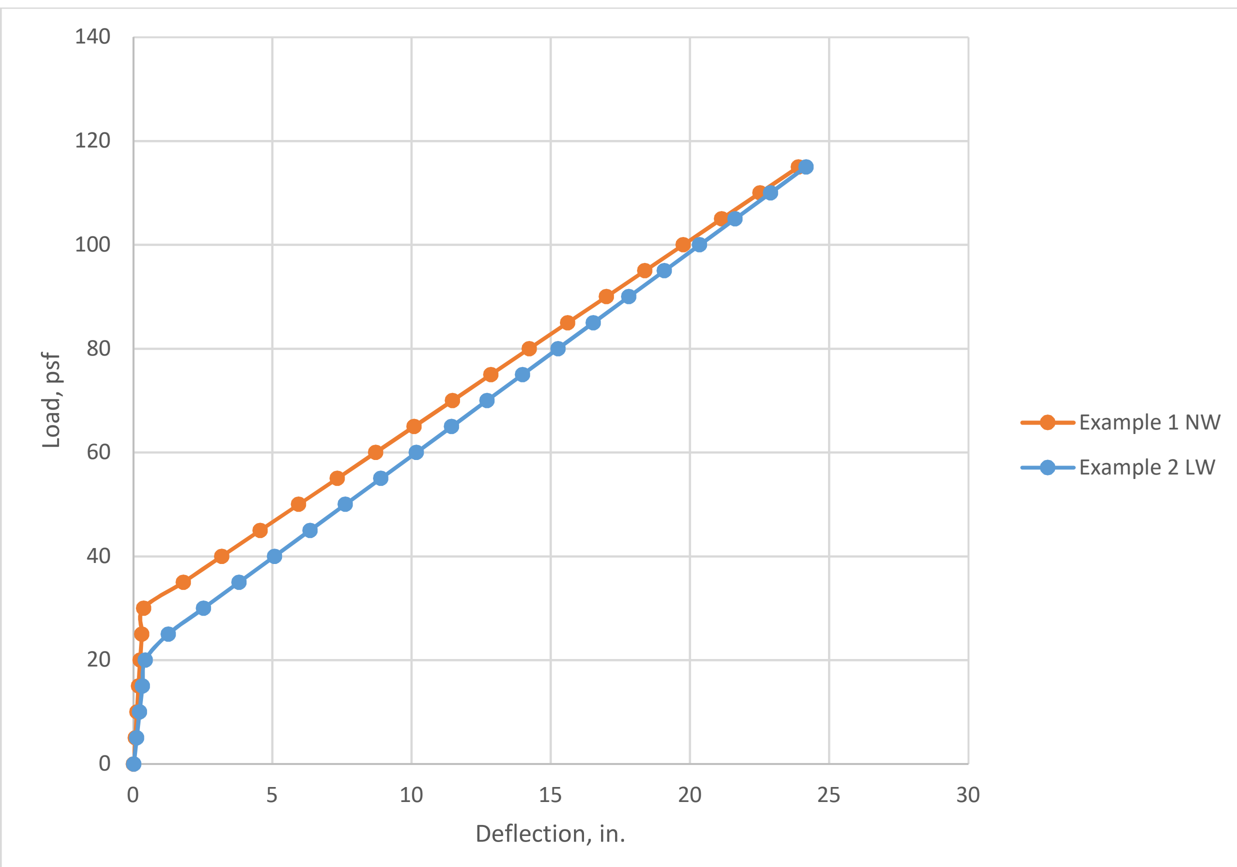

Figure 5-2: Design Examples – Load-Deflection Curves

Chapter 6 - Conclusions and Recommendations

The parametric study in this report calculated the deflection in slender lightweight tilt-up wall panels using ACI 318 (2019) code with various lightweight concrete factors λ and K values used in the modulus of rupture equation. Both factors had a minimal impact on deflections for lateral loading before the cracking moment had been reached. Once the panels cracked, larger deflections were observed in panels with small values for λ and K. As the panels approached the nominal moment capacity, the deflection curves converged. This implies that the current code equations are assuming stability governs for deflections near panel yielding.

A comparison of the deflections calculated with ACI code equations and the deflections observed in the Report of the Task Committee on Slender Walls (Simpson et al., 1982) was performed. This comparison suggests that the linear interpolation equation for service level deflection in slender tilt-up wall panels is slightly conservative for wall panels with small slenderness ratios. For more slender panels, however, the linear interpolation correlated well with the test data.

6.1 Design Recommendations

Without test data on slender lightweight concrete tilt-up wall panels, the true deflection behavior of them is unknown. Until testing and further analysis has been performed, a K value of 7.5 can be used for calculation of the modulus of rupture in accordance with current code. For conservative design, a lower K factor can be used, which would yield a larger deflection for a given load. It should be noted that the recommendation of a K factor of 7.5 would be used with the standard ACI 318 code equation shown in Equation 3-20. In this thesis, that was represented by a K factor of 5 and the removal of the (2/3) factors in Equation 3-20. While the lightweight concrete factor λ had a minimal impact when varied between 0.75 and 0.85, using λ = 0.75

would provide the most conservative design. Two design examples are shown in Chapter 5 describing the design of a normal weight and lightweight slender tilt-up wall panel.

6.2 Further Research

Deflection tests on lightweight slender tilt-up wall panels are required to accurately represent the behavior in design. Ideally, a test would be performed with the same panel properties and dimensions as the Report of the Task Committee on Slender Walls (Simpson et al., 1982) for ease of comparison. Tests could be performed with concrete mixes containing aggregates with various densities that correlate to different lightweight concrete factors per ACI code. Once deflections have been recorded, the deflections could be compared to the linear interpolation equation used for service level deflections.

The modulus of rupture equation for service level deflections could also potentially be revisited. There are a few reasons that would justify future research into the modulus of rupture for lightweight concrete: the current research is potentially outdated, the dispute over the modulus of rupture in high-strength lightweight concrete, and accounting for shrinkage effects. The current ACI 318 code equation for the modulus of rupture does not list references for test data, but is likely based on outdated research, as it has not changed in the last few decades. Concrete has likely changed since the modulus of rupture equation was developed, with new aggregates and different strength properties. The dispute over the accuracy of the modulus of rupture equation discussed in the literature review of this thesis has not been settled, and further research could be done to determine its accuracy. As the aggregate density is reduced, more shrinkage occurs. While not discussed in depth in this thesis, the impact of shrinkage on lightweight concrete in slender wall panels could require adjustments to the lightweight concrete modification factor or the modulus of rupture. Until further test data is available, this impact cannot be accurately measured.

References

Abi-Nader, G. G. (2009). *Erection Stresses in Reinforced Concrete Tilt-up Wall Panels*. University of Florida.

ACI Committee 318. (2019). *Building code requirements for structural concrete (ACI 318-19): an ACI standard: commentary on building code requirements for structural concrete (ACI 318R-19)*. American Concrete Institute.

ACI Committee 213. (2014). *Guide for Structural Lightweight-Aggregate Concrete*. American Concrete Institute.

ACI Committee 551. (2015). *Design guide for tilt-up concrete panels*. American Concrete Institute.

Almograbi, M. (2010). Durability Study of Lightweight Concrete Material Made from Date Palma Seeds (DPS). *Nasser Nations University*.

American Society of Civil Engineers. (2017). *Minimum Design Loads and Associated Criteria for Buildings and Other Structures (Asce/Sei 7-16)*. American Society of Civil Engineers.

ASTM C78/C78M-10 – *Standard Test Method for Flexural Strength of Concrete (Using Simple Beam with Third-Point Loading).*

ASTM C127-12 – *Standard Test Method for Density, Relative Density (Specific Gravity), and Absorption of Fine Aggregate.*

ASTM C469/C469M-10 – *Standard Test Method for Static Modulus of Elasticity and Poisson's Ratio of Concrete in Compression.*

Bremner, T. W., & Holm, T. A. (1986). Elastic Compatibility and the Behavior of Concrete. *ACI Journal Proceedings*, *83*(2). doi: 10.14359/10422

Cook, J. E. (2007). Proposed Changes to ACI 318-05 Modulus of Elasticity Formula Based on 25 Years of Research. *2007 Concrete Technology Forum Conference Proceedings*.

Embry, I. (2016, December 9). Concrete Mix Design for Structural Lightweight Concrete. Retrieved from https://www.ecoccs.com/Concrete_Mix_Design_for_Lightweight_Strength_Concrete.html.

Graybeal, B., & Greene, G. (2015). *Lightweight concrete: shear performance*. U.S. Department of Transportation, Federal Highway Administration, Research, Development and Technology, Turner-Fairbank Highway Research Center.

Hanson, J. A. (1961). Tensile Strength and Diagonal Tension Resistance of Structural Lightweight Concrete. *ACI Journal Proceedings*, *58*(7). doi: 10.14359/7972

Hanson, J. A. (1964). Replacement of Lightweight Aggregate Fines with Natural Sand in Structural Concrete. *ACI Journal Proceedings*, *61*(7). doi: 10.14359/7808

Herki, B. A., Safary, Z., & Khalid, O. (2016). Engineering Properties of Sustainable Lightweight Concrete Using Waste Polystyrene. *International Journal of Engineering and Innovative Technology*, *5*(12).

Hoff, G. C. (1992). High Strength Lightweight-Aggregate Concrete for Arctic Applications. *Structural Lightweight Aggregate Concrete Performance*.

Hognestad, E., Hanson, N. W., & McHenry, D. (1955). Concrete Stress Distribution in Ultimate Strength Design. *ACI Journal Proceedings*, *52*(12). doi: 10.14359/11609

Holm, T. A. (1980). Physical Properties of High Strength Lightweight-Aggregate Concrete. *Second International Congress of Lightweight Concrete*.

Heffington, J. A. (2000). *Development of High-Performance Lightweight Concrete Mixes for Prestressed Bridge Girders.* University of Texas at Austin.

International Code Council. (2015). International Building Code. Falls Church, Va. :International Code Council

Kripanarayanan, K. M. (1994). *Tilt-up load-bearing walls: A Design Aid*. Portland Cement Association.

Kosmatka, S. H., & Wilson, M. L. (2017). *Design and control of concrete mixtures* (15th ed.). Skokie, IL: Portland Cement Association.

LaRue, H. A. (1946). Modulus of Elasticity of Aggregates and its Effect on Concrete. *ASTM International Proceedings*, *46*.

Lukic, I., Malesev, M., Radonjanin, V., & Milovanovic, V. (2013). A Comparative Analysis of Environmental Impacts of Ordinary Concrete and Structural Lightweight Concrete. *Faculty of Technical Sciences, Novi Sad, Serbia*.

Malhotra, V. M. (1990). Durability of concrete incorporating high-volume of low-calcium (ASTM Class F) fly ash. *Cement and Concrete Composites*, *12*(4). doi: 10.1016/0958-9465(90)90006-j

Martin, D. P., Zimmer, A. S., Boldeuc, M. J., & Hopps, E. R. (2013, January). Is Lightweight Concrete All Wet? *Structure Magazine*.

Messenger, H. G., Harmon, T. G., Baur, K., Graziano, G. C., & Lorah, D. L. (2005). *United States Patent No. US 2005O258572A1.*

Meyer, K. F. (2002). Transfer and Development Length of 0.6-inch Diameter Prestressing Strand in High Strength Lightweight Concrete. *School of Civil and Environmental Engineering, Georgia Institute of Technology*.

Meyer, K. F., Buchberg, B. S., & Kahn, L. F. (2003). Development of High Strength Lightweight Concrete Mix Designs: A Practical Approach. *49th Annual PCI Convention & Exhibition*.

Müller-Rochholz, J. (1979). Determination of the elastic properties of lightweight aggregate by ultrasonic pulse velocity measurement. *International Journal of Cement Composites and Lightweight Concrete*, *1*(2), 87–90. doi: 10.1016/0262-5075(79)90014-9

Nassar, A. J. (2002). *Investigation of transfer length, development length, flexural strength and prestress loss trend in fully bonded high strength lightweight prestressed girders*. Virginia Polytechnic Institute and State University.

Ozyildirim, H.C., & Gomez, J.P. (1999). High Performance Concrete in a Bridge in Richlands, Virginia.

Park, W.-J., Kim, T., Roh, S., & Kim, R. (2019). Analysis of Life Cycle Environmental Impact of Recycled Aggregate. *Applied Sciences*.

Pauw, A. (1960). Static Modulus of Elasticity of Concrete as Affected by Density. *ACI Journal Proceedings*, *57*(12). doi: 10.14359/8040

Pfeifer, D. W. (1968). Sand Replacement in Structural Lightweight Concrete-Creep and Shrinkage Studies. *ACI Journal Proceedings*, *65*(2). doi: 10.14359/7462

Ramirez, J. A., Olek, J., & Malone, B. J. (2004). Shear Strength of Lightweight Reinforced Concrete Beams. *High-Performance Structural Lightweight Concrete*.

Russell, H. G. (2008). *Lightweight Concrete-Material Properties for Structural Design*.

Shideler, J. J. (1957). Lightweight-Aggregate Concrete for Structural Use. *ACI Journal Proceedings*, *54*(10). doi: 10.14359/11441

Simpson, W. M., Adham, S. A., Amrhein, J. E., Coil, J., Dobrowolski, J. A., Foth, U. A., … McLean, R. S. (1982). *Report of the Task Committee on Slender Walls*. Los Angeles, CA: The Committee.

Tasillo, C. L., Neeley, B.D., & Bombich, A. A. (2004). Lightweight Concrete Makes a Dam Float. *High-Performance Structural Lightweight Concrete*.

Trumble, R., & Santizo, L. (1992). The Advantages of Using Lightweight Concrete in a Medium Rise Building and Adjoining Post-Tensioned Parking Garage. *Structural Lightweight Aggregate Concrete Performance*.

Videla, C., & Lopez, M. (2000). Mixture Proportioning Methodology for Structural Sand-Lightweight Concrete. *ACI Materials Journal*, *97*(3). doi: 10.14359/4623

Videla, C., & Lopez, M. (2002). Effect of Lightweight Aggregate Intrinsic Strength on Lightweight Concrete Compressive Strength and Modulus of Elasticity. *Materiales De Construccion/Construction Materials*, *52*(265).

Ward, W. (2011). The Construction of Tilt-Up. *Tilt-Up Concrete Association*, *First Edition*.

Washa, G. W., & Fluck, P. G. (1952). Effect of Compressive Reinforcement on the Plastic Flow of Reinforced Concrete Beams. *ACI Journal Proceedings*, *49*(10). doi: 10.14359/11806

Appendix A - Permission for Use

The figures from ACI 551 and 213 are used with permission from Barry Bergin, Manager of Publishing Services with the American Concrete Institute. The graphs and figures from the *Report of the Task Committee on Slender Walls* are used with permission from Don Schinske, Executive Director with the Structural Engineers Association of California.